Università degli Studi di Padova

Dipartimento di Fisica e Astronomia
"Galileo Galilei"

Dipartimento di Biologia

Corso di Laurea Magistrale in Astronomia

Searching for the oxygen footprint of light-harvesting organisms

Relatrice: **Prof.ssa Nicoletta La Rocca**
Correlatore: **Prof. Riccardo Claudi**
Laureando: **Vito Squicciarini**

Anno Accademico 2018/2019

Contents

Chapter 1

Introduction

> *"There are infinite worlds both like and unlike this world of ours. [...] We must believe that in all worlds there are living creatures and plants and other things we see in this world."*
>
> *Epicurus, 4^{th} century B.C.*

The endless quest for the unknown, the eagerness to unveil the secrets of nature, is the fuel that propels and powers any scientific endeavour of the human species. "The courage of our questions and the depth of our answers, our willingness to embrace what is true rather than what feels good" [1] allow us to gradually expand, step by step, our knowledge of the Universe. Today we are living in an exciting age for science, where an ever-growing flow of data constantly challenges our models and opens up the spaces for new questions, but helps us to provide answers to the old ones. The unending pursuit to understand our place in the Cosmos, the longstanding philosophical issue on the origin and the distribution of life beyond Earth, summarised in the question "are we alone?" has recently abandoned the realm of speculation and entered the scientific debate. Astrobiology – the science aimed at studying the origin, the properties, the distribution of life in the Universe – emerged in the 1950s from a convergence among planetary sciences, the search for exoplanets, the studies on the origin of life and the Search for Extra Terrestrial Intelligence (SETI). Encompassing astronomy, physics, chemistry and biology, this rapidly expanding field of study belies, at its heart, the wilful search for *the answer*.

In order to assess in a scientific way the issue of extraterrestrial life, it is necessary to define it precisely, splitting it into three smaller pieces: whether there are other worlds, whether these worlds could sustain life, whether we have some means of actually discovering it.

The debate whether the Earth is the only stage in the cosmic arena permeated the speculations of ancient philosophers. The Greek atomists Democritus and Leucippus (5^{th} century BC) were the first to suggest that matter consists of atoms floating in an infinite vacuum. The casual aggregation of atoms was the blind force behind the birth and death of every object in the Universe, and the Earth was just one of these aggregates. In the words of the Roman poet Lucretius (1^{st} century BC),

> "It is in the highest degree unlikely that this earth and sky is the only one to have been created ... Nothing in the universe is the only one of its kind, unique and solitary in

[1] Carl Sagan, *Cosmos* (1980).

> its birth and growth ... You are bound therefore to acknowledge that in other regions there are other earths and various tribes of men and breeds of beasts".

But this was always a minority opinion, that was later totally overcome by the idealist school of Plato and Aristotle, which held the Earth as the centre of a teleological world and the man as the peak of the divine creation. In the Aristotelian view, stars and planets were thought to be aethereal spheres, perfect and immutable, while the Earth, composed of the four elements, was the land of creation and destruction, where everything is bound to be ephemeral. This view, incorporated by Christian theology, dominated the western thought for almost two millennia.

If we exclude the pioneering intuition of Nicolas Cusanus -who back in 1440 in his essay "Of Learned Ignorance" argued for an infinite universe, the unity of celestial and terrestrial matter and the idea that each star is a sun with its own planets- the spark that launched the scientific revolution was the publication of "De Revolutionibus Orbium Coelestium" in 1543. Copernicus' work, even if it was not intended to do it, changed forever man's picture of the Universe. The history of astronomy has been since then, in the words of Edwin Hubble, "a history of receding horizons". Moving the Earth away from the centre of the Universe set off a whole chain reaction. *The Earth is a planet, planets are earths.* If the Moon orbits the Earth, but the Earth orbits the Sun, there's not a single, universal point of attraction. Galileo Galilei's discoveries of the phases of Venus and Jupiter's moons were the confirmation of this newly-discovered truth. Maybe there's no need for a centre of the universe *at all.* A new physics was needed to describe the heavens: starting with Galileo, the effort was completed with Isaac Newton's Principia (1687), suggesting a Universe driven by a clockwork mechanism. In the 18th century, William Herschel's observations of double stars confirmed that the same laws of gravity and motion of the Solar System were at work everywhere. In 1861, William and Margaret Huggins spectroscopically detected the same elements in stars as Robert Bunsen and Gustav Kirchhoff had found in the Sun, finally proving that the Sun *is a star.* The same natural laws are valid in the whole Universe.

The observation of two *stellae novae* ("new stars") in 1572 and 1604 in the supposedly immutable sphere of fixed stars and Tycho Brahe's demonstration that a bright comet, lacking a measurable parallax, was a celestial phenomenon piercing the aethereal spheres which were thought to sustain planets, first showed that the Universe is indeed a dynamic place. The intellectual journey that eventually led to the modern vision of an evolving Universe began here.

The absence of an observable annual parallax in the position of the stars led to a profound consequence: stars are amazingly far, and the Universe is far more extended than everyone had ever dreamt of. In a sense of awe, Galileo Galilei, glancing at the Milky Way, resolved the whitish stripe into countless stars. In one of the first attempts at stellar photometry, Christiaan Huygens (1698) estimated the distance of Sirius, the brightest star of the night sky, as 0.4 light years. However, scientists were not able to really grasp the actual size of the Universe until Edwin Hubble, in 1924, proved that spiral nebulae like Andromeda and the Triangulum were indeed too far to belong to the Milky Way, and were instead independent galaxies. The discovery of the first extrasolar planet by Mayor & Queloz (1995), followed by thousands of detections in just 25 years, gave a definitive answer to the first piece of the question: other worlds do exist.

The strongest piece of evidence in favour of the existence of extraterrestrial life is the fact that we exist. The fact that we know that, at least once in the history of the Universe, life started on a planet around a main sequence star, that the same laws of physics apply, that the same chemical elements are everywhere, suggest that life should have evolved elsewhere as well. NASA's Hubble Space Telescope indicates that there might be an astonishing 1 trillion galaxies in the Universe. Since the Milky Way alone hosts 250 ± 150 billion stars, it appears extremely likely, from a statistical point of view, that the Universe is teeming with life. But conversely, the conditions for life to arise have often been described as very stringent (the "Rare Earth hypothesis", Ward & Brownlee 2000). Like a ∞/∞ division, a thorough assessment needs being performed to

recognise whether the former or the latter factor dominates.

The British philosopher William Whewell, in his essay "Of the Plurality of Worlds" (1853), warned that certain conditions are needed in order for life to arise and foresaw the idea of habitable zone:

> "The earth, alone, is placed at the border where the conditions of life are combined; ground to stand upon; air to breathe; water to nourish vegetables, and thus, animals...; and with this, a due supply of light and heat, and due energy of the force of weight. All these conditions are, in our conception, required for life; that all these conditions meet, elsewhere than in the earth's orbit, we see strong reason to disbelieve...That the earth is inhabited, is not a reason for believing that the other planets are so, but for believing they are not so."

Some years later, in 1871, Charles Darwin, after proposing his theory of evolution, began assessing the problem of the origin of life:

> "But if (and oh! what a big if!) we could conceive in some warm little pond, with all sorts of ammonia and phosphoric salts, light, heat, electricity, etc., present, that a proteine compound was chemically formed ready to undergo stillmore complex changes..."

The idea of an abiogenesis from a "primordial soup" was developed by Aleksandr Oparin (1924) and John Haldane (1929) and found a remarkable experimental validation thanks to the Miller-Urey experiment (1952). The experiment simulated the conditions which were thought to be present on primordial Earth: a highly reducing atmosphere, composed of a mixture of hydrogen (H_2), water vapour (H_2O), methane (CH_4) and ammonia (NH_3), liquid water, a source of heat and electrical sparks to simulate lightning. After one week, the solution was analysed and five amino acids, the building blocks of proteins, were identified. The experiment proved that, under the right conditions, a prebiotic chemistry can easily rise from scratch.

Molecules of life must be stable enough for organisms to thrive but flexible enough to allow a complex metabolism. These requirements are met by carbon-based molecules, which constitute the totality of Earth biochemistry. Other alternatives have been put forward; for example, a silicon-based life. Although silicon is in many respects similar to carbon, there are serious impediments to this idea. Firstly, the redox reaction $SiH_4 \leftrightarrow SiO_2$ requires much more energy than the reaction $CH_4 \leftrightarrow CO_2$. Secondly, silicon is not able to form long stable chains and hardly reacts with water. This is not a minor point, since water has a biological importance that goes beyond being a mere solvent: on a static level, it determines the stability of biological structures; on a dynamical level, it takes part actively and rapidly to every metabolic process, sometimes as an active part, sometimes as a means of transport. Finally, silicon is relatively less common than carbon in the Universe.

Even if a carbon-based chemistry were the only possible one, there could be virtually an infinite number of carbon biochemistries. In the absence of a unified theory of life, a prudent approach consists in searching for life that is similar to Earth's, as our very existence proves that, under Earth-like conditions, life can arise.

The habitable zone (Huang 1959) is defined as the ring around a star where liquid water can exist on a planet. It is primarily a condition on surface temperature. It is clear that the crucial parameters controlling the temperature of a planet are orbital distance and luminosity of its parent star. Recent discoveries of extrasolar planets seem to show that rocky planets in the habitable zone of their stars are indeed common. However, the problem is much more complex because the climate of a planet is heavily influenced by its atmospheric composition. Gases like H_2O, CO_2 and CH_4 have strong absorption bands in the infrared, trapping some heat that would be otherwise

reflected back to space. This "greenhouse effect" accounts for an additional +35 K on Earth, but on Venus, embedded in a 90-bar CO_2 atmosphere, it reaches +500 K! Given that we actually don't know the properties of exoplanet atmospheres, we are forced to rely on theoretical models trying to envisage which kinds of atmospheres could exist in different stellar environments.

While it is risky to infer general conclusions from the only example of inhabited world we know, it is interesting to notice that microbial life arose no later than about 500 Myr after Earth's formation, while complex, multicellular life only appeared 600 Myr ago (Jiang et al. 2011; Schiffbauer et al. 2012), suggesting that the former could be quite common, the latter accidental; the timescale of Earth's life, additionally, can be used to constrain the stellar classes which could be viable targets for the search of life. Since the main sequence lifetime is approximatively related to stellar mass according to the relation:

$$\frac{t_{MS}}{t_{sun}} \sim \left(\frac{M}{M_{sun}}\right)^{-2.5\sim3} \tag{1.1}$$

earlier stars than F-class ones likely evolve too fast to allow complex life to develop. This is not a great limitation, though, since the initial mass function favours late type stars with respect to early type stars. 75% of the stars are estimated to be M-type dwarfs (Henry 2004). This is why M-star planets are seen as an appealing target for the search for life.

But, even if we found a lot of planets that might be habitable, how could we know if they actually host life? In the first decades of the space era, direct inspection of the bodies of the Solar System was considered the chief means for looking for life. The Viking landers sent to Mars in the 1970s conducted biological experiments to look for signs of life on the red planet, but its results were controversial and gave no definitive answer (Adelman 1986; Horowitz et al. 1976; Levin & Straat 1976). Future projects targeting Jupiter's Europa are animated by the same purpose. But, of course, the immensity of galactic distances renders this method not viable for studying extrasolar planets.

A completely different approach directly stems from the faith in technological advancement which pervaded the end of the 19$^{\text{th}}$ century. The advent of electricity and new means of communication provided, for the first time, a portal that could bring the quest for extraterrestrial life out of the realm of fiction. Personalities like Tesla, Marconi, Lord Kelvin and David P. Todd suggested that wireless electrical or radio communications with Martians were feasible. The idea returned over a half-century later, when Giuseppe Cocconi and Philip Morrison (1959) proposed to search for interstellar communications by advanced civilisations of our galaxy. Radio messages might be transmitted at a wavelength of 21 cm (1420.4 MHz), perhaps a cosmic standard since it corresponds to the wavelength of emission by neutral hydrogen. For the first time, a once philosophical question became scientifically testable.

Independently from Cocconi and Morrison, astronomer Frank Drake (1961) tried to estimate the number of actively radio-communicating galactic civilisations N by means of the famous equation:

$$N = R_s \cdot f_p \cdot n_e \cdot f_l \cdot f_i \cdot f_c \cdot L \tag{1.2}$$

where R_s is the average star formation rate in the Galaxy; f_p is the fraction of those stars hosting planetary systems; n_e is the number of planets per system with a suitable conditions for life; f_l is the fraction of them that actually bears life; f_i is the fraction of inhabited planets in which intelligent life emerges; f_c is the fraction of radio-communicating civilisations; L is duration of their communication history. Simply put, it yields a rough guess of how many species *like ours* are out there. Drake's equation, by focusing not on the abstract concept of life, but rather to the practical search of advanced civilisations, inspired and paved the way for the SETI (Search for Extra-Terrestrial Life) project. In its deepest epistemological sense, the equation applies a truly reductionist approach by scientifically splitting the problem of finding advanced civilisations

into smaller and more tangible parts (Cabrol 2016). But its strength is also its weakness, for its formulation is strongly human-biased, both in the means employed to communicate and in the tacit assumption that they *wish* to communicate.

Although almost sixty years have passed since, no unambiguous signal of extraterrestrial origin has been found in SETI surveys. The only voice that has been resonating , in the background, is that of Fermi: "Where is everybody?". But in order to catch a possible signal, we must be listening at the right time, at the right frequency, and be pointing the right direction in the sky, supposing of course that the signal is actually pointing at us. Nevertheless, this all-or-nothing search goes on, as finding a signal would be a world-changing discovery.

A milder approach, where incremental -rather than abrupt- progress is being continuously achieved, characterises modern astrobiological research. The principle is that microbial life should be much more widespread than technologically advanced life, and that it is possible to shed light on the origin of life by paring biology down to minimal physical and chemical components. Assessing what kind of environment is more prone to biotic initiation and what biosignatures could remotely unveil the presence of life has become an increasingly beaten track. Looking back at our Earth, we clearly see that life has drastically modified the makeup of the atmosphere. Molecular oxygen, in particular, is completely out of chemical equilibrium and, without a continuous biological source, would disappear in a few million years (Leger et al. 1993). Oxygen shows a prominent absorption feature at 0.76 μm in Earth's spectrum. Photodissociation of oxygen, caused by solar UV radiation, generates ozone (O_3), a compound that shows evident absorption features at 9.6 μm. Finally, the presence of methane in Earth's atmosphere is totally incompatible with the presence of oxygen unless it is continuously replenished: as it turns out, abiotic production is a factor 30 (Segura et al. 2007) less than biological production. The Earth's integrated spectrum is in figure 2.2.

In addition to byproducts of its methabolic reactions, life reveals its own presence in the Earth's spectrum directly, through a spectral feature known as the *Red Edge*: it is linked to the high reflectance of chlorophylls at 700-850 nm (Kiang et al. 2007a,b) and has no abiotic counterparts.

Finding evidence either of O_2/O_3 and CH_4 out of chemical equilibrium in the spectrum of an extrasolar planet, or of a feature comparable to the Red Edge, would therefore be a proof of some kind of biological activity. Atmospheric studies of extrasolar planets have just begun. As Sagan once said, *"somewhere, something incredible is waiting to be known"*.

Chapter 2

Background

"There are countless suns and countless earths all rotating around their suns in exactly the same way as the seven planets of our system. We see only the suns because they are the largest bodies and are luminous, but their planets remain invisible to us because they are smaller and non-luminous. The countless worlds in the universe are no worse and no less inhabited than our Earth"

Giordano Bruno, De l'infinito universo e mondi, 1584

2.1 Planetary atmospheres: state of the art

The discovery of more than 4000 exoplanets in the last 25 years has rapidly established a whole new field of study. Astronomers are just beginning to grasp the exquisite menagerie of planetary systems, one that is far more complex than assumed before. The most common type of planet has roughly two Earth masses and is absent in the Solar System (Marcy et al. 2014b); super-Earths and mini-Neptunes build a bridge between rocky planets and gas giants; hot Jupiters challenged the standard theory of the Solar System formation; "water worlds" with a proportion of (solid or liquid) water mass relative to the entire planet higher than 70 % (Léger et al. 2004), are thought to have oceans hundreds of kilometres deep. The Solar System architecture is just one of a myriad of possibilities.

Atmospheric characterisation of exoplanets is currently viable through direct imaging and transits. The transit method, possible when the orbital plane of the exoplanet is almost parallel to the line of sight, exploits the fact that, when the planet transits in front of its parent star, it blocks some of its light. Some light filters through the planet's atmosphere and reaches our line of sight, keeping track of the spectral features of the atmospheric gases. The spectrum coming from the star during a transit will therefore carry a tiny footprint of the planet's atmosphere. After subtraction of the unperturbed stellar spectrum, it is therefore theoretically possible to identify these features and infer the atmospheric composition (Brown 2001; Tinetti et al. 2007). Transmission spectra primarily probe the upper atmosphere of planets, depending on the system's geometry and planet's atmospheric density. The angular size of the host star with respect to the exoplanet determines the critical deflection height, scaling with $1/T_{eff}^2$: it is possible to probe more deeply the atmosphere of worlds orbiting cooler stars for given planetary size and atmospheric profile (Kaltenegger 2017).

On the other hand, direct imaging discoveries are still very challenging because of the high contrast ratio between planet and star, which can reach values of 10^{-10} for an Earth-like planet (see, e.g., Chauvin et al. 2005; Lafrenière et al. 2007; Biller et al. 2013). Emission spectroscopy (Charbonneau et al. 2005), observing the lit hemisphere of the planet and comparing the total spectrum from the star+planet system with the stellar spectrum obtained during a secondary transit, sheds light on the thermal structure of the planetary atmosphere and the emission/reflection properties of its surface. In the emergent flux, what we observe is sum of the starlight reflected off the planet and the planet's emitted flux in the IR, dependent on the planet's temperature. Unlike a transmission spectrum, it probes different atmospheric depths, including the surface. Although the intensity of spectral features in both reflected and thermal spectra primarily depends on the abundance of the related chemical, the former is affected as well by the incoming stellar radiation at that wavelength, whilst the latter hinges on the temperature difference between the emitting/absorbing layer and the continuum. This allows observers to probe in the IR properties like the temperature of the emitting surface, while in visible light surface reflection properties can be detected, provided that the atmosphere is transparent in that range (Kaltenegger 2017).

2.2 Future prospects

Designs of direct imaging instruments exploiting internal coronagraphs or star-shade techniques are expected to be capable of observing nearby Sun-like stars to both detect exoplanets and spectroscopically characterise their atmospheres even with small (1-2 m) space telescopes. Ground-based high-contrast imagers will include SPHERE@VLT (Beuzit et al. 2008), focusing on warm and young planets, GPI@GEMINI (Larkin et al. 2014) and PCS@E-ELT (Kasper et al. 2013).

Ground-based facilities allowing the atmospheric characterisation of exoplanets include the High Dispersion Spectrograph (R = 45,000) at the Subaru 8-m telescope, CRIRES (Cryogenic High-Resolution Infrared Echelle Spectrograph) and its upgrade CRIRES+ at VLT (Dorn et al. 2014), GIARPS (GIAno+haRPS) at Telescopio Nazionale Galileo (Claudi et al. 2018). These spectrographs enable a different method to characterise the atmospheres of planets with high orbital velocities, namely a high spectral dispersion cross-correlation technique exploiting the Doppler shift in the planetary spectrum compared to the stellar spectrum (Snellen et al. 2010). Encouraging results were obtained by Bean et al. (2010), who managed to characterise the warm super Earth orbiting the M star GJ 1214b, and Snellen et al. (2010), who revealed carbon monoxide on the Hot Jupiter HD209458b flowing in a strong wind at $\sim$2 km/s from the dayside to the nightside of the planet.

Several space missions and ground-based experiments in the near future will begin to measure atmospheric transmission, reflection and emission spectra of extrasolar planets, trying to recover their molecular composition and search for evidence of biosignatures. Atmospheric characterisation of Super-Earths has become today feasible with instruments such as the Wide Field Camera 3 aboard the Hubble Space Telescope (HST) (Deming et al. 2013). Recently, for the first time, analysis of data from WFC3 has led to an exciting discovery: namely, the footprint of water vapour has been detected, for the first time, in the atmosphere of a super-Earth in the habitable zone of its parent star (Tsiaras et al. 2019).

Although NASA's Kepler Space Telescope, with more than 2000 confirmed discoveries, is considered a landmark for exoplanetary studies, it didn't provide many targets for atmospheric characterisation due to planets' faintness (Seager 2014). The TESS mission (Ricker et al. 2016), launched in 2018, is expected to find hundreds of transiting super-Earths, some of which in an M star's habitable zone, suitable for atmospheric observations by NASA's James Webb Space Telescope (JWST) (Clampin 2014; Clampin & Pham 2014). JWST, scheduled to launch in 2021, will observe in visible, near-IR, and IR windows.

The European Space Agency has decided to undertake an ambitious programme aimed at expanding our knowledge of exoplanetary systems. CHEOPS (Broeg et al. 2013), scheduled to launch in 2019, will perform ultrahigh precision photometry on bright stars already known to host planets, providing suitable targets for spectroscopic atmospheric characterisation. PLATO (2026, Rauer et al. 2014) is going to detect terrestrial exoplanets around solar-type stars, and ARIEL (2028, Tinetti et al. 2018) is going to measure the chemical composition and thermal structures of hundreds of transiting exoplanets. It is then of great importance to prepare theoretical models and databases to correctly interpret the findings of these future missions.

2.3 What kind of life are we looking for?

We don't know anything about extraterrestrial life and the form it may take, nor do we have a comprehensive, first-principle understanding of biology capable of predictions about it. Assuming that extraterrestrial life has nothing at all in common with the terrestrial one makes searching for it almost impossible. The opposite extreme of supposing it to be exactly identical to ours is simplistic and would risk missing most actual indications of extraterrestrial biology (Seager et al. 2005). All we have is the example of Earth's life, so a prudent approach is looking for life resembling to some degree to the terrestrial one.

Life has been described as a thermodynamically open system (Prigogine et al. 1972), which exploits gradients in its surroundings to create imperfect copies of itself, makes use of a chemistry based on carbon, and employs liquid water as a solvent in virtually every chemical reaction (Owen 1980; Des Marais et al. 2002). Our knowledge of chemistry strongly suggests (Kaltenegger 2017) that a carbon-based biochemistry is likely, and that liquid water is necessary (for speculations about alternative possibilities, see, e.g., Bains 2004; Chyba & Hand 2005; Baross 2007; Brack et al. 2010). Carbon is easy to oxidise and reduce, forms long and stable chains and is one of the most abundant elements in the Universe. Liquid water, due to its large dipole moment, is a strong polar-non polar solvent, has the capability to form hydrogen bonds and to stabilise macromolecules; it is liquid at a large range of temperature and pressures and has a great heat capacity that makes it able to tolerate a heat shock (Claudi 2017).

2.4 How can we detect it?

2.4.1 Biosignatures

The remote detection of life exploits the fact that life uses chemical reactions to extract, store, and release energy, producing by-products in its metabolic processes that, under the right conditions, can build up in the atmosphere to a detectable concentration. We call these gases *biosignatures* or *biomarkers*. Reviews of biomarkers, concentrating on spectral signatures, are given by Des Marais et al. (2002), Selsis (2003), Traub (2003), Kaltenegger et al. (2006), Beichman et al. (2007) and Kaltenegger et al. (2007).

Even though we can't know all the possible biosignatures (an attempt in this direction is in Seager et al. 2016) due to the aforementioned lack of a unified theory of life, we may begin by studying terrestrial biomarkers and their expected concentration under different environmental conditions. If a future mission detected some gases completely out of chemical equilibrium within their atmospheres, it would be a particularly intriguing discovery. Caution must be taken, of course, in assessing whether a simpler, abiotic explanation in those environments exists.

The most important biomarker on Earth is molecular oxygen. Constituting 21% of the atmosphere by volume, it is almost completely the waste product of the photosynthetic activity of autotroph organisms, since less than 1 ppm of atmospheric O_2 comes from abiotic processes

(Walker 1977). Without a continuous biological source, O_2 would rapidly drop to a concentration ten orders of magnitude lower than the current one (Walker 1977; Leger et al. 1993; Kasting & Catling 2003). Since O_2 is completely out of chemical equilibrium on the Earth, it is considered a robust biosignature (Leger et al. 1993). It is no surprise that its detection has been suggested for decades as a tracer of exoplanetary life (Owen 1980). The validity of this assumption will be thoroughly discussed in Chapter 3.

In addition to oxygen, methane is also far from equilibrium in Earth's atmosphere. On short timescales, O_2 and CH_4 react creating carbon dioxide and water; so, there must be a continuous supply of CH_4 to keep it at detectable concentrations. It turns out that, on Earth, the biotic to abiotic ratio of CH_4 production is about 30:1 (Segura et al. 2007). The abiotic source comes from volcanic emissions from hydrothermal systems where hydrogen, released by the oxidation of Fe by H_2O, reacts with CO_2 to form CH_4. The amount of CH_4 produced in this way depends on the oxidation degree of the planetary crust, so the detection of CH_4 alone cannot be considered evidence for of life, although its detection in an oxygen–rich atmosphere could be a hint of the presence of a biosphere (Claudi 2017).

Ozone is a photochemical product of oxygen, governed by the Chapman cycle (Chapman 1930). Angel et al. (1986) first underlined its significance as a potential biomarker: its strong absorption feature at 9.6 μm has a nonlinear dependence on O_2 abundance (Kasting et al. 1985), being paradoxically a more sensitive indicator of O_2 than O_2 itself (Schindler & Kasting 2000a). Detecting O_2/O_3 in combination with a reduced gas like CH_4 is considered strong evidence for biological activity (Lammer et al. 2009). O_2, O_3, CH_4 can be detected by low-resolution spectrographs (see, e.g., Kaltenegger & Selsis 2007; Segura & Kaltenegger 2010; Des Marais et al. 2002), although the concurrent detection of O_2 and CH_4 would be challenging, except maybe for a planet in a lower-UV radiation environment, like those around quiet M stars (Segura et al. 2005); observability reduces with increasing cloud cover and increases with the age of the system (Rugheimer et al. 2013).

As a rule of thumb, a reduced ultraviolet flux on the planet allows longer biosignature gas lifetimes and, consequently, higher concentrations to accumulate (Seager et al. 2013a). It is possible that biosignature gases that are negligible on present day Earth are abundant on other planets. Pilcher (2003) first suggested that CH_3Cl and organosulphur compounds, in particular methanethiol (CH_3SH), could be produced in high enough abundance by life, possibly becoming good biosignature candidates. Some sulphur compounds appear as promising biosignatures on anoxic planets: hydrogen sulphide (H_2S), carbon disulphide (CS_2), carbonyl sulphide (OCS) are produced by bacteria or fungi during the breakdown of organic material; dimethyl sulfoxide (DMSO: $CH_3 \cdot SO_2 \cdot CH_3$); dimethyl sulphide (DMS), the largest biological source of atmospheric sulphur, produced by marine organisms (Domagal-Goldman et al. 2011). All these gases might accumulate to potentially detectable levels.

The amount of atmospheric NH_3 is orders of magnitude lower than CH_4 because of its very short lifetime under UV irradiation. Under favourable conditions, NH_3 could build up to detectable levels, and its simultaneous detection with oxidised species would be interesting (Kaltenegger et al. 2010b). Perhaps the most promising of this group is nitrous oxide (N_2O), produced in abundance by life but only in negligible amounts by abiotic processes (Claudi 2017). It must be underlined, however, that the detection of oxidised forms of nitrogen or halogens is less likely than that of O_2, as they are all more reactive (and so damaging to life) and require more energy to be produced from environmental chemicals than O_2 (Seager et al. 2013a).

Although strictly not a biosignature, water is a precondition for life as we know it. Water absorption can be seen in the visible-NIR border at 0.7, 0.8 and 0.9 μm, in the NIR bands at 1.1, 1.7 and 1.9 μm, in the mid-IR between 5 and 8 μm and between 17 and 50 μm. The absence of water can be deduced, with an extremely high resolution, from the detection of highly soluble compounds like SO_2 and H_2SO_4 (Lammer et al. 2009).

2.4.2 The Vegetation Red Edge

Could a hypothetical alien observer find *direct* evidence for the existence of life on Earth by remotely looking at its spectrum? In principle yes, if life significantly modifies the reflection spectrum of the surface. In order to answer this question, let us look at the integrated spectrum of our whole planet, as if it were a single-pixel, spatially unresolved exoplanet. A simple, yet powerful solution consists in making use of Earthshine, i.e. the terrestrial light reflected back from the Moon. The idea was put forward by Jean Schneider in 1998 (Arnold et al. 2002) but actually dates back to 1912, when Vladimir Arcichovsky, in a prescient paper (Arcichovsky 1912), suggested to search for chlorophyll absorption features in the Earthshine spectrum to have an idea about what could be expected to be found in the spectra of other planets.

A leaf flaunts a peculiar reflectance spectrum. In the visible region most of the light is absorbed, triggering the plant's photosynthetic activity: the behaviour directly stems from the absorption properties of chlorophylls and other light-harvesting pigments. A small bump in reflectivity near 500 nm is called the "green bump" and is the reason for the green colour of plants. A more significant feature, due to the high reflectance of chlorophylls at 700-850 nm (Kiang et al. 2007a,b), is the so-called Vegetation Red Edge (VRE). If our eyes could see in the near infrared, plants would be seen as bright and "infrared". The Red Edge is not caused by pigments, but rather by the physical structure of the leaf and might be an evolutionary adaptation to avoid overheating (Gates et al. 1965).

Although the red edge is strong for an individual plant leaf, it is not granted that the signal can be distinguished in a full-planet spectrum. Observations of Earthshine, however, show that the idiosyncratic spectral features of photosynthetic pigments can indeed be revealed due to the vast vegetation coverage of Earth's surface. The rise in reflectivity is obviously weakened (it is typically less than 5%) but yet strong enough to remain a viable surface biosignature. The feature could be stronger for planets with a lower cloud-cover fraction or a larger vegetation coverage. The chlorophyll bump at 500 nm is, intuitively, much more difficult to observe.

It is likely that vegetation on extrasolar planets will be very different from that on Earth. For instance, Kiang (2008) hypothesises the colours and characteristics of extrasolar plants, depending on the temperature of the parent star. Even if the photosynthetic mechanisms were similar to the terrestrial ones, the vegetation red edge could possibly be shifted to different wavelengths (Kiang et al. 2007a,b).

Hence, looking for odd spectral features in the spectrum of scattered light from an extrasolar planet is one of the most promising methods to remotely search for life. But can a similar signal of non-biological origin be disguised as biological? Unfortunately, yes. Some minerals are known to show similar reflectance edges at approximately 750 nm (e.g., Seager et al. 2005). A typical example is that of Jupiter's Io, covered by volcanic sulphur allotropes with a sharp reflectance edge at 450 nm. The albedo of the satellite drastically increases from about 0 to 0.8 going redward this mineral edge (e.g., Spencer & Schneider 1996). So, caution should be taken when interpreting data: additional analyses concerning near IR and mid-IR (5-40 μm) absorption features (typical of most minerals) or atmospheric composition would suffice to rule out these false positives (Seager et al. 2005). It is nevertheless ensuring that the wavelength of Earth's vegetation red edge does not correspond to that of any known mineral (Sagan et al. 1993).

To sum up, the detection of a spectral feature that differs from known atomic, molecular, or mineralogical signatures would be noteworthy, suggesting maybe a biological origin. A concurrent detection of an atmospheric chemical disequilibrium would be even more intriguing.

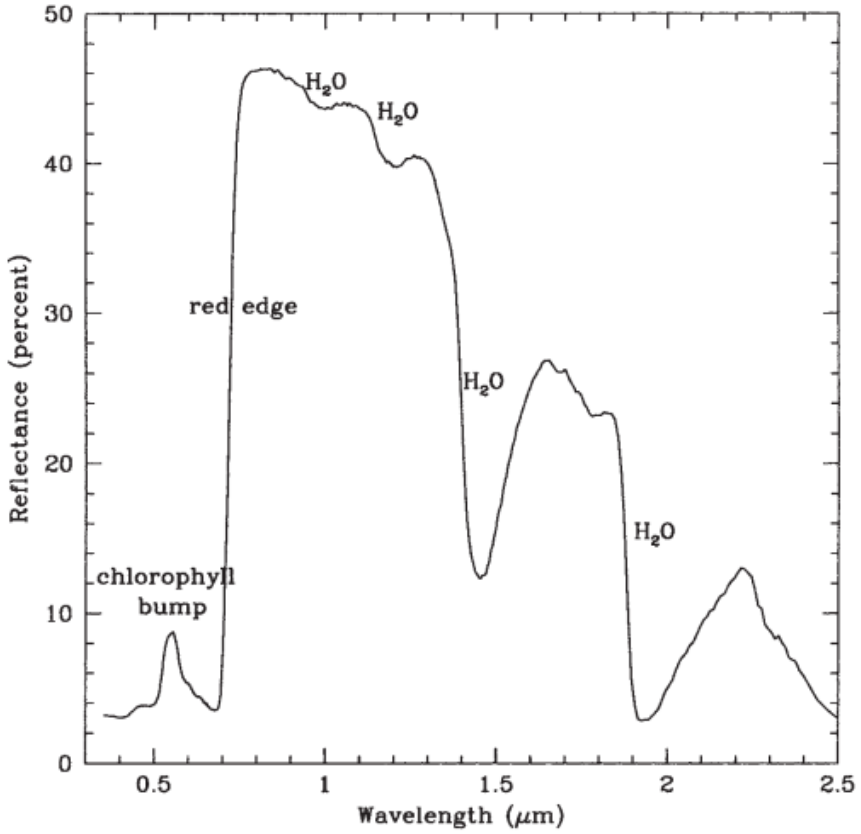

Figure 2.1: Reflectance spectrum of a deciduous leaf (data from Clark et al. 1993). The small bump at about 500 nm corresponds to the minimum of chlorophyll absorption and is the reason for the green colouration of plants. The much bigger bump at ~ 700 nm -the *Red Edge*- is instead related to the physical structure of the leaf. Figure from Seager et al. (2005).

2.4.3 Photometry

A related, but somewhat different, approach to the problem is photometric. Photometry can be thought as an extremely low-resolution spectroscopy, and the comparison of magnitudes of the same object taken in different bands can give a wealth of information about cloud, ice, continent, ocean, and forest cover, as well as the planet's rotation rate (Ford et al. 2001). The power of this approach ultimately stems from the different wavelength dependence of albedos of various surface components.

In addition to this, a time series of photometric data of an Earth-like planet could reveal the existence of weather and seasons. The difference among different images depends on cloud-cover fraction, as a higher cloud cover makes the planet more photometrically uniform and reduces the fractional variability (Seager et al. 2005).

2.4.4 The Earth's spectrum

Studies of Earthshine by Arnold et al. (2002) and Woolf et al. (2002) showed that the VRE is detectable in an integrated Earth spectrum; however, the feature is weak, of the order of 5%. Its

strength depends on many factors, like the ratio between ocean and continents in the hemisphere seen from the Moon, or the instantaneous cloud cover above the vegetation area. Hamdani et al. (2006) proved that the VRE appears larger when a larger continent fraction is facing the Moon. The observations detected also the existence of O_2 and H_2O absorption bands in the red part of the spectrum, and O_3 absorption bands, together with the effects due to Rayleigh scattering -the reason for the blue colour of our planet (Tikhov 1914)-, in the blue part.

The indirect effect of photosynthesis, that is the accumulation of a large amount of O_2, appears therefore easily detectable by a remote observer. O_2 has a strong visible signature, the saturated Frauenhofer A band, at 0.76 μm, visible with low/medium resolution, with a weaker feature at 0.69 μm, observable with high resolution. Since ozone is a photochemical product of oxygen, it is possible to infer the presence of O_2 by looking at the O_3 feature known as the Chappuis band, a shallow triangular dip in the visible (0.45-0.74 μm) or the 9.6-μm O3 band in the IR. The latter, in particular, is highly saturated and thus an excellent qualitative but poor quantitative indicator for the existence of O_2 (Angel et al. 1986; Leger et al. 1993; Kaltenegger 2017). N_2O is detectable at 7.8, 8.5 and 17.0 μm, but only with high resolution (Kaltenegger et al. 2010b).

An interesting thing to notice is that, although life on Earth has been thriving for almost 4 Gyr, spectral signatures changed significantly during the planet history. The Proterozoic Earth offers a striking demonstration of the fact that an inhabited world can completely lack atmospheric biosignatures (Cockell 2014). However, the O_3 band at 9.6 μm starts to be detectable for an O_2 level as low as 10^{-3} PAL (Leger et al. 1993; Segura et al. 2003). Earth's spectrum has shown this feature for more than 2 billion years, and a strong visible signature of O_2 at 0.76 μm for 0.8-2 billion years, depending on the detection sensitivity (Kaltenegger & Selsis 2007). CH_4 is not easily identified using low-resolution spectroscopy for present-day Earth, but its feature at 7.66 μm in the IR could be easily detectable before free oxygen started accumulating in the atmosphere. Varying the orbital distance, gravity, the atmospheric temperature/pressure profile or the cosmic ray flux -affecting chemical reaction rates- can deeply modify the appearance of an inhabited world's spectrum (Grenfell et al. 2007, 2008; Kaltenegger et al. 2010a). Again, *there are more things in heaven and earth than are dreamt of in our philosophy*[1].

2.5 Atmosphere in a test tube

The project "Atmosphere in a test tube", led by the Astronomical Observatory of Padova of the Italian Institute of Astrophysics (INAF) in collaboration with other INAF institutes and the Department of Biology of the University of Padova, intends to provide a database of extrasolar planet atmosphere spectra to interpret data that are going to be gathered by ground-based and space-based new generation instruments.

Its main goal is the study and the simulation of atmospheres of extrasolar planets, by means of a threefold approach:

- measuring the optical characteristics of planetary atmospheres built or modified in laboratory;
- observing the atmospheric modification caused by the biological action of biota, irradiated with sources simulating stars of different spectral type;
- studying the atmospheric alteration induced by photochemistry under a wide range of stellar environments.

[1] adapted from William Shakespeare's Hamlet (1.5.167-8)

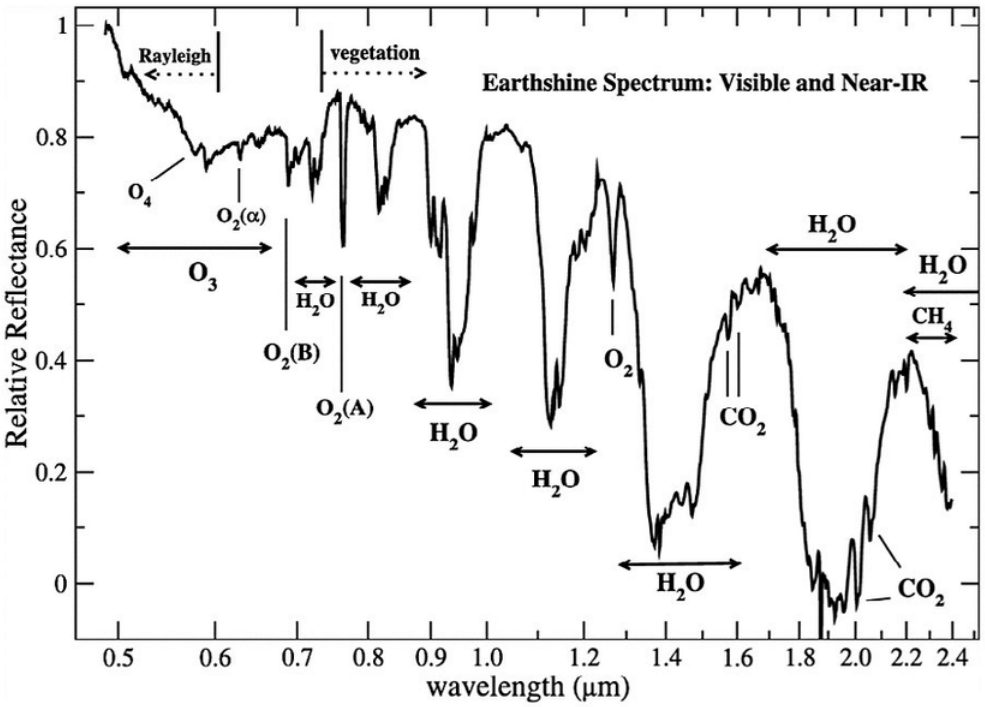

Figure 2.2: Reflectance spectrum of Earth in visible light and NIR, as obtained from Earthshine. Vegetation's footprint is distinguishable through the sharp rise in reflectivity, the *Red Edge*, at about 700 nm. The intensity of the signal increases with the fraction of land in the observed hemisphere. Figure from Turnbull et al. (2006).

An experiment of particular interest for the purpose of this thesis is the study of biosignatures in the simulated warm Earths and super Earths environments through a careful analysis of the effect of the irradiation quality of an M star on the oxygen production of photosynthetic bacteria (Claudi et al. 2016).

The instrument used to carry out the experiment was an environmental simulator composed by a sealed reaction cell. Even though the temperature inside the cell could be raised up to 100 °C or lowered down to -25 °C, biological samples were usually kept at a "comfortable" temperature of about 30 °C. The stellar simulator, an array of 25 different channels with different kind of LEDs, covered a wavelength range between 365 nm and 940 nm, larger than the photosynthetic pigment absorption range typical of the most common photosynthetic bacteria (280-850 nm), and was capable to reproduce the spectra of main sequence F, G, K and M stars.

The two bacteria chosen were *Chlorogloeopsis fritschii* and *Synechocystis PCC 6803*. These organisms usually don't have photopigments capable to photosynthesise the NIR part of the radiation, but the former is able to modify its photosynthetic apparatus in order to adapt to different light conditions if exposed in NIR light conditions, producing chlorophyll d and f. This feature is callen FarLip acclimation.

Analysis of data compared with the growth curves in different light conditions shows that both organisms are able to respond very well to the change from white light to M7 light and continue to grow using the visible part of the M7 spectra, although showing different growth rates. *Chlorogloeopsis fritschii*, having FarLip properties, could also exploit the far red wavelengths of the M-star light, while *Synechocystis PCC 6803* could not. The key result is that terrestrial

organisms are able to adapt and thrive in M-star environments, hence there's no physical obstacle to the possibilities of exploitation of M-star energy output by some kind of extraterrestrial light-harvesting complex.

Future experiments are going to directly lodge bacteria inside the environmental chamber in order to modulate even the gaseous mixture and temperature, possibly creating a database of organisms capable to resist in different planetary conditions. A complementary line of research will focus on the "red edge" feature, trying to understand if pigmentation could be influenced by a radiation spectrum different from the Sun's one.

A subtler question is how the presence of photosynthetic organisms would affect the atmospheric composition of an Earth-like exoplanet in the habitable zone of an M star, having taken into account a whole range of physical, chemical and geological constraints. That's what theoretical models try to assess.

Chapter 3

Is oxygen a good biomarker?

"Do you ever wonder if – well, if there are people living on the third planet?" "The third planet is incapable of supporting life", stated the husband patiently. "Our scientists have said there's far too much oxygen in their atmosphere".

Ray Bradbury, The Martian Chronicles, 1950

In paragraph 2.4.1 we have seen that virtually the totality of molecular oxygen in Earth's atmosphere stems from photosynthesis. It is impressive to acknowledge that oxygen mixing ratios should drop to $\sim 10^{-13}$ at the surface in the absence of a biotic source (Kasting et al. 1979; Pinto et al. 1980; Kasting & Walker 1981; Schindler & Kasting 2000b).

Yet, this fact does not grant *per se* that, under different environmental conditions, oxygen originating from abiotic processes could build up to a detectable concentration. It is crucial to understand when a detection is a false positive and when, instead, it is possible to confidently rule out any abiotic explanation.

Special attention should be devoted to photodissociation of H_2O and CO_2.

3.1 H_2O photolysis

XUV radiation ($\lambda < 200$ nm) is known to prompt intensive heating, ionisation and chemical modification of a planet's upper atmosphere (Yelle 2004; Tian et al. 2005; Penz et al. 2008; Guo 2011; Erkaev et al. 2013; Lammer et al. 2013; Shaikhislamov et al. 2014); this leads to hydrodynamic expansion of the ionised material, which reaches the exobase and comes into contact with the stellar wind flow, that carries it away to space (Khodachenko et al. 2015). In particular, it can photolyse water molecules:

$$\begin{aligned} H_2O + h\nu &\rightarrow H + OH \\ OH + OH &\rightarrow H_2O + O \\ O + O + M &\rightarrow O_2 + M \\ \hline \text{Net reaction: } 2H_2O &\rightarrow 4H(\text{escape to space}) + O_2 \end{aligned}$$

The rate of production of O_2 by photolysis of H_2O is dictated by the rate of hydrogen escape, which can be either energy-limited, meaning that a fixed fraction ϵ_{XUV} of the arriving energy gets

involved in H escape, or diffusion-limited, i.e. limited by diffusion through the homopause at $\sim$ 100 km (Hunten 1973; Walker 1977); while the former regime is typical of planets experiencing a runaway greenhouse, the latter naturally occurs in planets like the Earth, at a rate depending on the total hydrogen mixing ratio in the stratosphere: $f_{tot}(H) = f(H) + 2f(H_2) + 2f(H_2O) + 4f(CH_4) + ...$ (Kasting & Catling 2003). The modern Earth's stratosphere is very dry ($f(H_2O) \sim$ 3–5 ppmv) and reduced gases are also at or below the ppmv level, so the current rate of O_2 production from hydrogen escape is relatively low (Harman et al. 2015). The situation is reversed on planets whose atmospheres have a severe deficiency in nitrogen and carbon, leaving H_2O as their major constituent: they should be identifiable by noticing the absence of $N_2 - N_2$ absorption features (Harman et al. 2015).

Intuitively, planets that lose *a lot* of water can accumulate *a lot* of oxygen in their atmospheres. The classical example is a planet next to the inner edge of the habitable zone that loses its water in a runaway or moist greenhouse (Kasting 1988, 1997, 2010; Wordsworth & Pierrehumbert 2013), i.e. a "Venus-like" world. After hydrogen has escaped, O_2 could plausibly build up to concentrations of tens or hundreds of bars before being eventually absorbed by the planetary surface. For instance, since the equivalent pressure of the vaporised Earth oceans amounts to $\sim$270 bar, this process would provide an Earth twin with a 240 bar O_2 atmosphere. The process acts on timescales that are very short with respect to the system lifespan (a few tens to hundreds Myr, see Schindler & Kasting 2000b), so this kind of detection could be safely ruled out because of the lack of H_2O absorption bands (Harman et al. 2015).

A special case of runaway greenhouse involves planets orbiting M stars. According to Luger & Barnes (2015) (see also Ramirez & Kaltenegger 2014; Tian & Ida 2015), due to the long, highly luminous, pre-main-sequence lifetime of M stars, planets in the habitable zone could lose most or all their water inventory early in their lives, becoming filled with atmospheric O_2. The lack of strong H_2O absorption features would be, in this case, evidence against life (Harman et al. 2015). Other groups, like Hamano et al. (2013), have suggested that planets that start off in a runaway greenhouse state could have their O_2 absorbed by the magma ocean, perhaps removing the possibility of a false positive. However, their line of reasoning does not take into account a later resupplying of water.

Let us focus on this scenario, following Luger & Barnes (2015). The pre-main sequence phase of a M dwarf lasts about 10 Myr for M0 stars and 1 Gyr for M8 stars. The contraction of these stars and the subsequent luminosity decrease causes their HZs to shift inward by up to an order of magnitude. Since M star planets likely form within the first 10 Myr of the system life, most planets in the HZs of MS M stars were inside the inner edge during pre-main sequence. Thus, any initial water inventory is at severe risk of being violently wiped out: a runaway greenhouse is triggered, the stratospheric mixing ratio of water approaches unity and oxygen starts accumulating in the atmosphere, at a rate depending on the XUV flux impacting the atmosphere.

If the stellar XUV flux does not exceed a critical threshold $\mathcal{F}_{crit}$, oxygen does not escape and its accrual rate $\dot{m}_O^{atm}$, regardless of the regime of hydrogen escape, is proportional to the energy-limited mass loss rate $\dot{M}_{EL}$ (Erkaev et al. 2007):

$$\dot{m}_O^{atm} = 8\dot{M}_{EL} = 8 \cdot \frac{\epsilon_{XUV} \pi \mathcal{F}_{XUV} R_p R_{XUV}^2}{G M_p K_{tide}} \tag{3.1}$$

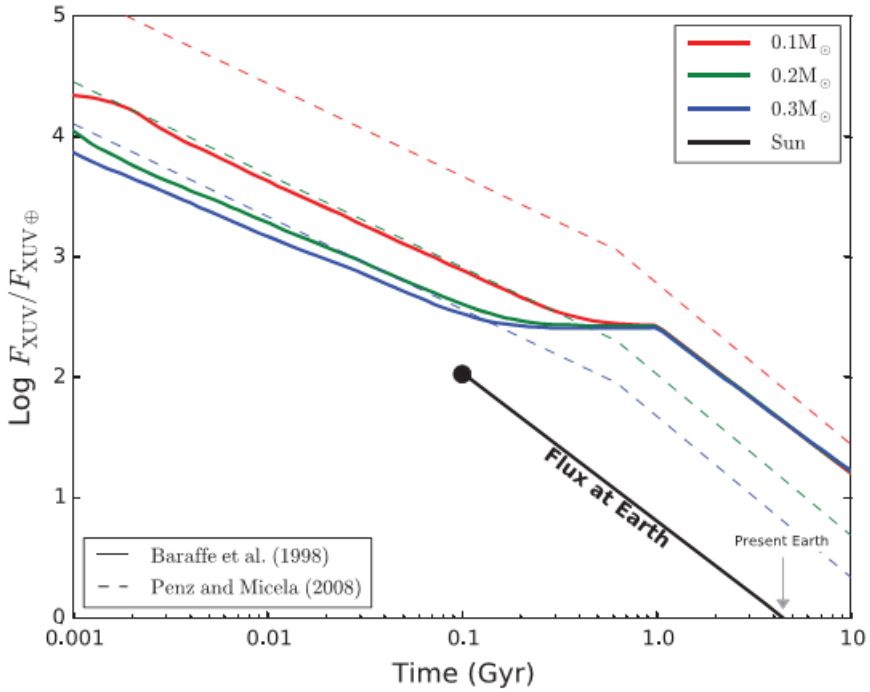

Figure 3.1: Evolution of the XUV flux at the HZ inner edge for 0.1, 0.2 and 0.3 $M_\odot$ stars -according to Ribas et al. (2005) (solid lines) and Penz & Micela (2008) (dashed lines)- scaled to that received by present Earth, $F_\oplus = 4.64 \cdot 10^{-3}$ W m^{-2}. The Sun's flux at Earth in time is shown for reference. Figure from Luger & Barnes (2015).

where M_p and R_p are planetary mass and radius, R_{XUV} is the radius where photolysis takes place (that we can safely equate to R_p) and K_{tide} is a tidal correction that never departs significantly from unity (decreasing with decreasing stellar mass, it is ~ 1 for G-star HZ planets and still ~ 0.88 for a planet at the inner edge of a $0.1M_\odot$ star).

When instead the XUV flux exceeds $\mathcal{F}_{crit}$, the hydrogen flow is so violent that it drags some oxygen with it (hydrodynamical escape), implying a constant rate of O_2 buildup:

$$\dot{m}_O^{atm} = \left(\frac{320\pi G m_H^2 b M_p}{kT} \right) \tag{3.2}$$

depending only on planet mass M_p and flow temperature T. Here, m_H represents the mass of a hydrogen atom, k the Boltzmann constant and b the binary diffusion coefficient for H and O atoms.

Assuming $b = 4.8 \cdot 10^{19}$ (T/K)$^{0.75}$ m^{-1} s^{-1} (Zahnle & Kasting 1986) and an average thermospheric temperature $T = 400$ K (Hunten et al. 1987; Chassefière 1996), it is found that:

$$\mathcal{F}_{crit} := 0.18 \left(\frac{M_p}{M_\oplus} \right) \left(\frac{R_p}{R_\oplus} \right)^{-3} \left(\frac{\epsilon_{XUV}}{0.30} \right)^{-1} \text{W m}^{-2}, \tag{3.3}$$

~ 39 times higher than the current XUV flux impacting the Earth's upper atmosphere. The O_2 buildup rate can reach an impressive 5 bar/Myr for Earth-mass planets and 25 bar/Myr for super-Earths. The destiny of free O_2 depends on the efficiency of O_2 sinks: either the surface undergoes extreme oxidation, removing the totality of free O_2, or the planet develops an atmosphere with

hundreds to thousands of bar of O_2. Both the quantity of H_2O lost and the final O_2 pressure scale with planet mass: it is possible that some recently discovered habitable super-Earths such as GJ 667Cc could have lost $\sim$ 10 TO and built up $\sim$ 2000 bar of O_2 (Figure 3.1). The effect might be somewhat weakened, if a substantial magnetic field is present[1].

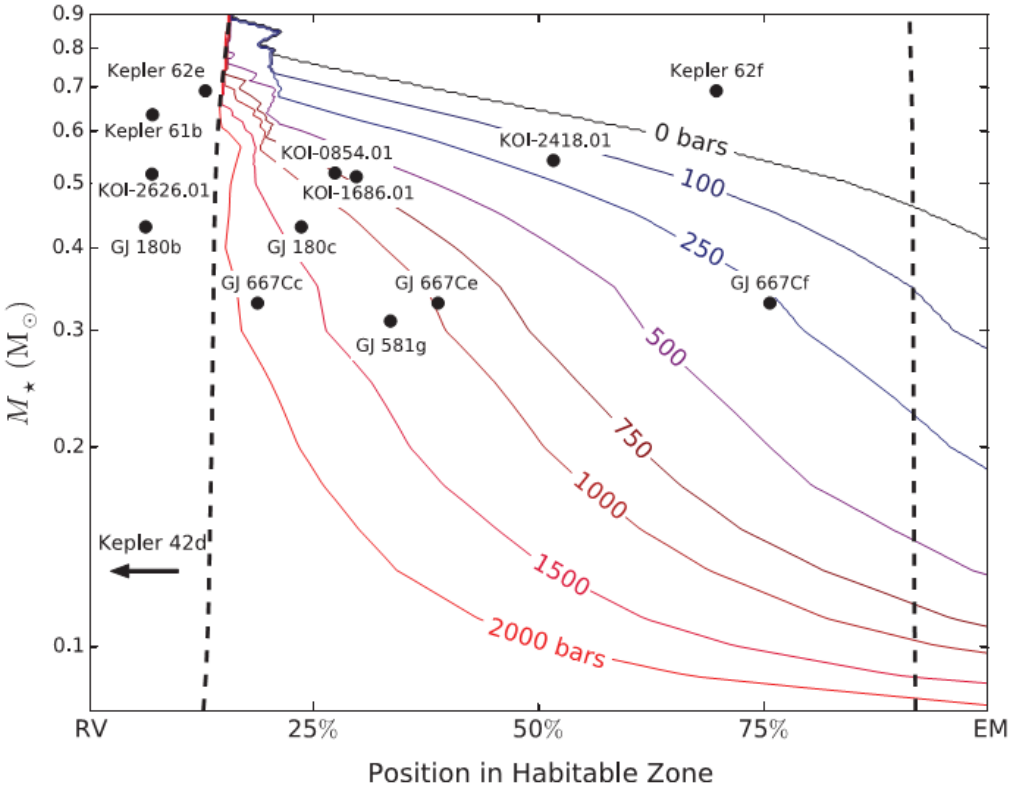

Figure 3.2: Free O_2 atmospheric pressure reached at the end of the runaway greenhouse in known super-Earths, provided that all O_2 remains in the atmosphere. The simulations assumed planet masses of $5M_\oplus$ and initial water reservoirs of 10 Earth oceans. The main sequence habitable zone is bounded by the "runaway greenhouse limit" and the "maximum greenhouse limit" (see Chapter 4 for details). Figure from Luger & Barnes (2015).

Another case of planet able to retain a lot of oxygen is a planet just beyond the outer edge of the HZ, a "Mars-like" world with a frozen surface. Such a surface is not an efficient O_2 sink, so O_2 from photolysis of H_2O can accumulate. Mars itself has $\sim$0.1% O_2 in its atmosphere thanks to this process. Mars' O_2 concentration could theoretically have been even higher but, due to its low gravity, nonthermal processes such as dissociative recombination of ions, i.e. $O_2^+ + e \rightarrow O + O$, give

[1]A bit counterintuitively, since radiation effortlessly penetrates the magnetosphere. However, by affecting the ascending streaming of the induced planetary wind plasma, the magnetic field creates a bubble, disconnecting the stellar wind plasma from the planetary environment and rendering much less effective the loss process. According to a model for Hot Jupiters by Khodachenko et al. (2015), mass loss decreases as a function of magnetic field intensity, approximately according to the expression -fitted to their Figure 13-:

$$\frac{\dot{m}(B)}{\dot{m}(B=0)} = \frac{e^{-\beta B} + 0.15\gamma e^{-\alpha(B-1)}}{1 + 0.15\gamma e^{\alpha}} \tag{3.4}$$

with $\alpha = 0.09$, $\beta = 2$ and $\gamma = 0.3$. A field intensity of 1 G reduces the mass loss by about one order of magnitude.

O atoms sufficient kinetic energy to escape (McElroy 1972). A planet of ~ 2 Mars masses, that is at the same time massive enough to hinder these nonthermal loss processes and light enough not to maintain a high flux of reduced gases from its interior, could accumulate O_2 very effectively. The absence of H_2O in the lower atmosphere of such planets could be confirmed in the future using direct imaging (Harman et al. 2015).

Both the cases illustrated here should not be considered worrisome, provided that the atmospheric composition can be constrained (Schindler & Kasting 2000b; Harman et al. 2015).

3.2 CO_2 photolysis

Photodissociation of CO_2 provides a second path to abiotic O_2 production. FUV radiation can photolyse CO_2:

$$CO + h\nu \rightarrow CO + O$$

Direct recombination of CO with O is slow, however, because it is spin-forbidden. Hence, O atoms recombine with each other to form O_2:

$$O + O + M \rightarrow O_2 + M$$

where "M" is a third molecule, needed to carry off the excess energy from the collision.

This process might potentially bring to an atmospheric buildup of O_2 (Hu et al. 2012). The NUV/FUV ratio is the key parameter affecting the steady state concentrations of CO and O_2 (Tian et al. 2014; Harman et al. 2015), while careful assumptions about oxygen sinks need to be evaluated. See Harman et al. (2015) for a comprehensive discussion on this topic.

Planets orbiting F and G stars are predicted not to produce significant amounts of free O_2 via this process, regardless of the CO_2 concentration in the atmosphere, if outgassing rates of reducing gases similar to Earth's are assumed (Harman et al. 2015)[2]. There's some uncertainty in the models for planets with null or little outgassing rates, with Harman et al. (2015), on the one hand, predicting no detectable O_2 levels and Hu et al. (2012) predicting instead an O_2 mixing ratio as high as 10^{-3} and a O_3 column integrated number density of about 1/3 of the present-day Earth's levels. However, it seems physically implausible to find Earth-like planets with such low outgassing rates, unless they are very old, so we can safely neglect this case.

The situation becomes delicate when looking at planets around K and M stars. Such planets are more likely to accumulate O_2 due to a higher FUV/NUV stellar flux ratio, as compared to the Sun. Planets around K stars are expected on average to reach 10^{-3} PAL, a value comparable to the terrestrial one just after the Great Oxidation Event. The detailed knowledge of sinks is required, so an abiotic explanation of the signal can't be confidently ruled out. The situation for planets around M stars is even worse: according to Tian et al. (2014), a planet with 5% CO_2 and Earth-like volcanic outgassing rates could reach an O_2 surface mixing ratio of $\sim 2 \cdot 10^{-3}$ and, under some conditions, O_2 levels as high as 0.1 PAL. Such high concentration might be avoided, again, on planets with sufficient surface sinks for O_2 (e.g., dissolved ferrous iron in the oceans), or if CO and O_2 react rapidly in solution (Harman et al. 2015).

Planets in which this mechanism is at work should again exhibit weak H_2O features (Selsis et al. 2002; Segura et al. 2007). Future telescope observations, including JWST, should be able to identify CO bands at 2.35 μm or 4.6 μm together with CO_2 at 2 μm or 4.3 μm, hints of strong CO_2 photolysis. Calculations show that CO at 2.35 μm and O_4 (typical of high-O_2 post-runaway atmospheres) at 1.06 μm and 1.27 μm could be seen with an $S/N > 3$ in JWST-NIRISS with just 10 transits (Schwieterman et al. 2016).

[2]F star planets might reach mixing ratios as high as 10^{-3} in the high atmosphere, easily spottable in transit observations (Harman et al. 2015), but have essentially no O_2 at the surface. A high O_3/O_2 ratio is expected, suggesting an "upper" rather than "lower" source of O_2 (Domagal-Goldman et al. 2014)

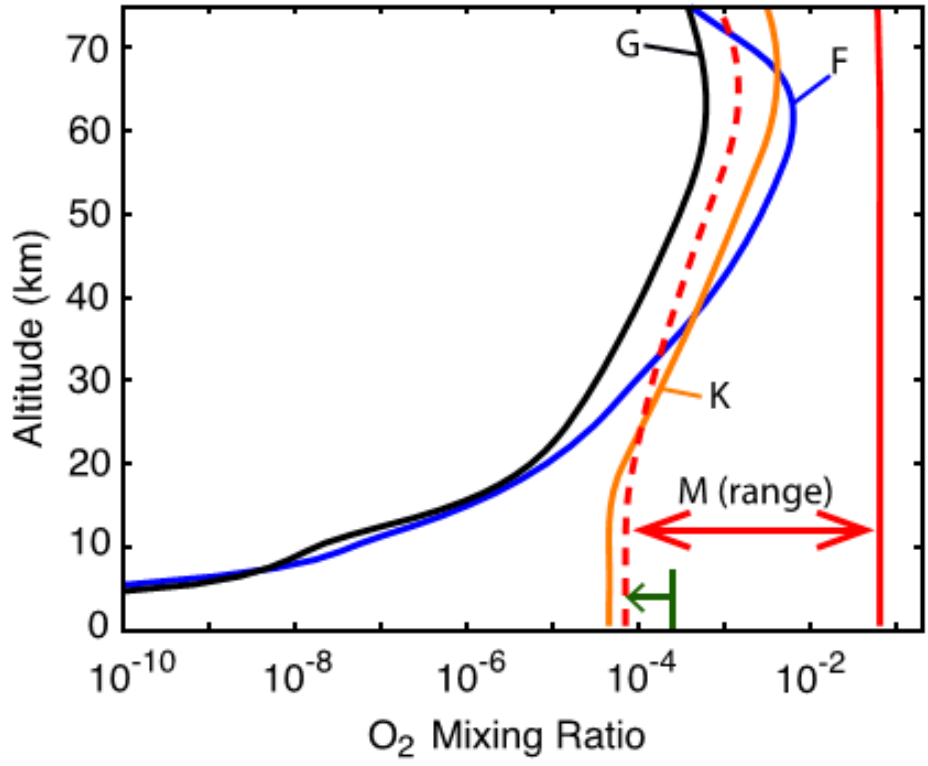

Figure 3.3: O_2 vertical profiles for lifeless planets orbiting σ Bootis ("F"), the Sun ("G"), ϵ Eridani ("K"), and GJ 876 ("M (range)"). Solid curves indicate upper limits on O_2, i.e. when O_2 sinks are small. The dashed curve is the "low-O_2" case for the M-star planet. The upper limit on Proterozoic O_2 from Planavsky et al. (2014) is shown for comparison. Figure from Harman et al. (2015).

3.3 Conclusions

The question of oxygen as a biosignature is complex and has experienced an obstreperous evolution over the last decades. The last developments seem to suggest that:

- abiotic oxygen is not expected to build up in exoplanets orbiting F and G type stars;
- photolysis of water can sometimes produce great amounts of oxygen, but these false positives can be safely ruled out if H_2O spectral features are absent;
- photolysis of CO_2 is negligible for planets around F and G type stars, while it seems an important problem for planets around K and M stars. Seeing O_2 on a planet around these stars is not by itself evidence for life.

What seems to emerge from the big picture is a need for extreme caution in interpreting alluring O_2 detections. Stronger constraints on atmospheric chemistry are desirable to definitely rule out any abiotic explanation. Lovelock (1965) and Lippincott et al. (1967) suggested looking for a double biosignature, i.e. the concurrent presence of O_2/O_3 and a reduced gas like CH_4 or N_2O. This kind of double detection is considered strong evidence for biological activity (Lammer et al. 2009).

Chapter 4

The Habitable Zone

"At the table in the kitchen, there were three bowls of porridge. Goldilocks was hungry. She tasted the porridge from the first bowl. "This porridge is too hot!" she exclaimed. So, she tasted the porridge from the second bowl. "This porridge is too cold", she said. So, she tasted the last bowl of porridge. "Ahhh, this porridge is just right", she said happily and she ate it all up."

Joseph Cundall, Goldilocks and the Three Bears, 1849

From the moment that Galileo, glancing at the chalky stream crossing the night sky, first discovered that *"the Galaxy is nothing else than a congeries of innumerable stars distributed in clusters"*[1], its immensity never ceased to amaze. Recent discoveries have confirmed the long-held suspicion that the Milky Way is literally teeming with planets: thousands of them have been detected by missions like Kepler (cf. Chapter 2), and their number keeps growing. However, many of these rocky worlds are barren wastelands, too hot to sustain life as we know it, whilst many others are, at the other hand, frozen deserts. Just like Goldilocks, astronomers began searching for the conditions that seem to "fit just right" for life to develop and thrive: hence the notion of *Goldilocks zone* or, more formally, *habitable zone*.

4.1 The classical habitable zone

The concept of habitable zone was introduced by Huang (1959, 1960) and is largely employed by space missions aimed at selecting promising astrobiological targets for extensive follow-up observations. Simply put, it is the ring around a main sequence star in which a rocky planet is able to support liquid water on its surface[2] [3]. It corresponds, essentially, to a condition on its

[1] ... "To whatever region of it you direct your spyglass, an immense number of stars immediately offer themselves to view, of which very many appear rather large and very conspicuous but the multitude of small ones is truly unfathomable". *Sidereus Nuncius*, 1610.

[2] The assumption of Earth-like life is implicit in the definition (see Paragraph 2.21 for details)

[3] Curiously, a rough computation of a liquid water zone is already present in Newton's Principia (1667): "Our water, if the earth were located in the orbit of Saturn, would be frozen, if in the orbit of Mercury it would depart at once into vapours. For the light of the sun, to which the heat is proportional, is seven times denser in the orbit of Mercury than with us: and with a thermometer I have found that with a sevenfold increase in the heat of the summer sun, water boils off" (Book III, Section 1, Prop. VIII, Corol. 4).

temperature. Since the flux received by the planet decays as r^{-2}:

$$F(r) = \frac{L}{4\pi r^2} \tag{4.1}$$

Where L is the parent star luminosity, planets closer to their stars are expected to be hotter. The zeroth-order estimate of temperature of a planet defines the effective temperature as the temperature at which the total power received from the star equals the thermal emission of the planet:

$$P_{abs} = \frac{LS_{abs}(1-A)}{4\pi D^2} \tag{4.2}$$

$$P_{em} = S_{rad}\epsilon\sigma T^4 \tag{4.3}$$

$$P_{abs} = P_{em} \iff T = \sqrt[4]{\frac{S_{abs}}{S_{rad}}\frac{L(1-A)}{4\pi\sigma\epsilon D^2}} \tag{4.4}$$

where D is the planet-star separation, σ is the Stefan-Boltzmann constant ($5.67{\cdot}10^{-8}$ W m^{-2} K^{-4}) and the ratio S_{abs}/S_{rad} is taken $\frac{1}{4}$ for a rapid rotator and $\frac{1}{2}$ for a slow rotator (e.g., a tidally locked planet). The albedo parameter A quantifies the fraction of incident radiation that is reflected by the planet; the emissivity ϵ is the ratio between the thermal radiation effectively emitted from a surface and the one emitted from an ideal black body surface at the same temperature.

This straightforward calculation would suggest a provisional way to define the HZ as the region around a star in which the effective temperature is in the range [273.15 K, 373.15 K]. But this line of reasoning is too simple for a series of reasons.

The most important one is evident if suited values for the Earth (A=0.306, $\epsilon = 1$, $S_{abs}/S_{rad} = 1/4$) are inserted into equation (4.4). The computed effective temperature (252 K) is noticeably lower than the globally averaged temperature of the planet (288 K). The difference between model and data ($\Delta T = 36K$) is caused by the greenhouse effect, an additional warming caused by heat absorption by gases like H_2O and CO_2, which are optically thick at most infrared wavelengths. The effect depends sensitively on the atmospheric makeup: on Venus, possessing a 90-bar CO_2-rich atmosphere, it reaches an astonishing $\sim$ 510 K (Sagan 1962). The surprising conclusion is that the effective temperature gives almost no information about the actual temperature of a planet provided with a substantial atmosphere; a detailed chemical analysis of its atmosphere is crucial (Kaltenegger 2017).

Computation of the greenhouse effect is difficult. A commonly used approximation is the following (Hart 1978):

$$\Delta T = ((1 + 0.75\tau)^{0.25} - 1) \cdot T_{eff} \cdot F_{conv} \tag{4.5}$$

where $F_{conv} = 0.43$ is a factor that takes into account atmospheric convection and τ is the optical thickness of the atmosphere, sum of the optical depths of each greenhouse gas. For the Earth, $\tau_{CO_2} = 2.34$ and $\tau_{H_2O} = 0.15$.

Moreover, while the initial makeup stems from the somewhat random mechanisms of planet formation, the chemical evolution of an atmosphere depends sensitively and often in unpredictable ways on the incoming flux and the spectral energy distribution of the parent star. So, we begin to grasp that the problem is far more complex than previously assumed and does not simply involve distance from the host star, although the latter influences and limits the possible mechanisms at work in an atmosphere. Planet habitability should be examined case-by-case, because the kaleidoscope of conceivable planets includes a wide range of atmospheric compositions, due to the stochastic nature of planet formation and evolution.

Although implicitly assumed in the literature, it needs to be underlined that the inner edge boundaries have nothing to do with the boiling point of water. Disruptive effects on the water

reservoir can be triggered, for an Earth-like planet, at a mean surface temperature as low as 340 K (Kasting et al. 1993). Indeed, 1-D climate models (Kasting et al. 1993; Selsis et al. 2007; Pierrehumbert & Gaidos 2011; Kopparapu et al. 2013, 2014) predict that, for a water-rich planet like the Earth, two kinds of habitability limits appear at the inner edge of the HZ: 1) a moist greenhouse limit, where the stratospheric water vapour mixing ratio becomes $> 10^{-3}$, making the planet lose water by photolysis and subsequent hydrogen loss in a few tens to hundreds Myr, and 2) a runaway greenhouse limit, where the thermal radiation flux from the planet reaches its maximum, leading to a rapid and unstoppable surface heating which makes the oceans evaporate (Kasting 1988). Moist greenhouse seems to be the real process endangering habitability, since it occurs at lower incoming fluxes than runaway greenhouse. The reason is that the vertical distribution of water vapour is strongly dependent on temperature. The tropopause, i.e. the top of the convective layer, climbs from 10 km to 170 km as T_{sup} goes from 280 K to 420 K and the mixing ratio of stratospheric H_2O increases from $\sim 10^{-5}$ to ~ 1 (with a steep transition at T_{sup}=340 K). In this situation, the surface H_2O mixing ratio exceeds the critical value of 0.2, making "cold-trapping" of water vapour at the tropopause ineffective (Ingersoll 1969). The upward flow of hydrogen is no more diffusion-limited (Hunten 1973; Walker 1977) and hydrogen produced by H_2O photolysis can rapidly escape to space (Kasting & Pollack 1983). Updated 1-D models for the Sun place the moist greenhouse limit at 0.97 AU and the runaway greenhouse limit at 0.95 AU (Kopparapu et al. 2013).

With regard to the outer edge of the HZ, two critical distances were introduced by Kasting et al. (1993). The "first condensation limit" is the distance at which, keeping a fixed surface temperature of 273 K, CO_2 clouds first start to form; at the time, absent a complete understanding of the radiative effect of CO_2 clouds, these were thought to cool down the atmosphere; recent studies, however, have shown that clouds actually provide a small additional greenhouse effect (Forget & Pierrehumbert 1997; Forget et al. 2013; Kitzmann 2017), leading to relinquishment of the concept. The "maximum greenhouse" limit, still widely used today, is instead the maximum distance at which a cloudless CO_2 atmosphere can maintain $T_{sup} = 273K$. The greenhouse effect, in fact, does not increase monotonically with CO_2 partial pressure: after reaching a maximum value at pCO_2=8 bars, condensation of CO_2 and increased Rayleigh scattering reverse the trend. The limit is encountered at 1.70 AU in the Solar System (Kopparapu et al. 2013).

Complementary to theoretical estimates, two observational estimates of the limits of the HZ can be inferred by looking at the Earth's closest neighbours, Venus and Mars. Geological evidence of surface fluvial features and, perhaps, even large oceans on the currently *red* planet strongly suggests a once more clement and wetter climate (e.g., Craddock & Howard 2002; Ramirez & Craddock 2017) until $\sim$ 3.8 Gyr ago. Being then the Sun's luminosity only $\sim$ 75% of the present one (Gough 1981), the flux on early Mars defines an "Early Mars limit" at 1.77 AU. The apparent contradiction with the more internal maximum greenhouse limit could be solved by invoking the presence of additional greenhouse gases like H_2 or CH_4 (Kasting 1991). The geological absence of any liquid water footprint in the last $\sim$ 1 Gyr of Venus' history defines the "recent Venus" limit. The Sun was only 92% as bright $\sim$ 1 Gyr ago, giving an inner edge at $\sim$ 0.75 AU. Although commonly used in the literature, inferring a conclusion from the absence of evidence against it makes this over-optimistic limit unreliable. The volcanic activity on Venus deeply differs from Earth's, due to an extremely thick lithosphere that is not susceptible to plate tectonics; but, since tectonics acts as an effective way to disperse internally-produced heat, the interior of the planet heats up, until the whole lithosphere sinks inside the mantle during global resurfacing episodes (Herrick 1994; Turcotte et al. 1999). As a result, the surface of Venus carries no signs of its ancient history. A more cautious approach should start from the observation of the very high atmospheric D/H ratio ($> 100\times$ Earth's; Donahue et al. 1982), suggestive of high hydrogen escape and hence of a giant episode of water loss. If such episode happened in the very first phases after formation (Kasting 1988), the lack of oxygen in Venus' present atmosphere could be explained by absorption

by the early magma ocean. According to Ramirez (2018), nearly 500 bars of oxygen ($\sim 2\times$ Earth's oceans) could be removed by the process. This allows to define an "early Venus limit" (Ramirez 2014) at 0.86 AU.

Early studies of long-term climate stability of our planet seemed to indicate a fragile, unstable equilibrium against a runaway greenhouse and a runaway glaciation, emphasising the positive feedbacks of the greenhouse effect and the planetary albedo: the former intensifies with T_{sup} because of increased atmospheric H_2O (Manabe & Wetherald 1967), the latter goes up as T_{sup} decreases because of increased ice and snow coverage (Kasting et al. 1993). On the one hand, according to Rasool & de Bergh (1970), the oceans would have never condensed had Earth been 4 to 7% closer to the Sun; on the other hand, Budyko (1969), Sellers (1969) and North (1975) predicted runaway glaciation had it been 1 to 2% farther from the Sun. Hart (1978) undertook an ambitious simulation concerning the evolution of the Earth's atmosphere, modelling a wide range of physical, chemical and biological processes and including, for the first time, solar evolution. He concluded that the stability strip is extremely narrow, spanning from 0.95 AU to 1.01 AU.

Subsequent studies have shown that these estimates were actually over-pessimistic. What these estimates were neglecting was a strong negative feedback, capable of stabilising planetary climates: the connection between CO_2 levels and surface temperature (Walker et al. 1981), first intuited by Urey (1951). On long time scales ($t > 10^6$ yr), the CO_2 concentration is regulated by reactions with the crust, in a process called *carbonate-silicate cycle*. Carbon dioxide is taken away by weathering of calcium and magnesium silicates in rocks, followed by precipitation and burial of carbonate sediments. The reaction can be summarised as:

$$CaSiO_3 + CO_2 \rightarrow CaCO_3 + SiO_2 \tag{4.6}$$

The process, though acting at a slow pace, is able to remove all the carbon in the atmosphere-ocean system in $\sim$ 400 million years (Holland 1978; Berner et al. 1983). The inverse reaction, pumping CO_2 back in the atmosphere-ocean system, is carbon metamorphism: when the seafloor is subducted, carbonate sediments are subjected to high temperatures and pressures; calcium silicate is reformed, releasing gaseous CO_2 through volcanoes (Kasting et al. 1993). The combination of the two reactions maintains CO_2 concentration in a steady state.

Weathering reactions, occurring at appreciable rate only when liquid water is present, are dependent on temperature, acting thus as a planetary thermostat. For instance, if the Earth suddenly cooled down, rainfall would decrease, causing a decrease in production of carbonic acid, responsible of silicate weathering; this would cause a buildup of CO_2 in the atmosphere, which in turn would strengthen the greenhouse effect, heating up again the planet.

The theory implies that, the more a planet with an active carbonate-silicate cycle is far from its star, the more abundant is expected to be CO_2, until it should become, near the outer edge, a major atmospheric component (Lammer et al. 2009). The CO_2/climate buffer is expected to break down when CO_2 starts to condense (Whitmire et al. 1991), because of increased planetary albedo and reduced lapse time in the convective region of the atmosphere, both rendering the greenhouse effect less effective (Kasting et al. 1993).

The concepts exposed herein epitomise the classical view of the HZ. Although universally adopted in the literature, it is worth mentioning some criticism about the concept. The habitable zone outlined here is, strictly speaking, *the circumstellar region in which a terrestrial-mass planet with an Earth-like atmospheric composition (CO_2, N_2, H_2O) can sustain liquid water on its surface* (Kopparapu 2018). Different atmospheric makeups, the behaviour of physical and chemical processes under unknown environments, coupled to the difficulty of disentangling the pervasive contribution of life to them, deceitfully threaten to make models assessing the issue of planetary habitability strongly Earth-biased (Moore et al. 2017). Instead of getting rid of the concept altogether, it has been moderately suggested (Tasker et al. 2017) to modify terminology by replacing

the term "habitable zone" with a more scientifically accurate "temperate zone", putting the emphasis on stellar radiation (i.e., the real observable) without being at risk of confusing both the scientific community and the general public[4]. Nevertheless, the whole concept should be used, as we know, as a handbook to select targets detected by space and ground-based mission for follow-up observations: keeping this advice in mind, the notion keeps being undoubtedly useful. Future spectroscopic characterisation of exoplanets will prove invaluable, providing a remarkable way to test and put constraints on theoretical predictions. In the last years, ambitious efforts have been undertaken to model planets with different mass, atmospheric composition and stellar environment, in order to get some insight on what may happen on such worlds.

Name	d (AU)	Flux/$F_\oplus$	Author
Inner edge			
Moist greenhouse limit	0.97	1.06	Kopparapu et al. 2013
Runaway greenhouse limit	0.95	1.11	Kopparapu et al. 2013
Early Venus limit	0.86	1.35	Ramirez 2014
Recent Venus limit	0.75	1.78	Kasting et al. 1993
Outer edge			
Maximum greenhouse limit	1.70	0.35	Kopparapu et al. 2013
Early Mars limit	1.76	0.32	Kasting et al. 1993

Table 4.1: Inner and outer edge for the Solar System's HZ according to different models.

4.2 Unearthly worlds

The classical HZ definition assumes that the only greenhouse gases in the modelled planets are CO_2 and H_2O. Indeed, the default atmosphere in most simulations has traditionally been the Earth's. What if other gases are present? The boundaries of the HZ will shift (e.g., Heng 2016). In particular:

- nitrogen (or any other inert molecule) abundance influences the inner edge. Since instability against water loss arises as soon as the ground H_2O mixing ratio exceeds 20%, increasing pN_2 stabilises the atmosphere. Hence, higher pN_2 correlates with wider HZs (Kasting et al. 1993; Wordsworth & Pierrehumbert 2014);
- accrual of SO_2 in a CO_2-rich atmosphere, in case of small photochemical sinks and saturation of the surface, could provide an additional thermostat stabilising the climate, pushing the outer edge further from the star than carbonate-silicate alone would allow (Kaltenegger & Sasselov 2010);
- adding H_2 to an atmosphere greatly influences the outer edge: a 40-bar hydrogen atmosphere would push the outer edge of the Solar System to 10 AU (Pierrehumbert & Gaidos 2011); however, being so light, hydrogen rapidly escapes to space. If a continuous source is lacking, hydrodynamic escape would remove 50 bar of primordial H_2 from a super-Earth HZ planet in just a few million years (Wordsworth 2012). Yet, some 0.3 bar could be sustained in an Earth-like atmosphere through volcanism and would extend the HZ outward by approximately

[4]While the point raised here is undoubtedly sensible, the phrase "habitable zone" is so pervasive in the literature that it will be used in this dissertation too.

30–35% for A to M host stars (Ramirez & Kaltenegger 2017). It is interesting to notice that, according to Ramirez (2017) and Wordsworth et al. (2017), ∼3% H_2 and less than two bars of CO_2 could have ensured warm surface conditions on early Mars; the scenario looks even more intriguing, as measurements from Martian meteorites argue for a highly-reduced early Martian mantle capable of high hydrogen outgassing (Warren & Kallemeyn 1996). Finally, the addiction of H_2 increases the atmospheric scale height, making detection of bioindicators in transit spectroscopy easier (Hu et al. 2012; Seager et al. 2013b). The inner edge is almost unaffected (∼0.1–4%) because H_2 warming is negligible in H_2O-dominated atmospheres (Ramirez 2018);

- methane is characterised by a peculiar duplicity: it acts as a powerful greenhouse gas in planets orbiting stars earlier than a mid-K (4500 K), but it produces a strong anti-greenhouse effect in planets orbiting cooler stars (Ramirez 2018). If CH_4 concentration is 10% that of CO_2, the outer edge can increase by over 20% for the hottest stars (T_{eff} = 10,000 K) and decrease by a similar amount for the coolest stars (T_{eff} = 2600 K). Interesting enough, CH_4 warming could be the solution to the faint young Sun paradox (Kasting 2004). High CH_4 outgassing rates are unlikely, though, unless the mantle is highly reduced (Ramirez 2018).

The importance of the CO_2 cycle has been stressed in the previous section. But, in order to have a strong carbonate-silicate cycle, plate tectonics is thought to be essential, recycling carbon from the surface to the interior of the planet (Kump et al. 2000; Sleep & Zahnle 2001). Changes in tectonic and volcanic activity deeply affect the global climate (Kasting & Catling 2003). It is not clear whether physical limitations to the existence of tectonics, such as "shuts down" as soon certain outgassing rates or atmospheric pressure thresholds are reached, exist (Ramirez 2018). The process may be favoured for planets between one and five Earth masses (Noack & Breuer 2014), until for $M \geq 5M_\oplus$ increased resistive forces under high gravity may reduce subduction tendency (e.g., Noack & Breuer 2014; O'Neill & Lenardic 2007), although there is no general consensus about it (e.g., Valencia et al. 2007). On the other hand, a minimum mass, crucial to avoid rapid loss of internal heat, seems to be required (Sleep 2000; Gaidos et al. 2005; Gaidos & Selsis 2007). Having stressed the complexity of extrapolating our limited knowledge of Earth's geodynamics to different planets, a tentative estimate of a critical mass for tectonic habitability could be 0.3 $M_\oplus$ to achieve a 5 Gyr tectonic lifespan (Williams et al. 1997; Scalo et al. 2007). The existence of a lower geological limit for habitability is not worthless, for the least massive stars could be unable to create planets above this threshold (Scalo et al. 2007).

Worlds with inefficient volcanism, such as stagnant-lid super-Earths (Noack 2014), are characterised by a rigid, nearly immobile lithosphere; no subduction is possible, hence strongly limiting recycling of surface material back into the mantle[5]. Outgassing is strongly limited if pressure and pressure gradient in the uppermost part of the mantle are very high; such conditions can be reached for either large core-mass fractions (iron is denser than silicates, increasing gravity and thus pressure) or for high planet masses ($M \geq 5M_\oplus$). Low-mass planets may not be able to outgas sufficient amounts of greenhouse gases due to a limited reservoir of volatiles in their mantle (Noack et al. 2017). On the other hand, planets with a high radiogenic production and total internal CO_2 budget could maintain temperate and stable climates for billions of years (Foley & Smye 2018). Given that they do not experience plate tectonics – a property detectable by higher pCO_2 than the carbonate-silicate cycle would allow ($pCO_2 \geq 0.1$ bar) (Kasting et al. 1993) –, they are extremely sensitive to the opposite fates of runaway glaciation and runaway greenhouse; hence their HZs are very narrow, like in Hart (1978).

The effect of rotation on planetary climates has been thoroughly examined by Yang et al.

[5]Nevertheless, some kind of surface recycling via burial by lava flows should still possible (e.g., Pollack et al. 1987; Hauck & Phillips 2002; Hirschmann & Withers 2008; Gillmann & Tackley 2014; Lenardic et al. 2016).

(2013a, 2014), who found that slowly or synchronously rotating planets should have a more internal inner edge, because stronger convection on the dayside generates thick and water clouds near the substellar point, increasing the albedo. CAM5 simulations (Bin et al. 2018) quantify the inner edge decrease in $\sim$ 0–19%. In addition to this, it has long been established that changes in the ocean/land fraction influence the global climate (Abe et al. 2011). At the two ends of the spectrum we encounter exotic environments, suggestively dubbed as *ocean* and *desert worlds*.

Ocean worlds, thought to have water envelopes hundreds to thousands of kilometres deep (Grasset et al. 2009; Léger et al. 2004; Sotin et al. 2007) are of great astrobiological interest. A starting point to assess their habitability is the fact that the minimum physical requirements in order for life to emerge must be present:

- building blocks of life;
- catalytically active surfaces;
- an energy source.

The first ones either come from external sources like comets, meteorites or dust particles, or spring from abiotic chemical processes à la Miller–Urey (Miller 1953), from photodissociation chemistry -like in Titan (Khare et al. 1986) or Pluto (Summers et al. 2015). The requirements, if met, occur at the interface between basaltic crust and water shell, where a source of chemical disequilibrium providing the necessary energy for a proto-metabolism can be provided by alteration processes such as serpentinisation. These mechanisms also furnish reduced chemical species, pivotal to generate energy and build the molecules of life (e.g., Russell et al. 2010). With an ice layer blocking the connection between the surface and the ocean, the emergence of life seems implausible (Maruyama et al. 2013; Noack et al. 2016). Moreover, the high pressure at the bottom of deep water–ice layers could also hinder volcanism at the water–mantle boundary, unless plate tectonics exists. Tectonics, by continuously creating new crust, keeps it thin enough to allow considerable upward heat flux, which in turn can lead to temporary melting at the base of the ice layer. The periodic appearance of lower ocean could provide time windows in which life can thrive. To summarise, water-rich planets that are the best candidates for the origin and evolution of life are planets with a shallow ocean (up to several tens to hundreds of kilometres), a low planet mass, or a high surface temperature (that still allows for existence of biomolecules). A shallow ocean also favours the existence of long-term volcanism, and thus leads to more life-friendly conditions at the ocean floor. While planets with less than one Earth mass can be habitable even if possessing substantial amounts of water, super-Earths can conversely only be considered as habitable planets, if they contain a low water percentage by weight (Noack et al. 2016).

Desert worlds, i.e. planets with an extremely low water content, possess wider habitable zones than the classical one: at the inner edge, their weak H_2O greenhouse effect enhances thermal infrared emission to space and creates a dry stratosphere, which limits water vapour photolysis and subsequent H escape to space. At the outer edge, land planets better resists global freezing because there is less water for clouds, snow, and ice, the elements triggering the positive ice-albedo feedback (Abe et al. 2011).

A key factor controlling the width of the habitable zone is the planet's mass. Assuming a H_2O-dominated atmosphere at the inner edge and a CO_2-dominated one at the outer edge and scaling the N_2 partial pressure with planetary radius, Kopparapu et al. (2014) have shown that larger planets have wider HZs than smaller ones, with the inner edge moving inward because of smaller H_2O column depth, requiring higher temperatures to trigger a moist greenhouse. The outer edge is instead more or less unaffected, thanks to the balancing effects of increased greenhouse effect and increased albedo. Super-Earths can sustain and retain thicker atmospheres than the Earth. While on Earth thermal and non-thermal escape are significant just for H and He, the smaller Mars

also loses C, N and O at large enough rates to impoverish its atmospheric supply over geological time (McElroy 1972), as recently confirmed by data from the MAVEN mission (Jakosky et al. 2015; Brain et al. 2015; Cui et al. 2019). This fact suggests that, in order to efficiently preserve its atmosphere over time, a planet should be several times more massive than Mars. A pivotal role in determining the sensitivity to non-thermal escape belongs to magnetic fields (Tian et al. 2009), even though the strength required to shield the atmosphere from early stellar activity is not known (see, e.g., Grießmeier et al. 2009; Lammer et al. 2011; Tian et al. 2014). In order to power a magnetic field, an iron core, an adequate rotation speed and elevated heat fluxes at the boundary between mantle and core are needed (e.g., Stevenson 2003), and plate tectonics might be necessary to fulfil the last requirement (Elkins-Tanton & Seager 2008; Barnes et al. 2009; Stamenković et al. 2012): more massive planets are generally expected to possess stronger fields. Both tectonic activity and the internal dynamo last longer for larger planets, for their lower surface/volume ratio increases the cooling time of the interior: Earth is still geologically active, whereas Mars has been geologically dead for perhaps 2 billion years and devoid of a magnetic shield for ~ 4.1 Gyr (Acuña et al. 1999; Lillis et al. 2013)

According to a certain line of thinking (e.g., Heller & Armstrong 2014), some worlds can be characterised by even more favourable conditions for life than those present on Earth. Examples of "superhabitable worlds" would encompass slightly bigger, more massive, more water-rich, warmer and older planets.

This exciting new field of planetary modelling is on the verge of encountering actual data coming from next-generation instruments. Their meeting will prove valuable to test and constrain models, letting astronomers get a glimpse of the mechanisms shaping the exquisite diversity of planetary systems.

4.3 Non-solar stars

The models of the habitable zone have been traditionally developed based on the Solar System; hence, attempts have been made to extrapolate the results to other kinds of stars, in order to provide a more comprehensive picture of the matter of habitability[6].

Since the stellar flux on the top of a planet's atmosphere, the key parameter determining atmospheric equilibrium and evolution, is given by:

$$F = \frac{L}{4\pi d^2}, \tag{4.7}$$

a fourfold increase in luminosity L must be accompanied by a twofold increase of the orbital distance d in order to keep F costant. This fact allows us to define a simple scaling law:

$$d = 1 \text{ AU} \cdot \left(\frac{L/L_\odot}{S_{eff}} \right)^{0.5} \tag{4.8}$$

(Kasting et al. 1993), where S_{eff} is the flux that corresponds to the distance of interest (i.e., the inner edge) in our Solar System. However, the wavelength dependence of the interactions between matter and radiation suggests that, alongside the integrated flux, the stellar energy distribution of a star should play an important role in atmospheric warming (e.g., Kasting et al. 1993; Kopparapu et al. 2013). Indeed, keeping S_{eff} constant, a redward shift of the peak of the stellar Planckian, i.e. considering a less massive star, results in a more efficient heating, because 1) Rayleigh scattering

[6]The focus will be put, as usual, on single stars. The question of habitability around binary stars is complicate, as unusual dynamical and climatic constraints need being used at once. Kasting et al. (1993) estimates that $\sim 5\%$ of external binaries and $\sim 50\%$ of internal binaries could possess habitable planets in stable orbits.

is weaker at longer wavelengths ($\propto \lambda^{-4}$), and 2) molecular absorption is stronger in the near-infrared than in visible light (Kasting et al. 1993). Therefore, planets around cool K and M stars are warmed more efficiently than G-stars companions, which in turn show more absorption than planets orbiting warm F and A stars. A widely used correction to the value of S_{eff} to be inserted in equation (4.8) is given by the following parametrisation:

$$S_{eff} = S_{sun} + a \cdot T^* + b \cdot T^{*2} + c \cdot T^{*3} + d \cdot T^{*4} \tag{4.9}$$

(Ramirez 2018), where T* is the difference between the stellar and the Sun's effective temperatures, and S_{sun} the flux relative to the distance of interest for the Sun.

At the inner edge, the critical value for S_{eff} triggering a runaway greenhouse increases by $\sim$ 30% for an F0 star and decreases by $\sim$ 30% for an M0 star; the critical flux for a moist greenhouse changes by $\sim$ +10% and $\sim$ 10%, respectively. At the outer edge, the maximum greenhouse limit modifies by $\sim \pm$30% (Kasting et al. 1993), where again the increase refers to the F0 star, the decrease to the M0 star, and occurs at higher CO_2 pressures for cooler stars ($\sim$ 20 bars for an M8; Ramirez 2018).

When the stabilising effect of the carbonate-silicate cycle is weakened because of low volcanic outgassing rates, oscillations between fleeting ice-free and protracted globally glaciated conditions, known as "limit cycles", should occur (Tajika 2007). Since the planet's albedo, due to the same two reasons exposed with regard to atmospheric warming, is higher for an F0 parent star and lower for M0 star (Kasting et al. 1993), planets around F-stars are the most vulnerable to the positive ice-albedo feedback, hence to limit cycles (Shields et al. 2013), while M-stars might have a somewhat larger outer edge than 1D models predict (Turbet et al. 2017).

The effect of stellar mass on habitability is far more pervasive than simply moving the position of the habitable zone: on the one hand, the luminosity evolution of stars results in a shift of the HZ over time (see paragraph 4.4 for details); on the other hand, the lifetime of the star itself poses an upper limit on the time available for life to emerge and thrive. It is interesting to notice that microbial life arose no later than about 500 Myr after Earth's formation, while complex, multicellular life employed almost 4 Gyr to appear (Jiang et al. 2011; Schiffbauer et al. 2012). Since the main sequence lifetime is approximatively related to stellar mass according to the relation:

$$t_{MS} \propto \left(\frac{M}{L}\right) \propto M^{1-\alpha} \tag{4.10}$$

where $\alpha = 4$ for $M \in [0.43M_\odot, 2M_\odot]$, $\alpha = 3.5$ for $M \in [2M_\odot, 55M_\odot]$ (Salaris & Cassisi 2005), earlier stars than F class probably evolve too fast ($t_{MS} < 2$ Gyr) to allow complex life to develop. This is not a great limitation, though, since the initial mass function favours late type stars with respect to early type stars, and $\sim$ 75% of our Galaxy's stars are estimated to be M-type dwarfs (Henry 2004). Thus, it is no mystery that M-star planets are seen as an appealing target for the search for life.

A problem arising for stars later than $\sim$ K3 is that, given the strong dependence on distance of tidal forces ($\propto r^{-3}$), habitable planets dangerously become at risk of tidal locking (Cuntz & Guinan 2016). The tidal radius:

$$r_t = 0.0027 \left(\frac{P_0 t}{Q}\right)^{1/6} M^{1/3} \tag{4.11}$$

is the radius inside which an Earth-like planet in a circular orbit around a star of age t would be tidally-locked. P_0 is the original rotation period of the planet, Q a planet-specific factor quantifying energy dissipation, M the stellar mass (Peale 1977; Kasting et al. 1993). Comparing

it with the distance of the inner edge:

$$r_{ie} = 1 \text{ AU} \cdot \left(\frac{L/L_{\odot}}{S_{eff,ie}} \right)^{0.5} \propto L^{0.5} \propto M^{\alpha/2} = M^2 \tag{4.12}$$

where $\alpha = 2$ for less massive stars than the Sun, we see that, with lower and lower M, at some point $r_{ie} < r_t$.

The consequence would be a preference for the very common late-G and early to mid-K stars as preferred targets for the search of life (Kasting et al. 1993). However, tidal locking can be avoided in planets around stars up to M0 if equipped with a 1-bar atmosphere, up to M3 if provided with a ∼10 bar envelope (Leconte et al. 2015). Tidal-locking does not rule out habitability, but it may obstruct the existence of a planetary dynamo (e.g., Cuntz & Guinan 2016). A more extensive discussion on the question of M-star system habitability will be presented in paragraph (4.5).

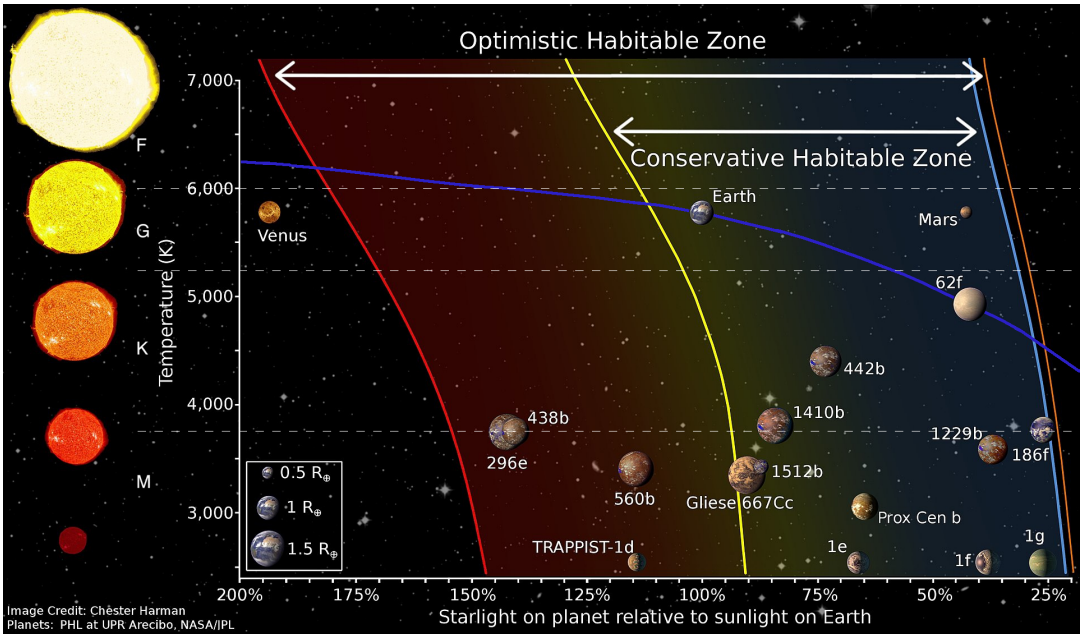

Figure 4.1: Boundaries of the habitable zone for stars of different spectral class. The red and orange lines (*recent Venus* and *early Mars*, respectively) delimit the optimistic HZ, while the yellow and sky blue lines mark the conservative HZ, adopting the *runaway greenhouse* and the *maximum* CO_2 *greenhouse* as limits. The distance d=1 AU (blue line) has been plotted to put the HZ sizes into perspective. Some of the most promising known exoplanets are shown too. Adapted from Chester Harman.

4.4 The continuous habitable zone

Having obtained an estimate of the orbital range in which a planet might be able to sustain liquid water on its surface, a subtler issue needs being considered. Stars brighten throughout their main sequence evolution (Hoyle 1958) and undergo dramatic luminosity variations before and after the main sequence. Consequently, the main sequence habitable zone, linked to the stellar flux and the spectral energy distribution, moves outward over time (see, e.g., Villaver & Livio 2007; Danchi & Lopez 2013; Rushby et al. 2013; Luger & Barnes 2015). On the one hand, planets that are born

frozen could be later cold-started by a luminosity increase (Kasting et al. 1993); on the other hand, planets that are currently in the HZ can cross the inner edge at some point in future. Our own Earth is destined to experience a moist greenhouse in 1 Gyr which will vaporise the oceans (Ward & Brownlee 2004), dooming complex life to total extinction (Lovelock & Whitfield 1982)[7]. Hence, a particularly useful concept has been defined: the continuous habitable zone (CHZ), namely the circumstellar region that has been habitable throughout the whole system lifespan.

Given that the Sun's luminosity at the start of the MS was $\sim 70\%$ of its present value (Gough 1981), the outer edge of the CHZ can be computed through equation (4.8), yielding: d=1.39 AU (maximum greenhouse limit) and d=1.48 (early Mars limit) (Kasting et al. 1993). If the CHZ is not null, its inner edge must correspond to the present one. The width of the CHZ around a star is strongly dependent on t_{MS}: for the Sun, it is roughly 0.5 AU. A more massive star gets through the stages of its evolution at a faster pace, so it possesses a CHZ for shorter times. Conversely, the slow luminosity evolution of K and M stars ensures the presence of a stable HZ for several to tens of Gyr. A second variable influencing the CHZ is metallicity: stars with higher metallicity have a slower evolution, hence their habitable planets will dwell longer in the HZ (e.g., Danchi & Lopez 2013).

Another issue worth mentioning is what happens before and after the MS phase: after a protostar is born, it experiences gravitational collapse under its own weight, until the onset of nuclear reactions in the core makes it settle in the MS. During this pre-MS evolution the stellar luminosity decreases, thus the HZ at the beginning of the MS is more internal than the pre-MS HZ (Kaltenegger 2017). The pre-MS duration strongly depends on stellar mass, lasting up to 2.5 Gyr for some M stars. This could on the one side raise the question of pre-MS HZ habitability (Ramirez & Kaltenegger 2014), on the other side put at risk the later MS habitability because of long-lasting severe conditions during pre-MS troubling the wannabe habitable planets. The same late-type stars, once leaving the main sequence, can spend billions of years (9 Gyr for an M1 star) in the post-MS phase, making planets in their post-MS HZs the last stronghold for life in the distant future of the Universe (Ramirez & Kaltenegger 2016).

4.5 The case of M stars

Ascertaining which planetary systems offer the highest likelihood of hosting worlds amenable to life, alongside the environmental conditions which most affect long-term habitability, is one of the ultimate goals of exoplanetary astronomy.

We have seen that, due to their enormous abundance and their prolonged lifespan, implying a very stable habitable zone, M stars[8] look very promising from an astrobiological point of view. Indeed, more and more attention has been put upon these stars over the last decade: 3000 out of the 150,000 stars forming the Kepler sample were M stars, and about 200 exoplanets, many of which in the HZ, have been detected around them (e.g., Anglada-Escudé et al. 2013; Quintana et al. 2014); even a greater number has been found by instruments employing radial velocity, transits and gravitational microlensing, and more of them are expected to be found with the début of next-generation telescopes. Astrometric data from GAIA will aid both to directly detect a handful of giant planets around M stars (Sozzetti et al. 2013) and to calibrate radii and distances of known M stars (Bailer-Jones 2005), thus increasing the precision on planet size estimates. NASA's TESS mission, due to its typical 27-day observing window, exhibits a strong bias toward short period planets (Sullivan et al. 2015): 75% of the newly-discovered small worlds

[7]The last niches of unicellular life could last up to 2.8 Gyr (O'Malley-James et al. 2014).

[8]When referring to "M stars", we will always refer to main sequence M stars, the so called *red dwarfs*. M-type supergiants like Antares and Betelgeuse are extremely massive stars that are born and die in a few Myr: a blink of an eye, astronomically speaking.

are expected to be hosted by M stars (Sullivan et al. 2015), hence qualifying M stars as preferred targets for atmospheric characterisation by the James Webb Space Telescope. Finally, PLATO will be able to perceive transits even beyond the snow line (Rauer et al. 2014). Ground-based spectrographs like MINERVA-Red (Blake et al. 2015), SPIRou@CFHT (Étienne Artigau et al. 2014), CARMENES@CAHA (Quirrenbach et al. 2012), Habitable Planet Finder@HET (Mahadevan et al. 2010), CRIRES+@VLT (Dorn et al. 2014), NIRPS@La Silla (Wildi et al. 2017) are expected to join this collective effort.

Interestingly enough, planets in the HZ of are easier to detect for M stars because decreasing stellar mass implies higher M_{planet}/M_{star} and R_{planet}/R_{star} ratios, resulting in 1) stronger transit signals[9]; 2) augmented transit probability because of closer orbits[10]; 3) increased radial velocity signals[11]; they are particularly befitting atmospheric characterisation via transmission spectroscopy (e.g., Kreidberg et al. 2014); finally, they are more prone to exhibiting strong bands of biogenic N_2O, CH_3Cl and CH_4 (Scalo et al. 2007; Rauer et al. 2011), because the lower ultraviolet flux from quiet M stars implies longer biosignature lifetimes and thus, fixing the production rate, higher equilibrium concentrations (Seager et al. 2013a).

Recent exoplanet detections around M stars have shown that their planetary systems tend to be closely-packed, with a scarcity of gas giants (2-4 times fewer than around G stars, see Johnson et al. 2007) and a prevalence of rocky planets in the range [1.0–2.8] $R_\oplus$ (3.5 times more common than around F, G and K stars, Mulders et al. 2015), one third of which in the habitable zone (Shields et al. 2016). Estimates yield a ∼40% occurrence of multiple-planet systems (Rowe et al. 2014); an astounding example of it is Trappist-1, an M8 star with its brood of seven rocky planets (Gillon et al. 2017). These facts seem to point to the existence of different mechanisms at work during planet formation around such small stars (Shields et al. 2016).

However, when talking of M star worlds, a whole bunch of environmental problems comes into view, requiring an extremely careful consideration in order to assess their habitability. The aforementioned high occurrence of closely-packed, multiple-planet systems implies a high probability of dynamical interactions inside these systems, whose consequences for planetary habitability need being examined (e.g., Shields et al. 2016). A larger planetary obliquity increases seasonality (Ward 1974; Williams & Pollard 2003; Dobrovolskis 2013), possibly expanding the habitable surface fraction (Spiegel et al. 2009) and acting against the danger of global glaciation (Spiegel et al. 2010; Armstrong et al. 2014). High-eccentricity planets suffer from a strong temperature range between apoastron and periastron (Bolmont et al. 2016), possibly endangering habitability (Barnes et al. 2008). Tidally-induced heating in the interiors of such planets is a double-edge sword: it could enhance habitability, by extending the lifespan for plate tectonics on small planets (Barnes et al. 2008; Jackson et al. 2008), but also lead, especially around $M < 0.3M_\odot$ stars, to a Venus-like runaway greenhouse state (Barnes et al. 2013) or to a Io-like magma ocean world (Driscoll & Barnes 2015).

A serious concern stems from the consideration that, lying the HZs of M stars so close to their host stars, planets are probably tidally locked, like the Moon with respect to the Earth (cf. Equation 4.12). This should imply a huge temperature difference between the dayside and the nightside, in a similar fashion to what we observe on Mercury (Chase et al. 1976). If the nightside gets cold enough, the atmosphere start condensing on the surface, leading to a rapid depletion of the whole gaseous reservoir; it is necessary, therefore, a strong enough heat flux from the dayside to maintain the nightside above the freezing point of the main atmospheric components. Haberle et al. (1996) with a 1-D model and later Joshi et al. (1997) with a more advanced 3-D

[9] 1.3 mmag for an Earth transiting an M4V star, 0.084 mmag in front of a Sun-like star (Charbonneau & Deming 2007).

[10] 1.5% for an M4V star, 2.7% for an M8V, 0.48% for the Sun (Charbonneau & Deming 2007).

[11] However, radial velocity detections should be taken with extreme caution, since the typical rotation period of M stars overlaps with the HZ orbital period (Newton et al. 2016; Vanderburg et al. 2016).

model showed that a $\sim$ 1-1.5 bar CO_2 atmosphere is dense enough to avoid such a scenario[12]. Subsequent studies (Joshi 2003; Wordsworth et al. 2010; Edson et al. 2011; Yang et al. 2013b; Yang & Abbot 2014; Hu & Yang 2014; Cullum et al. 2014) have confirmed that winds and ocean currents could provide an efficient heat transport system, with wind speeds that do not exceed 10 m s^{-1} even at the terminator (Joshi et al. 1997).

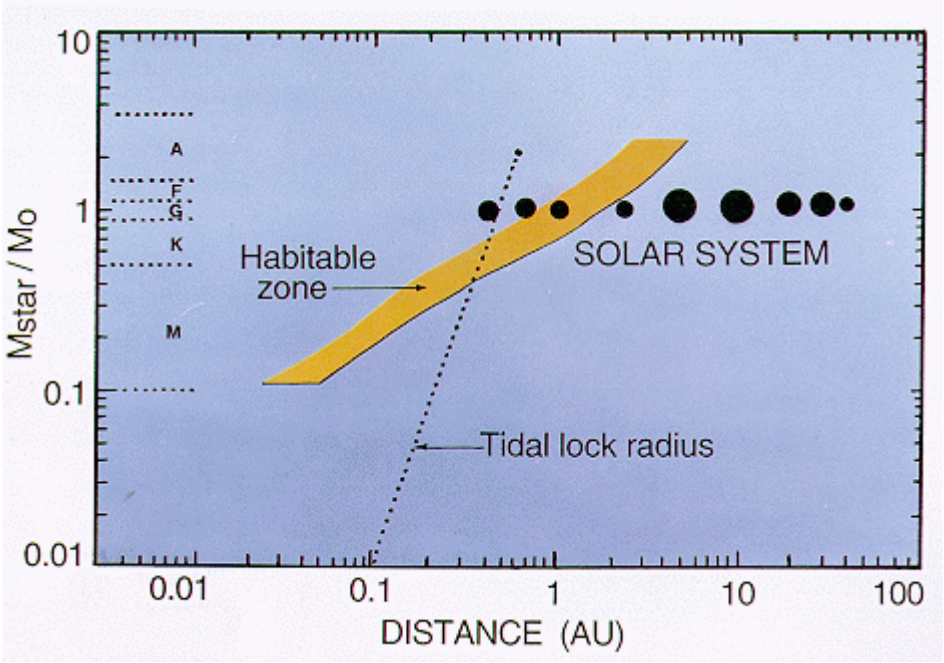

Figure 4.2: The tidal lock radius plotted here is the radius inside which an Earth-like planet in a circular orbit around its star would end up in synchronous rotation in $t \leq 4.5$ Gyr because of tidal damping. The process becomes more and more significant for HZ planets as the stellar mass decreases. Figure from Kasting et al. (1993).

Even if tidal locking does not directly put in trouble the atmosphere survival, yet it endangers it indirectly. Slow rotation hinders the onset of a strong magnetic field: Grießmeier et al. (2005), applying scaling laws for the magnetic dipole moments taken from different theoretical models (Busse 1976; Stevenson 1983; Mizutani et al. 1992; Sano 1993), estimated the magnetic moment $\mathcal{M}$ of a tidally locked Earth-like planet orbiting a 0.5 $M_\odot$ star at 0.2 AU as $0.022\mathcal{M}_\oplus < M < 0.15\mathcal{M}_\oplus$; the atmosphere is left almost defenceless against the activity of the perilously close star[13]. The intense stress on the atmosphere, especially in the first, turbulent phases of stellar life, may strip it completely, unless it is replenished in some way when the star enters a quieter state (Lammer et al. 2009).

In fact, in addition to the usual, black-body emission, M stars are characterised by strong non-Planckian emission, caused by the activity of the chromosphere that drains energy from the stellar interiors. This activity can take the form of variations of the star luminosity due to stellar

[12]Similar pressures, incidentally, are capable of sustaining large oceans on an Earth-like planet in the HZ (Joshi et al. 1997)

[13]A planet's magnetic field acts like a shield for the upper atmosphere, protecting it against stellar wind. While its presence on Earth fends the charged solar wind particles at a safe distance of $10R_\oplus$ (Khodachenko et al. 2007; Lammer et al. 2007), its absence on Mars enables them to dive to the roiling depths of Martian atmosphere (up to 270 km from the land; Lundin et al. 2004), dramatically enhancing non-thermal atmospheric loss.

spots, recurrent flares, coronal mass ejections, stellar cosmic rays, strong coronal X-rays and chromospheric UV emission (Ayres 1997; Gershberg 2005; Scalo et al. 2007). Many observations of clusters have shown that late-type stars slow down their rotation according to the expression:

$$P_{rot} \propto t^{-1/2} \tag{4.13}$$

(e.g., Skumanich 1972; Newkirk 1980; Soderblom 1982; Ayres 1997) because of angular momentum loss. A strong correlation exists between P_{rot} and the activity level (Wilson 1966; Kraft 1967). Hence, younger stars are more magnetically active, show a stronger X and UV emission and expel large flares (e.g., Keppens et al. 1995; Ribas et al. 2005). Moreover, the fraction of magnetically active stars increases with later spectral type, probably because of longer and longer activity lifetimes (West et al. 2008; Mirzoyan 1990; Stauffer et al. 1991).

A planet in the HZ of an M star faces a coronal X-ray flux 10^3 - 10^4 stronger than Earth's during non-flaring states and 10^5 - 10^6 during flares (Scalo et al. 2007). X-rays and EUV radiation hit the upper layers of the atmosphere, i.e. the thermosphere, heating it to high temperatures and enhancing thermal and nonthermal atmospheric loss rates (Scalo et al. 2007), especially considering the longer duration of EUV activity with respect to G stars[14] (Allard et al. 1997). If Proxima Centauri b had an Earth-like atmosphere, its escape time would be as short as 10 Myr (Airapetian et al. 2017). Even if the atmosphere does not completely disappear, the surface may be totally sterilised like the present Martian surface (e.g., Pavlov et al. 2002).

Stellar wind, whose dynamic pressure could exceed by orders of magnitude that of the Sun (Garraffo et al. 2017), constitutes an additional forcing on the planet, ionising, heating, chemically transforming and gradually eroding the atmosphere (Kulikov et al. 2007; Lammer et al. 2008; Tian et al. 2008). However, it must be kept in mind that the Earth managed to endure during the first 100 Myr of the Sun's main sequence a XUV (0.1-120 nm) flux ∼100 times stronger and a solar wind 100-1000 times denser than today, and a XUV flux still ∼ 6 times stronger than today as late as 3.5 Gyr ago (Ribas et al. 2005). Planets around M stars, though, have to face similar harsh conditions for longer times (Shields et al. 2016).

The active photosphere produces starspots much larger (in %) than the Sun's, causing luminosity reductions up to 40% for several months (Rodono 1986) which, according to Joshi et al. (1997), can result in a 40 K decrease in surface temperature. Flaring events, whose intensity and duration is extremely irregular (Kunkel 1969; Pettersen & Coleman 1981; Giampapa & Liebert 1986; Worden et al. 1984), can sometimes reach an appreciable fraction of stellar dimension (Osten et al. 2005; Güdel et al. 2004) and luminosity. Mostly typical of young stars, they decay with a 1 Gyr e-folding time (Stauffer & Hartmann 1986; Demarque et al. 1986) as rotation slows down due to stellar winds (Heath et al. 1999). The frequency of energetic flares increases with higher $log(L_X/L_{bol})$ (Audard et al. 2000)[15], while the differential frequency N of events is related to its peak or total energy E via a power law:

$$N(E) = aE^{-x} \tag{4.15}$$

where $x = 2 \pm 0.4$ (Gershberg & Shakhovskaia 1983; Audard et al. 2000). Flares more energetic than 10^{25} J, the strongest solar flare ever recorded (Haisch et al. 1991; Woods et al. 2004), can

[14]For Sun-like stars, according to Ribas et al. (2005), the XUV flux (0.1-120 nm) at an orbital distance d evolves in time through:

$$F_{XUV}(t) = \begin{cases} 2.97 \cdot 10^{-2} \cdot t_0^{\beta} \cdot \frac{L_{star}}{L_\odot} \left(\frac{d}{1AU}\right)^{-2} \text{W m}^{-2} & t \leq t_0 \\ 2.97 \cdot 10^{-2} \cdot t^{\beta} \cdot \frac{L_{star}}{L_\odot} \left(\frac{d}{1AU}\right)^{-2} \text{W m}^{-2} & t > t_0 \end{cases} \tag{4.14}$$

where $\beta = -1.23$ and $t_0 = 100$ Myr. The expression holds for K and M stars too, but the latter have a longer $t_0 = 1$ Gyr.

[15]During the saturation phase $L_X \sim 7 \times 10^{21}$ W, then it decreases according to (4.14) (Ribas et al. 2005; Lammer et al. 2009; Luger & Barnes 2015).

take place up to 10 times per day for some M stars. During these flares the UV flux in the range 200-300 nm, usually at least an order of magnitude below the one on Earth, can temporarily exceed up to ten times the Sun's (Scalo et al. 2007). The consequence of such energetic, frequent and unpredictable events could be an atmospheric chemistry constantly out of equilibrium, since the recovery timescale may not be able to keep pace.

Electromagnetic activity is certainly accompanied by high-energy particle fluxes: since X-rays in flares are harder than solar ones, particles too should be more energetic (Tarter et al. 2007). Stellar cosmic rays may be much stronger than those hitting the Earth (Scalo et al. 2007), possibly leading to ozone-depleting reactions (Grenfell et al. 2007, 2008). Strong coronal mass ejections deeply affect the exoplanetary magnetosphere (Khodachenko et al. 2007; Lammer et al. 2007), causing its significative withdrawal. In order to maintain a magnetosphere extension capable of shielding an atmosphere ($2 \times R_p$, according to Lammer et al. 2007), the magnetic field strength should be between tens to hundreds of Gauss, well beyond the capability of rocky planets. The problem is particularly serious for mid- and late-type M dwarfs (Kay et al. 2016).

In a recent paper, Kopparapu et al. (2017) simulated with a 3-D model the evolution of atmospheres of ocean planets around M stars. Quite unexpectedly, a moist greenhouse can be triggered around M stars with $T_{eff} > 3000$ K at much lower surface temperatures (~ 280 K) than around the Sun ($T > 350$ K; Wolf & Toon 2015; Popp et al. 2016). Therefore, these planets can simultaneously suffer from heavy water loss and remain habitable for hundreds of million or even some billion years, smoothly shifting from water-poor to dry conditions. The induced change in the atmospheric temperature profile has however disrupting consequences on the cloud cover, dropping the albedo and leading in most cases to the onset of a runaway greenhouse at lower fluxes than classical models predict. Planets at the inner edge of stars with $T_{eff} < 3000$ K directly enter a runaway state, without experiencing a moist greenhouse.

A third, severe problem of M stars has been briefly alluded in paragraph 4.2. The lightest M stars can take more than 1 Gyr to settle in the main sequence (Laughlin et al. 1997; Burrows et al. 2001), decreasing their luminosity by ~ 100 times in the process. Planets in the main sequence HZ, besides facing strong stellar activity, can reach surface temperatures of 1000 K in this stage, well above the threshold for runaway greenhouse. Water losses will be therefore much higher than those witnessed in the early Solar System. While Venus, according to Ramirez & Kaltenegger (2014), could have lost some $\sim 3 \times 10^{23}$ moles of H_2, i.e. ~ 4 Earth oceans, during two runaway greenhouse episodes at $1 < t < 7$ Myr and $20 < t < 50$ Myr, and our planet too could have been stripped of ~ 0.25 Earth oceans[16], M star planets might potentially be stripped of up to several tens of Earth oceans (Luger & Barnes 2015; Tian & Ida 2015; Bolmont et al. 2017; Bourrier et al. 2017). The possibility of total annihilation of both the atmosphere and the water content is concrete. Even if the atmosphere does not completely disappear, it would bear marks of the process: enormous amounts of oxygen, produced by photolysis of H_2O and CO_2 (Luger & Barnes 2015; Tian 2015; Tian et al. 2014; Harman et al. 2015), especially if O_2 sinks are small (cf. Chapter 3).

However, this fate can be avoided if those planets are born with much more water than Earth or are refilled with it later, when the star has reached its main sequence state. Recent studies indicate that ocean worlds with a few tens of percent of water can indeed exist (Alibert & Benz 2017) and be common M-star systems because 1) M-star disk densities are thought to be higher than average (Hansen 2015; Unterborn et al. 2018), 2) the absence of gas giants could help volatile acquisition (Morbidelli et al. 2016) and 3) planetary migration from the outer stellar system at

[16]Summing up the O_2 content of continents, oceans and atmosphere, some $\sim 2.5 \cdot 10^{21}$ mol of O_2 turn out to be present (Catling et al. 2001), mostly inside ferric iron (derived from oxidation of ferrous iron). This is almost twice the number of moles of reduced carbon in the crust ($\sim 1.3 \cdot 10^{21}$ mol, Wedepohl 1995): since C and O_2 are in ratio 1:1 in organic matter, the excess oxygen was likely produced by photolysis of water (Catling & Kasting 2017). This explanation is consistent with the lower D/H ratio of 3.8 Gyr old hydrated minerals (Pope et al. 2012).

later epochs. On the other hand, arguments for a prevalence of dry planets– either due to low protoplanetary disk mass or early harsh XUV flux– are given by Lissauer (2007) and Raymond et al. (2007). The debate, therefore, is still far from over.

Planets with a sufficient mass to be geologically active[17], both tectonically active or stagnant-lid, can store a great amount of water and CO_2 in their silicate mantle, which is slowly released in the atmosphere through outgassing. Indeed, this is the origin of the atmospheres of Venus, Earth[18] (cf. Section 7.1.1) and Mars. Godolt et al. (2018) have shown that a surface ocean and a secondary atmosphere can indeed form when the star has concluded its most tormented phase. If this is the case, the planet would carry no memory of its primary atmosphere and have plenty of time for geological evolution.

To summarise, the main advantage of M stars as cradles of life is undoubtedly their extremely long lifespan. In spite of the strong challenges they have to face, M star habitability is not necessarily impeded, provided that at least a part of the atmosphere is able to survive them or to be replenished. The existence of bulwarks such as strong gravitational fields, large initial atmospheric pressure, strong magnetic fields, would facilitate the task (Tian 2009). This is why Super-Earths are seen with increasing interest (e.g., von Bloh et al. 2007; Irwin et al. 2009). Water can either be present as a residual of a huge initial reservoir, outgassed from the interior or, alternatively, be delivered to the planet from the outer zone of the system in later replenishment episodes. Once a quiet and stable stellar environment has been reached, tens of billions of years of chemical experiments can begin, perhaps igniting eventually the spark of life.

[17] We may consider, following Williams et al. (1997), the threshold of 0.3 $M_\oplus$ for a 5 Gyr tectonic lifespan.
[18] Negletting, of course, the conversion of CO_2 into O_2 operated by life.

Chapter 5

Photosynthesis on an alien world

"Apparently the vegetable kingdom in Mars, instead of having green for a dominant colour, is of a vivid blood-red tint."

H.G. Wells, The War of the Worlds, 1898

Photosynthesis is the power station that sustains and feeds virtually all[1] life on Earth (Bar-On et al. 2018). As every metabolic process of living organisms results in an increase of entropy of the Earth system, the second principle of thermodynamics demands a continuous energy input from the outside to secure ecosystems against heat death. This *outside* happens to be the Sun: out of the $1.5 \cdot 10^{25}$ J impacting the planet each day, $\sim 1\%$ is captured by light-harvesting organisms and stored as chemical energy[2] (Garrett & Grisham 2008). Oxygenic photosynthesis[3], as we have seen in Section 7.4, can be summarised as:

$$6H_2O + 6CO_2 + energy \rightarrow C_6H_{12}O_6 \tag{5.1}$$

and yields, after an intricate succession of biochemical steps, organic fixation of CO_2, mediated by the enzyme ribulose-1,5-bisphosphate carboxylase/oxygenase (Rubisco) (Rothschild 2008). Responsible for a removal of $1.049 \cdot 10^{14}$ kg C yr^{-1} (Field et al. 1998), photosynthesis needs light because it is an endergonic process, i.e. going against its thermodynamic potential (Garrett & Grisham 2008). But was it a lucky accident on the path followed by terrestrial evolution (e.g., Gould 1989) or rather an inevitable evolutionary consequence of physical, chemical and biological conditions present on the early Earth (Conway Morris 1998)?

At the heart of photosynthesis lies the photoreactivity of *chlorophyll*. Chlorophylls are molecules with four pentagon-shaped rings known as pyrroles, among which a magnesium atom is nestled. Their peculiarity resides in their light-harvesting capacity due to their aromaticity, i.e. the feature of having delocalised electrons in their structure; the ΔE between different states of these electrons lies in the visible window. Whenever light is absorbed, an electron is excited to a higher orbital, becoming sensitive to stripping by an apposite acceptor, resulting in an oxidation–reduction reaction. Thus, photon energy is converted into chemical energy (Garrett & Grisham 2008).

[1] Excluding some prokaryotes which thrive on chemiosynthesis. Photosynthesis is conducted by some eukaryotes (plants and algae) and six phyla of bacteria (*Cyanobacteria, Chlorobi, Chloroflexi, Firmicutes, Proteobacteria and Acidobacteria*; Bryant et al. 2007).

[2] The remaining energy is either absorbed by land and oceans ($\sim 2/3$) or reflected back to space ($\sim 1/3$).

[3] There exists also an anaerobic (anoxygenic) photosynthesis, where a reductant other than water is used.

Many chlorophylls exist: plants usually combine two of them ("a" and "b"), having slightly differing absorption spectra, to improve their efficiency in collecting light (Figure 5.1); some algae possess chlorophylls c1 and c2, while cyanobacteria have evolved chlorophylls d and f. Anoxygenic photosynthesis employs bacteriochlorophylls a,b,c,d,e,g, characterised by an enhanced infrared response. In addition to them, a bunch of *accessory light-harvesting pigments* exists[4] that enables organisms to exploit a wider range of wavelengths[5] (e.g., Stomp et al. 2004), transferring then the collected energy to active chlorophylls (Garrett & Grisham 2008).

Interestingly enough, terrestrial oxygenic photosynthesis exploits just a quite narrow window of the electromagnetic spectrum (400-700 nm), the so-called *photosynthetically active radiation* (usually abbreviated as PAR). More energetic photons cause damage to the molecules of life (Becker & Wang 1989), while, at the other extreme, the sharp cut-off at $\sim$ 700 nm -the Red Edge, cf. Section 2.4.2- could be caused by necessity of protecting against overheating and protein denaturation (Gates et al. 1965).

This is the key to success of terrestrial life, which intuitively tuned its light-harvesting machinery to match the peak of the Sun's spectral energy distribution. How could photosynthesis -if it existed- vary in other stellar environments, like those found around the ubiquitous M stars? As we have seen in Chapter 4, M-star planets are seen as an appealing target for life search because of extremely long lifespans, stable climates and resistance to global-scale glaciations. The main difference between planets in the HZ of a G star and an M star does not lie in the total flux, but rather in the spectral energy distribution. Since decreasing a blackbody's temperature shifts its energy peak to longer wavelengths:

$$\lambda_{max} \approx \frac{2898 \mu \text{m K}}{\text{T}}, \tag{5.2}$$

the visible output of a G2V star (peaked at $\lambda \approx 500$ nm) is, in percentage, greater that the one of an M0 star (peaked at $\lambda \approx 760$ nm). Moreover, M stars show significant deviations from an ideal blackbody in the PAR window because of line blanketing[6]. The combination of the two effects implies a much lower PAR emission from the M0 star as compared to the G2 star (Gale & Wandel 2017).

If we call F_E the total flux at our planet and F_{PAR} the flux in the PAR window, a planet receiving 1 F_E from its parent star would experience just $\sim 1/3 F_{PAR}$ if $T_{eff} = 4000$ K and $\sim 1/12 F_{PAR}$ if $T_{eff} = 2800$K. Tidal locking would enhance F_{PAR} by a factor ~ 3 in the subsolar point, assuming the same cloud coverage as Earth's (Heath et al. 1999). The reduced insolation does not pose an insurmountable obstacle, though, for 1) only $\sim 0.01 F_E$ is harnessed by Earth's plants (Pianka 1974) and 2) marine photosynthesis is known to be able to work at just $5 \cdot 10^{-4} F_E$ (P McKay 2000). Even worlds as far as Titan and Enceladus, theoretically, receive enough energy ($F \sim 0.01 F_E$) to power photosynthesis. So, if exoplanets orbiting M stars are not able to support photosyntesis-based biospheres, this is probably unrelated to the properties of their parent stars' spectrum.

Experimental evidence for the possibility of photosynthetic processes under the irradiation of M stars has been provided by the project *Atmosphere in a test tube* (cf. Section 2.5). Terrestrial cyanobacteria like *Chlorogloeopsis fritschii* and *Cyanobacterium aponinum*, although specifically evolved to gather light from a G star, are able to adapt and thrive in M-star environments: there

[4] E.g., carotenoids, bilins, flavins and pterins.

[5] These pigments are crucial to adapt to various environmental conditions. For instance, since wavelengths $\lambda \in [450, 550$ nm] are the most efficient at penetrating water but chlorophylls have a poor response in that range, accessory pigments like *fucoxanthol* and *phycoerythrin* allow aquatic plants to make the most of light underwater (Heath et al. 1999).

[6] Line blanketing is the decrease in intensity of a star's spectrum due to many closely spaced, unresolved absorption lines.

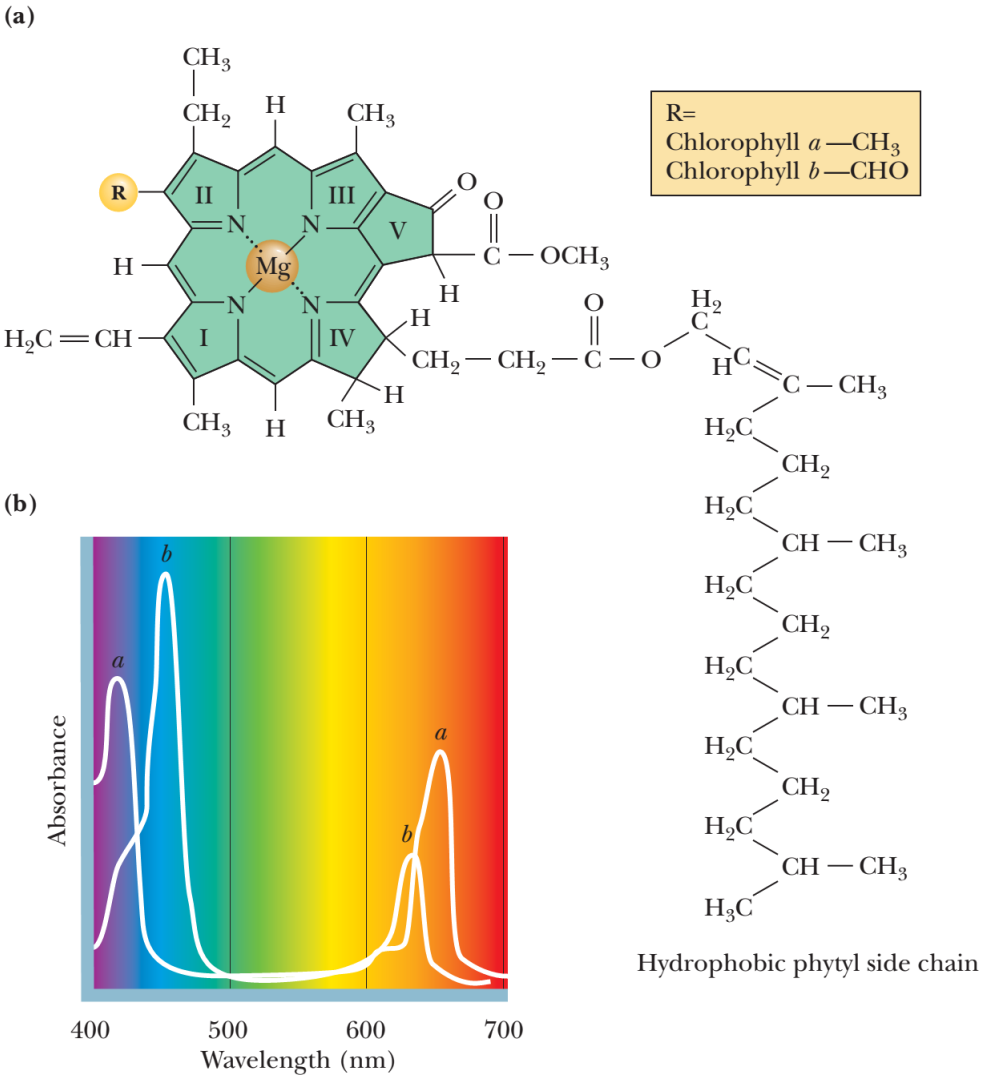

Figure 5.1: Structures (a) and absorption spectra (b) of the pigments chlorophyll a and b, commonly found in plants. Their poor green response is the reason for the colour of Earth's vegetation. Figure from Garrett & Grisham (2008).

is no physical obstacle, therefore, to the possibilities of exploitation of M-star energy by some kind of light-harvesting complex (Claudi et al. 2016).

It is reasonable to think that, just like earthly organisms adapted to the spectrum of the Sun, evolution should shape light-harvesting complexes of exoplanetary life to make the most of their own star's irradiation. In this regard, it is noteworthy that some prokaryotes like green bacteria, purple bacteria and heliobacteria have managed to extend redward their absorption capabilities (Gregory 1977): the genus *Chlorobium* up to 840 nm, *Rhodospirillum rubrum* and *Rhodopseudomonas capsulata* up to 870 nm, the genus *Chromatium* up to 890 nm and *Rhodopseudomonas viridis* even to 960 nm (Permentier et al. 2001). All of them, however, do not employ water as a hydrogen donor, hence they do not release oxygen. Is it possible to envisage an oxygenic photo-

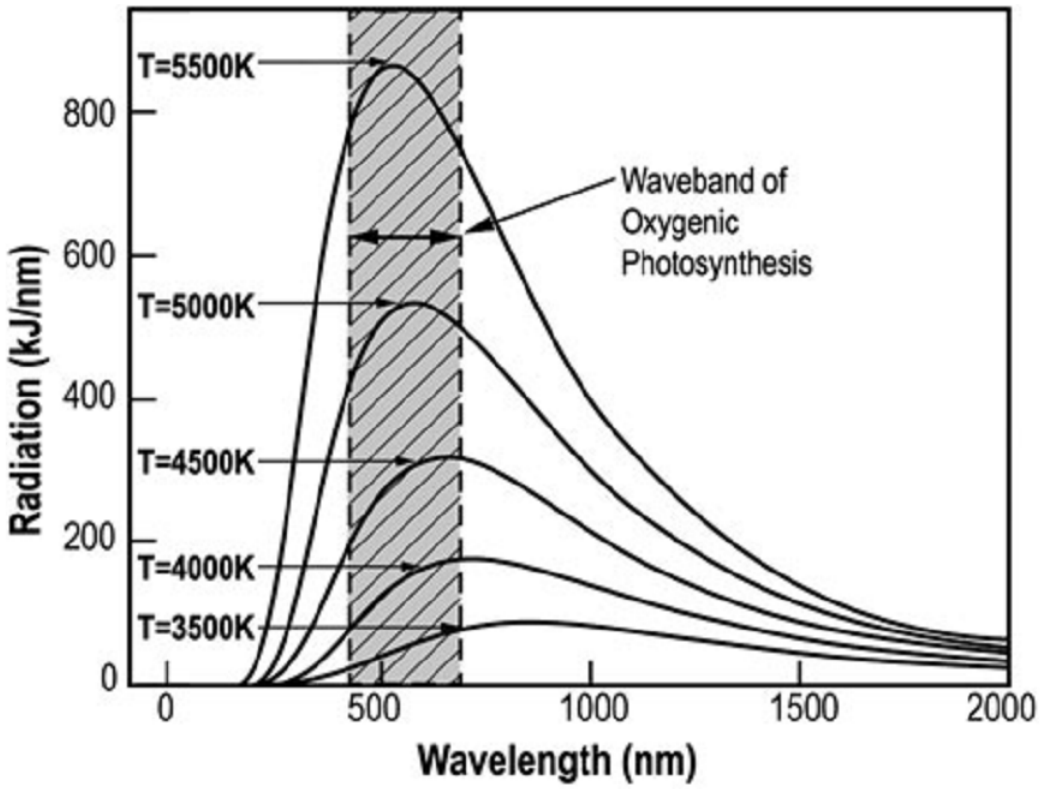

Figure 5.2: Planckian curves of various temperatures, showing the shift of cooler star radiation towards the near infrared. The PAR accurately matches the region of the Sun's spectrum ($\sim T = 5500$ K curve) where most of the energy is emitted. Figure from Gale & Wandel (2017).

synthesis with a similar near-infrared response? In principle yes, by means of a series of linked photosystems that employ more photons per every fixed CO_2: terrestrial photosynthesis uses two (Falkowski & Raven 1997), so it is energetically constrained to $\lambda < 730$ nm. The limit can be pushed to 1050-1095 nm if the use of a third photon is envisioned (Wolstencroft & Raven 2002; Tinetti et al. 2006), or even 1400–1460 nm if four photons are used (Hill & Bendall 1960; Hill & Rich 1983; Heath et al. 1999).

Wolstencroft & Raven (2002) have discussed in detail the possibility that oxygenic photosynthesis appears on exoplanets, taking into account astrophysical, chemical, climatic and biological processes. They concluded that the possibility is concrete and that light-harvesting should be a universal feature of life, because it relies on an exceptionally abundant source like water and represents an effective way to harvest enormous amounts of energy, extremely prone to strong positive evolutionary selection[7]. The biochemical details of these complexes should be case specific, dependent on a large set of environmental constraints, with a three- or four-photon favoured around M stars. Whether this can lead to oxygen buildup is another matter, which will be thoroughly tackled in Chapter 8: oxygenation time, we will see, depends sensitively on the balance between

[7]In the same way as on Earth the evolutionary selection preferred it to the less efficient -and nutrient-limited- chemolithotrophic reactions (Wolstencroft & Raven 2002; Kiang et al. 2007b).

sources and sinks of oxygen[8]. Since the biotic source of O_2 is related to the total biomass, it is pivotal to assess the maximum biomass that is sustainable on a world: while on Earth the limiting factor to biomass growth is the replenishing of nutrients (especially phosphorus), other worlds could be light-limited, i.e. receiving too little PAR to sustain Earth-like biospheres (Lehmer et al. 2018; Lingam & Loeb 2019b); as a result of the decreased O_2 source, they would have longer oxygenation time or even, if $F_{source} < F_{sink}$, accumulate no free oxygen at all. Oxygen-rich planets would be remotely detectable, as discussed in Chapter 2, through O_2/O_3 spectroscopic features or a Red(der) Edge (Segura et al. 2005).

5.1 The limits of life

As we have seen in Chapter 4, the climatic conditions on planets orbiting around M stars are idiosyncratic -from an earthly perspective-, with a marked difference between dayside and nightside, a whimsical stellar behaviour deeply affecting their atmospheres and a preference for dry, desiccated environments. But to what extent can life -actually, the only kind of life we know- survive?

Vascular plants are seen to irremediably lose photosynthetic capacities at 48 °C (Hüve et al. 2011), while some photosynthetic prokaryotes can endure up to 70–75 °C (Brock 1967); non-oxygenic hyperthermophiles can in some conditions bear 122 °C (Takai et al. 2008). On the other hand, Priscu et al. (1998) discovered microbes in liquid water inclusions in Antarctic ice, where the external temperature is below the freezing point, and some psychrophiles have been found to thrive at -15 °C (Mykytczuk et al. 2013). In general, under the common designation of *extremophiles* are grouped living beings thriving in extreme environments: unusual temperature, pressure, radiation flux, pH, dryness, salinity. Ranging from the hot springs of Yellowstone (Segerer et al. 1993) to the arid wasteland of the Atacama Desert (McKay et al. 2003), subglacial lakes in Antarctica (Bulat et al. 2004), the hypersaline waters of the Red Sea (Krumbein et al. 2004), the hot, high-pressure, surroundings of hydrothermal vents (Prieur et al. 1995), sulfide chimneys and black smokers (Baross 1983), earthly life seems to be stubbornly resilient and ubiquitous.

In addition to direct observations of modern Earth environments, many experiments have been performed to study the tolerance of terrestrial life to extreme conditions resembling the early Earth (Cnossen et al. 2007; Westall et al. 2011; Grosch & Hazen 2015), Mars (Navarro-González et al. 2003; Cockell & Raven 2004; Diaz & Schulze-Makuch 2006), icy moons like Europa (F. Chyba 2000; Chyba & Phillips 2002; Marion et al. 2003) and interplanetary space (Paulino-Lima et al. 2010). The lesson we learn is always the same: *where there is water, there is life.* In absence of a water supply, "anhydrobiosis" can befall organisms, halting metabolism altogether and prompting denaturation of lipids, proteins and nucleic acids, and the production of harmful oxygen species when exposed to harsh stellar radiation (Cox 1993; Dose et al. 1995; Rothschild & Mancinelli 2001).

5.2 UV and life

The main hindrance to surface life on M-star planets derives from the frequency and intensity of stellar flares (Dole 1964) and from the strong stellar XUV flux (Segura et al. 2010). Coupled with the likely absence of strong magnetic fields (Grießmeier et al. 2005), this could mean exposure of the surface to an incessant stellar and cosmic ray shower, with harmful biological implications:

[8] As a remainder, Earth's atmosphere was anoxic for several hundreds Myr after the emergence of photosynthesis and has achieved O_2 levels comparable to present ones only for the last $\sim$ 700 Myr (cf. Section 7.1.2), giving a remarkable example of how a world with photosynthetic organisms does not have to be highly oxygenated.

high-energy particles and radiation are known to generate significant damage to living beings; UV rays, in particular, inhibit photosynthesis (Harm 1980; Jagger 1985; Ries et al. 2000) and fatally damage DNA, lipids and proteins (Lindberg & Horneck 1991; Cockell 1998). Like on early Earth, life could be confined to its cradle, i.e. deep ocean environments, where the XUV flux is sufficiently shielded (Kiang et al. 2007a).

Nevertheless, some organisms (notably *Deinococcus radiodurans*, Battista 1997) are capable of bearing large doses of high-energy radiation by means of antioxidants, enzymes and repair mechanisms, and to reverse the effects of lethal UV doses after being exposed to visible light (*photoreactivation*, Rambler & Margulis 1980). Algae are able to repair damaged DNA and, like some plants, can synthesise UV-absorbing compounds such as flavonoids and flavones (del Moral 1972; Caldwell 1981) for self-protection.

Once the active chromospheric emission of the star has calmed down, the bias toward longer wavelengths proper of cooler stars implies at the same time a lower UV emission than the Sun's and a preference for UVA (315-400 nm) over UVB (280-315 nm). Since the latter is both the main responsible of biological damage on Earth and, through its interaction with the genome, a key factor shaping molecular evolution, is it likely that significant metabolic and biological differences are present. Additionally, visible damage, that on Earth accounts for $\sim 10\%$ of the total, would be proportionally more important, possibly weakening the importance of an ozone shield (Scalo et al. 2007).

An interesting perspective is that of Buccino et al. (2007), who underline the key role of UV radiation in the origin of life (Toupance et al. 1977; Ehrenfreund et al. 2002). The UV flux at Earth was probably two or three times larger 4 Gyr ago (Scalo et al. 2007), and the concomitant lack of an ozone shield made it an important energy source, involved in biosynthesis. A moderate flare activity could paradoxically be beneficial, triggering biogenic processes, while episodic strong flares could create a strong selective pressure for living organisms rather than automatically impeding their existence.

5.3 A purple world

Whilst nearly all light-harvesting organisms employ a chlorophyll-based photosynthetic system, there is at least one alternative system making use of a different pigment, rhodopsin. The process, although able to collect energy for metabolism, is unable to fix carbon from CO_2 (Bryant & Frigaard 2006). Because of its extreme simplicity with respect to chlorophyll-based photosynthesis, a hypothesis has been put forward, namely that the appearance of retinal[9]-based organisms predates photosynthesis (Sparks et al. 2006; DasSarma & Schwieterman 2018).

Since rhodopsin is characterised by a single absorption peak in the green-yellow part of the solar spectrum, it appears deep purple (Stoeckenius 1976). If the *Purple Earth* hypothesis is correct, it is possible that other planets, too, exhibit a *Green Edge*, opening new interesting possibilities in the search of biosignatures (Schwieterman et al. 2018).

5.4 Vegetation

Photosynthesis is pivotal if the rise of complex organisms hinges, like on Earth, on a substantial presence of free oxygen[10] (Catling et al. 2005). Some tentative, perhaps Earth-biased consider-

[9]Retinal is a subcomponent of rhodopsin.

[10]However, the presence of O_2 in a prebiotic atmosphere, to which M star planets can be susceptible due to water photolysis (cf. Chapter 3), should be considered a strong factor against life: the assembling of more and more complex molecules is virtually possible in an oxidising environment.

ations regarding a possible exoplanet vegetation have been speculatively put forward in the last two decades.

Something resembling higher plants could be sustained on tidally locked HZ planets, on the basis of modelled temperature profiles. Their light-harvesting pigments, adapted to match their parent star's spectrum (Kiang et al. 2007a), should make the best of a reduced photon availability. The substellar point (the one seeing the star directly overhead) would be favoured because of a higher insolation but could also suffer more from stellar flares. Moving away from the substellar point increases the path to be crossed by stellar light, diminishing the availability of light (Heath et al. 1999). At the terminator, the effect of flares would be quite small, the damaging radiation would experience a significative extinction, the winds would not be so strong (5–10 m/s, according to Joshi et al. 1997), but the overall insolation would be rather small (Tarter et al. 2007).

On Earth, evolution has strongly encouraged the development of leaves (Boyce & Knoll 2002), a particularly efficient means of poising energy collection and heat dissipation. Tinetti et al. (2006) calculated that a leaf-like structure performing photosynthesis via a three-photon process on an M-star planet would possess an *Infrared Edge* at 1050 nm and be detectable through a substantial bump over the continuum of $\sim 70\%$ (cloudless case) and $\sim 10\%$ (cloudy case). If similar structures have truly arisen on other worlds, they would open up exciting new horizons in our never-ending quest for the unknown.

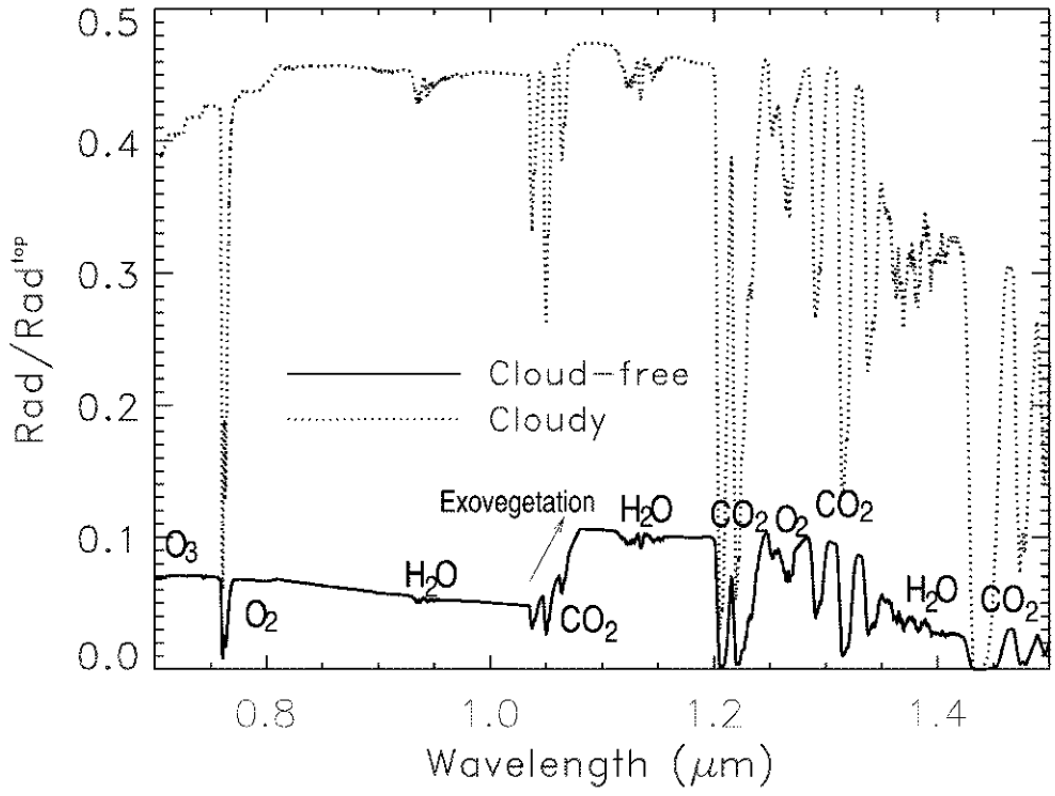

Figure 5.3: The effect of a vegetation performing a three-photon oxygenic photosynthesis on the disk-averaged spectrum of an M star Earth-like planet. The Red Edge at 1050 nm is clearly visible in the cloudless case and still distinguishable, although blurred, in the cloudy case. Figure from Tinetti et al. (2006).

Chapter 6

The model

"We are just an advanced breed of monkeys on a minor planet of a very average star. But we can understand the Universe. That makes us something very special."

Stephen Hawking, 1988

Having discussed in previous chapters the methods aimed at detecting and characterising exoplanets, the conditions that make them *habitable*, the plausibity of oxygen as a biomarker, the evolutionary thrust toward the emergence of light-harvesting complexes, let us now delve into the kaleidoscope of planetary environments; before commencing this inquiry, a detailed mathematical analysis of O_2 evolution needs being provided for the planet that we know best: our own Earth.

The model presented here has been developed in Python and includes several physical, chemical and geological processes producing ("sources") and destructing ("sinks") oxygen on our planet. Details on these processes will be provided in this chapter, while the set of equations will be presented in Section 7.2. The model should be able to reproduce the oxygenation history of our planet and recover a final O_2 level of 1 PAL[1]. Numerical simulations, at the heart of Chapter 7, will allow a gauge of the free parameters by means of a comparison with actual reconstructions of O_2 levels from geological records. After calibrating the model, the parameters and the equations will be varied in Chapter 8 to conjecture about the oxygen presence under different planetary conditions.

Particular care shall be devoted to the biological factor. While on Earth biomass is limited by availability of nutrients, planets around cooler stars appear to be light-limited, i.e. limited by the amount of PAR they receive. This observation will prove to be crucial in assessing both the question of oxygen accumulation and, if so, oxygenation time. The boundary between the two regimes will depend not only on the properties of the parent star's spectrum and the planetary size, but also on the extent of the PAR window exploited by light-harvesting complexes. This issue will be the focus of Section 8.2.1. A final discussion of results will be presented in Chapter 9.

Since the quantities mentioned in this dissertation come from experiments, papers and books encompassing almost the whole spectrum of scientific research (physics, astronomy, biology, chemistry, geology) and each field has its own measurement conventions, the choice was made to refer as more as possible to the *International System of Units* (SI).

[1] 1 PAL (Present Atmospheric Level) is the current O_2 level in the atmosphere. It corresponds to a mixing ratio of 0.2096 or, equivalently, to an amount of matter of $\sim 3.8 \cdot 10^{19}$ mol.

6.1 Physical parameters

6.1.1 Temperature

Although temperature does not appear explicitly in the model, it is tacitly assumed to be in the range that both allows the presence of liquid water (see Chapter 4) and does not hinder photosynthesis (see Chapter 5). Indeed, the model is primarily concerned with *Earth-like* (cf. Section 2.3) biospheres.

6.1.2 Star spectrum

A physical limitation to the unlimited growth of biomass is posed by the availability of stellar light powering photosynthesis. While on Earth light is abundant and the shortage of nutrients is the ultimate factor controlling biomass levels, the question whether different stars emit sufficient PAR to allow for biospheres comparable to the terrestrial one needs being carefully assessed.

Stars are usually modelled as blackbodies. However, due to strong line blanketing, the approximation gets less and less accurate for cooler and cooler stars. In order to simulate realistic stars, synthetic spectra ranging from F0 to M8, spanning the interval [115,2500 nm] with a resolution of 0.5 nm, have been taken from the ESO database (Pickles 1998). These spectral flux densities have been subsequently put in physical units by comparison with Noll (2014) and converted into spectral photon densities, because the photon-pigment interaction, at the heart of photosynthesis, is fundamentally a quantum process.

Since these spectra do not take into account atmospheric absorption, the transmission profile of Earth's atmosphere was retrieved by dividing the solar irradiance at the top of the atmosphere and that at sea level taken from ASTM G173-03 Reference Spectra (Gueymard 2001, 2003). Referring to an airmass=1.5, i.e. a zenital distance of 48.5°, they can be considered good approximations of globally averaged insolations.

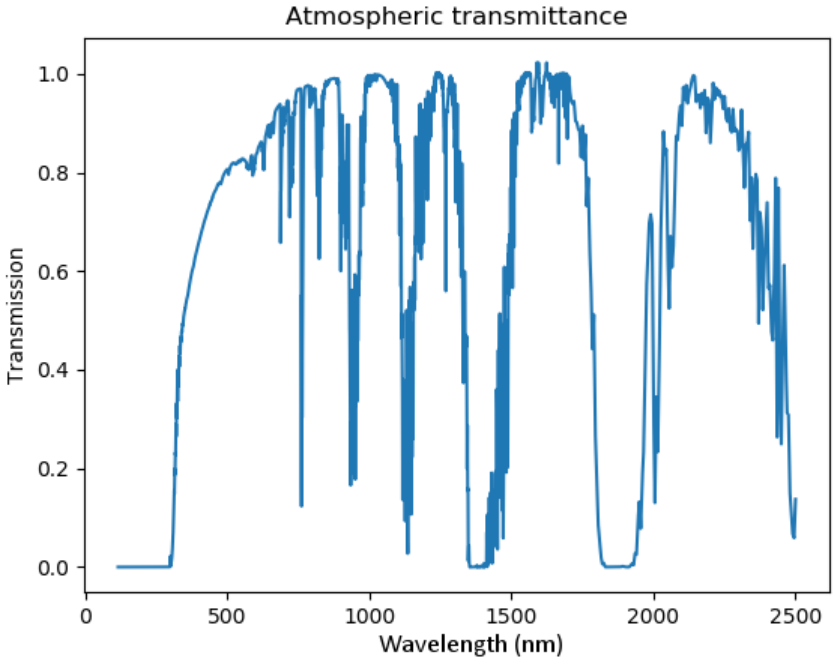

Figure 6.1: Transmission spectrum of Earth's atmosphere.

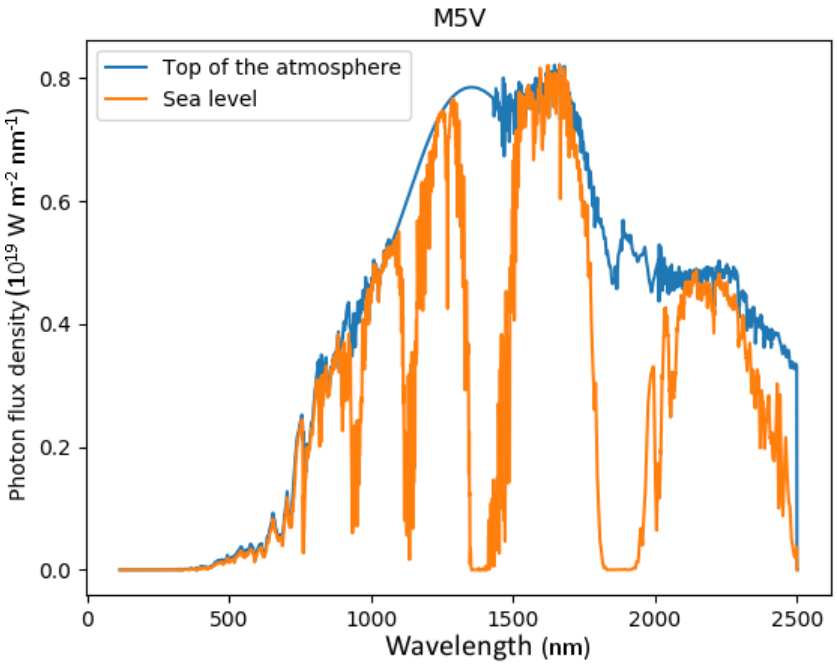

Figure 6.2: One of the stars used in the model, belonging to spectral class M5. The discrepancy between the stellar spectrum (blue curve) and the equivalent Planckian (here not shown) is evident. The spectrum at sea level (orange curve) has been computed convoluting the blue curve with the transmission spectrum shown in Figure 6.1.

6.2 Geological parameters

One of the main O_2 sinks is the outgassing of reduced gases during volcanic activity, both on land and at the seafloor. The time evolution of volcanic outgassing is thought to follow an exponential decay (e.g., Hart 1978):

$$F_{volc} = F_0 \cdot e^{-t/\tau} \tag{6.1}$$

The equivalent hydrogen outgassing rate[2] was about three times higher than today on early Earth, according to Catling & Kasting (2017). After comparing their table 8.1 and their estimate of a $\sim$ 11 Tmol yr^{-1} flux of hydrogen equivalents (excluding SO_2) for the early Earth, a value of $\tau = 4.4$ Gyr was chosen.

Conceptually similar to volcanism, methamorphism causes squeezing and heating, but not melting, of carbonate rocks, releasing large amount of CO_2. Especially common in rift valleys and mountain belts (Kerrick 2001; Kerrick et al. 1995), the process is often accompanied by release of reduced gas (Mörner & Etiope 2002; Etiope et al. 2008; Svensen & Jamtveit 2010), sprouting from reactions such as:

$$C + 2H_2O \rightarrow CO_2 + 2H_2$$

and

$$2C + 2H_2O \rightarrow CO_2 + CH_4$$

Some CH_4 is generated also within hydrothermal vents at mid-ocean ridges, both in the hotter axial vents and the cooler off-axis vents (like the Lost City vent field on the Mid-Atlantic ridge, Kelley et al. 2005). When ultramafic rock like peridotite are exposed to water, they are altered to form serpentine minerals – in a process known as serpentinisation. The overall reaction can be written as:

$$3FeO + H_2O \rightarrow Fe_3O_4 + H_2$$

When dissolved CO_2 is present in water, CH_4 can be produced as well (McDermott et al. 2015). The ratio of produced CH_4:H_2 is about 1:15 (Cannat et al. 2010; Keir 2010), while the ratio of CH_4(serp):CH_4(biotic) is about 1:1000 (Catling & Kasting 2017). This process appears to be today a minor sink for oxygen; however, there is evidence[3] that serpentinisation was important in Archean. Following the finding (Herzberg et al. 2010) that the seafloor should have been both thicker and more Mg-rich due to higher mantle temperatures and a correspondingly greater degree of partial melting at mid-ocean ridges, implying higher serpentinisation rates, the hypothesis was here made to tie the time evolution of this sink to Earth's upward heat flow:

$$Q(t) = \left(\frac{4.5}{4.5 - t}\right)^{\eta} \tag{6.2}$$

where η=0.7 (Claire et al. 2006).

Methane is created also thermogenically, scilicet, from thermal breakdown of organic matter operated by metamorphism, at a rate of $1.25–2.5 \cdot 10^{12}$ mol yr^{-1} (Etiope 2009). Contrary to the previous process, this mechanism is an important O_2 sink at the present time (accounting for $\sim$ 50% the total geological sinks), but it was smaller during the Archean because of a reduced amount of buried organic matter. Assuming that a part of the buried matter experiences, after some time, thermal breakdown, this contribution has been assumed to be proportional to $B(t)$.

[2]It is the hydrogen flux that would consume the same amount of O_2 that is actually consumed by the mixture of gases ejected by volcanoes.

[3]Namely, the widespread presence of greenstone belts: folded, heterogeneous regions, sometimes several thousand kilometres long, rich in dark-green, altered mafic to ultramafic igneous rocks.

Moving now to O_2 sources, it is worth noting that the main source of terrestrial oxygen, although of evident biological origin, is determined by a geological process: organic carbon burial. Photosynthesis and respiration continuously transform O_2 into CO_2 and vice versa[4]:

$$CH_2O + O_2 \leftrightarrow CO_2 + H_2O \tag{6.3}$$

But, every time that some organic matter is buried underground, it escapes oxidation because it is taken away from the availability of free oxygen. Every mole of buried carbon results in a mole of free O_2 released in the atmosphere: this burial rate -and not, as it could be thought by intuition, the instantaneous photosynthetic production, is the source, in the long run, of the whole oxygen reservoir of our planet (Catling & Kasting 2017).

In a similar fashion, O_2 is produced by burial of other redox-sensitive species like iron oxides and pyrite. Some iron-reducing oceanic bacteria are capable of reducing ferric oxide (Fe^{3+}) to ferrous oxide (Fe^{2+}) releasing oxygen in the process:

$$\frac{1}{2}Fe_2O_3 \rightarrow FeO + \frac{1}{4}O_2 \tag{6.4}$$

that they can subsequently use to oxidise organic material dissolved in water (Fredrickson et al. 1998; Bleam 2017). Other bacteria are known to degrade organic matter in a chemical chain whose final result is the reduction of sulfate and ferric iron (Fe^{3+}) to pyrite (FeS_2) (Berner 2004):

$$\begin{aligned} \text{Oxygenic photosynthesis} &: 15H_2O + 15CO_2 \rightarrow 15CH_2O + 15O_2 \\ \text{Sulphate reduction} &: 15CH_2O + 2Fe_2O_3 + 16H^+ + 8SO_4^{2-} \rightarrow 4FeS_2 + 23H_2O + 15CO_2 \\ \hline \text{Net reaction:} &: 2Fe_2O_3 + 16H^+ + 8SO_4^{2-} \rightarrow 4FeS_2 + 8H_2O + 15O_2 \end{aligned}$$

Since in both cases oxygen is not taken from the ocean-atmosphere system but rather from a mineral, burial of Fe^{2++} and pyrite constitutes a net source of free O_2. Assuming that the ratio between the bacterial mass involved in the process and the total biomass remains constant in time, the time evolution of carbon, Fe^{2+} and pyrite burial will be the same.

6.3 Chemical parameters

Oxygen is, after fluorine, the most electronegative element of the periodic table. Despite being the third most common element in the Universe, it is rarely found in its molecular form O_2 in planetary atmospheres: its capability to *oxidise* molecules implies that, whenever free oxygen is present, it promptly reacts with metals and hydrogen-bearing molecules. Respiration can be seen, in this regard, as the way that life uses to exploit the oxidising potential of oxygen to garner energy for its own purposes.
Reduced gases emitted from volcanoes are a major sink of O_2:

$$\begin{aligned} &2H_2 + O_2 \rightarrow 2H_2O \\ &CH_4 + 2O_2 \rightarrow CO_2 + 2H_2O \\ &CO + 1/2O_2 \rightarrow CO_2 \\ &SO_2 + H_2O + 1/2O_2 \rightarrow H_2SO_4 \\ &H_2S + 2O_2 \rightarrow H_2SO_4 \end{aligned}$$

[4]The two processes are actually far more complex and rich in exquisite details, requiring an intricate biochemical machinery to work.

All the above reactions are considered in the model, although in a simplified manner: instead of delving into the intricate details of reactions and redox-balance computation of the evolving atmosphere[5] (like, e.g., in Claire et al. 2006; Hu et al. 2012; Harman et al. 2015), the fluxes of reduced gases are simply converted into negative O_2 fluxes. Indeed, we are not interested in studying the temporal variation of molecules other than O_2.

On the Earth, the appearance of oxygenic photosynthesis occurred in a strongly reduced environment: the oceans were, in fact, much richer in iron than today. The majority of iron in igneous rocks is found in its ferrous (Fe^{2+}) state. According to a recent estimate by Zheng et al. (2018), the concentration of Fe^{2+} in Archean oceans was $\sim 8 \cdot 10^{-2}$ mol m^{-3} in shallow waters and $\sim 6 \cdot 10^{-1}$ mol m^{-3} in deep waters, while today the average value is just $4 \cdot 10^{-5}$ mol m^{-3} (Catling & Kasting 2017). Such high quantities of iron, partially replenished by a continuous iron flux from the seafloor and continents, impeded for much time the accumulation of free O_2 in the oceans, combining with it to form ferric iron (Fe^{3+}), that settled on the seafloor. Evidence for it is the enhanced $[Fe^{3+}]/[Fe^{2+}]$ ratio found in sedimentary rocks and the widespread presence of banded iron formations dating back to the Archean (Holland 1973).

A rough mathematical explanation of the process is provided. Oxygen trapped in ferric iron inside *soft* rocks, i.e. sedimentary rocks, amounts, according to Catling & Kasting (2017), to $\sim 1.3 \cdot 10^{20}$ mol. Since the total iron content in the anoxic Archean oceans -assuming a mean concentration $[Fe^{2+}] \sim 5 \cdot 10^{-1}$ mol m^{-3} and a total oceanic volume equal to the present one, $V_{oceans} \approx 1.37 \cdot 10^{18}$ m^3, Sverdrup et al. (2003)- was:

$$(0.5\text{mol Fe m}^{-3}) \cdot (1.37 \cdot 10^{18}\text{m}^3) \approx 7 \cdot 10^{17}\text{mol Fe}$$

and the hydrothermal flux of Fe^{2+} was much higher than today (Holland 2006):

$$F_{Fe^{2+}} \sim 3 \cdot 10^{12}\text{mol yr}^{-1},$$

a time lag of ~ 300 Myr between the onset of photosynthesis and the appearance of free oxygen requires a number of O_2 moles[6] of:

$$\frac{1}{4}(7 \cdot 10^{17} + 3 \cdot 10^8 \cdot 3 \cdot 10^{12})\text{mol} \approx 2.3 \cdot 10^{20}\text{mol},$$

much larger than the present amount of atmospheric O_2 ($\approx 3.8 \cdot 10^{19}$ mol) and comparable to the soft rock reservoir.

Once virtually all oceanic Fe^{2+} had been depleted, oxygen began to leak to the atmosphere, where it encountered a slightly reducing environment, with a significant methane partial pressure of $\sim 3 \cdot 10^{-3}$ bar (Kasting & Brown 1998; Claire et al. 2006). CH_4 was produced both by volcanoes and methanogen bacteria and quickly suffered a similar fate as oceanic iron.

The oxygenation of the atmosphere, started some ~ 2.4 Gyr ago in the so-called *Great Oxidation Event* (GOE), lead to dramatic consequences for both the equilibrium chemistry of our planet and the subsequent direction taken by biological evolution. When the abundant iron and sulphate rocks present on land first came in contact with free oxygen, a new major sink for O_2 was established: an oxidation process known as *weathering*. Weathering, a familiar example of

[5] Redox balance is, basically, conservation of free electrons. Models studying the evolution of the atmosphere must consider that, every time a species is oxidised, another species must be reduced. The combined atmosphere-ocean system must satisfy redox balance, unless mass loss to space is present.

[6] The reaction

$$2FeO + \frac{1}{2}O_2 \rightarrow Fe_2O_3$$

requires 4 moles of Fe for each mole of O_2.

which is rust, constitutes today the main sink of O_2 and can be thought as the reverse reaction of carbon, Fe^{2+} and pyrite burial:

$$\text{Carbon weathering} : C + O_2 \rightarrow CO_2 \tag{6.5}$$

$$\text{Pyrite weathering} : FeS_2 + \frac{15}{4}O_2 + \frac{7}{2}H_2O \rightarrow Fe(OH)_3 + 2H_2SO_4 \tag{6.6}$$

$$Fe^{2+}\ \text{weathering} : FeO + \frac{1}{4}O_2 \rightarrow \frac{1}{2}Fe_2O_3 \tag{6.7}$$

These reactions depend, quite intuitively, on oxygen abundance:

$$F_{weath} = k_w[O_2]^\beta \tag{6.8}$$

but the exact way in which they do is of difficult assessment (Holland 2003). For instance, Claire et al. (2006) tried many values in their simulations, spanning from $\beta = 1/3$ to $\beta = 0.4$, while Hart (1978) assumed a linear behaviour ($\beta = 1$). Different values of β will be investigated here, with the caveat that the expression must yield the measured weathering flux for $t = t_{now}$.

Another chemical factor involving oxygen is a cluster of reactions taking place in the upper atmosphere: under the action of UV radiation from the Sun, stratospheric oxygen continuously turns in ozone and vice versa, in the so-called Chapman cycle (Chapman 1930):

$$\begin{aligned} O_2 + h\nu &\rightarrow O_2^* \rightarrow 2O\cdot \\ O\cdot + O_2 &\rightarrow O_3 \\ O_3 + h\nu &\rightarrow O_2 + O \\ O_3 + O &\rightarrow O_2 \end{aligned}$$

which can be thought as a balance reaction:

$$2O_3 \leftrightarrow 3O_2 \tag{6.9}$$

The main result of the cycle is the conversion of UV photons into thermal energy, which is the main cause of stratospheric heating. But more importantly, by absorbing the dangerous UV radiation, ozone acts like a shield protecting terrestrial life. On Early Earth, the harsh UV flux sterilised the continental surface impeding, until enough oxygen built up, its colonisation by life[7].

Since ozone accounts only for $6 \cdot 10^{-7}$ bar in Earth's atmosphere, we can safely neglect it in our model.

6.4 Biological parameters

The source of virtually all free molecular oxygen on Earth is life. As we have seen, many autotrophs are able to harvest the energy of the Sun by means of photosynthesis, combining water and carbon dioxide into an energetic sugar, namely *glucose*:

$$6H_2O + 6CO_2 \rightarrow C_6H_{12}O_6 \tag{6.10}$$

which is the ultimate source of energy for the majority of terrestrial organisms. The net primary production of Earth organisms is $1.049 \cdot 10^{14}$ kg C yr^{-1} (Field et al. 1998), evenly distributed between land and oceans[8], and is equivalent to an O_2 release of $\sim$ 3500 Tmol yr^{-1}, assuming

[7] Although the timing of actual land colonisation by complex organisms is unrelated to it; see Chapter 9.

[8] Despite being the oceanic biomass just 0.2% of the global biomass, it account for 46% of the photosynthetic production. This discrepancy is due to the much shorter turnover time, i.e. rate the rate at which organic matter is recycled, in oceans (2-6 days) than on land ($\sim$ 19 years) (Field et al. 1998).

that the former is mostly in the form of CH_2O (Lingam & Loeb 2019a) . However, the rate of carbon fixation equals the rate of carbon depletion if the total living biomass does not change and no carbon is taken away from the system: carbon in living beings is continuously recycled by the combined action of photosynthesis and respiration; the net source of O_2 is, as we have seen, buried carbon. Interestingly enough, the fraction κ of the net primary production that escapes oxidation and gets buried appears constant in time, and has been estimated by Holland (2002) as $\kappa \sim 2.9 \cdot 10^{-3}$.

It is possible, therefore, to estimate the sedimentation rate of organic matter F_{bur} as a function of biomass as:

$$F_{bur} = \frac{1000}{30}[S_{land} \cdot B_{land} + S_{ocean} \cdot B_{ocean}] \tag{6.11}$$

where the constant $1000/(30 \text{ g mol}^{-1})$ converts kg into moles and the parameters $S_{ocean} = \alpha_o \kappa \approx 0.1421 \text{ yr}^{-1}$ and $S_{land} = \alpha_l \kappa \approx 3.6 \cdot 10^{-4} \text{ yr}^{-1}$ incorporate the different turnover rates in oceans and continents through the constants $\alpha_o = 49$ and $\alpha_l = 0.124$.

The living biomass itself constitutes a (minor) reservoir of carbon. Every new mole of C nestled in biomass corresponds to a mole of O_2 released in the atmosphere. Hence, the rate of variation of the total living biomass gives rise to an additional oxygen source/sink, depending on its sign:

$$F_{bio} = \frac{1000}{30}\frac{dB}{dt} \tag{6.12}$$

but, given that the total living biomass ($\sim 4.5 \cdot 10^{14}$ kg) corresponds to $\sim 1.5 \cdot 10^{16}$ mol O_2 and that, even if it the whole growth episode were to be unrealistically concentrated in just 1 Myr, it would give a flux $F_{bur} \sim 0.01$ Tmol yr^{-1} $\ll F_{bur} \sim 10$ Tmol yr^{-1}, this contribution can be disregarded.

To model Earth's biomass, the following expression was chosen:

$$B(t) = B_0 + \frac{B_1}{1 + e^{-\lambda_1(t-t_1)}} + \frac{B_2}{1 + e^{-\lambda_2(t-t_2)}} + \frac{B_3}{1 + e^{-\lambda_3(t-t_3)}} + \frac{B_4}{1 + e^{-\lambda_4(t-t_4)}}. \tag{6.13}$$

The function:

$$f(x) = \frac{L}{1 + e^{-k(x-x_0)}} \tag{6.14}$$

is widely known in biology and is called *logistic function*: it is used to model the growth of bacteria in broth, as it catches the exponential growth typical of unrestrained populations, followed by a slowdown and the final settling at a constant level, determined by the availability of nutrients (see, e.g., Zwietering et al. 1990). We hypothesise that terrestrial life, as a whole, acts like a gigantic bacterial culture whenever it is exposed, somehow, to the availability of fresh resources. Looking at the curve of oxygen (cf. Section 7.1.2), we guess that at least four similar episodes occurred, so we adopt a function with four bumps. B_0 is the biomass at the start of the simulation; the parameters $\{\lambda_i\}$ are related to the rapidity of the exponential growth; the $\{t_i\}$, finally, shift horizontally the sigmoids and can be thought as the central moments of the accretion episodes.

When dealing with an exoplanetary generalisation of this concept, a distinction between two cases must be made. As mentioned in Section 6.1.2, the maximum biomass attainable on a world is dictated by the availability of two elements:

- light;
- nutrients.

As soon as a shortage of one of them is encountered, biomass can no longer grow: we say that we are in a *light-limited* or in a *nutrient-limited* regime.

On Earth, it can be shown that the current land primary productivity can be sustained by a minimum PAR flux $\tilde{F}_l \approx 3.6 \cdot 10^{20}$ photons m^{-2} s^{-1} (Field et al. 1998), some $\sim 40\%$ of the actual $F_{PAR,\oplus}$, while oceans require just $\tilde{F}_o \approx 7.35 \cdot 10^{19}$ photons m^{-2} s^{-1}, $\sim 7\%$ of $F_{PAR,\oplus}$. Therefore, the net primary productivity of our planet is nutrient-limited. This will not be the case for much cooler stars than the Sun, where the reduced PAR[9] flux will be the key factor determining the saturation biomass. This will have major repercussions on the oxygen buildup, as we will see.

6.5 Other parameters

6.5.1 Planetary radius and water coverage

On Earth, the limitation on biomass growth stems from the limited availability of nutrients. However, the meagre substance for terrestrial and ocean biomass is different.

Earthly life compulsorily requires some elements to build its key molecules: hydrogen, carbon, nitrogen, oxygen, phosphorus and sulphur. In particular, phosphorus is found in nucleic acids and ATP, the molecules controlling information storing and metabolism (Westheimer 1987; Kamerlin et al. 2013), but its major inorganic sources (minerals like apatites) are nearly insoluble in water (Schlesinger & Bernhardt 2013): hence, oceans have to rely on transport of this key element from the continents. The availability of phosphorus is therefore the bottleneck for water life (Tyrrell 1999; Sarmiento & Gruber 2006; Filippelli 2008). An extremely intriguing hypothesis, supported by tentative evidence, ties the emergence of animals during the late Proterozoic to increases of phosphorus delivery to oceans (Knoll 2017; Reinhard et al. 2017). If this is the case for extraterrestrial life too, the process needs detailed consideration.

Following Lingam & Loeb (2019a), we may write the net primary production of the oceans Π_o as:

$$\Pi_o \propto \phi_P f_o R^2, \tag{6.15}$$

where ϕ_P is the steady-state concentration of dissolved P and f_o is the fraction of planetary surface covered by bodies of water. Computation of ϕ_P requires a delicate assessment of the balance between sources and sinks of phosphorus. The three sources S_r, S_a and S_w of phosphorus are material weathered and then carried by rivers, deposition of dust, aerosols and volcanic ash from air and submarine weathering of the seafloor by water:

$$S_r \sim 3 \cdot 10^{10} \text{ mol yr}^{-1} \left(\frac{f_o}{f_\oplus}\right) \left(\frac{1-f_o}{1-f_\oplus}\right) \left(\frac{R}{R_\oplus}\right)^2 \tag{6.16}$$

$$S_a \sim 1 \cdot 10^{10} \text{ mol yr}^{-1} \left(\frac{f_o}{f_\oplus}\right) \left(\frac{1-f_o}{1-f_\oplus}\right) \left(\frac{R}{R_\oplus}\right)^2 \tag{6.17}$$

$$S_w \sim 1.3 \cdot 10^{8} \text{ mol yr}^{-1} \left(\frac{f_o}{f_\oplus}\right) \left(\frac{R}{R_\oplus}\right)^2 \tag{6.18}$$

The amount of weathered material transported by rivers depends on the fraction of the surface covered by lands and, less intuitively, on the ocean fraction too, because only a fraction f_o of the land has been shown to receive precipitations (Lingam & Loeb 2019a). The material brought by air increases with the land fraction and the fraction of it that is deposited in oceans is clearly f_o. Seafloor weathering is so low, despite being $f_o > f_o(1-f_o)$, because the weathering rate depends in an exponential fashion on pH (Adcock et al 2013) and the pH of seawater is 2.4 units higher than rainwater's.

[9] We will make use of the terrestrial boundaries on PAR, as well as those of the three- and four-photon processes envisaged by Wolstencroft & Raven (2002).

The two main sinks of phosphorus are burial of marine sediments and precipitation at hydrothermal vents (Paytan & McLaughlin 2007), showing the scaling law:

$$L_P \propto M \tag{6.19}$$

because of the ultimate dependence on the heat flow, related to planetary mass (Lingam & Loeb 2018). Making use of the mass-radius relation $M \propto R^{3.7}$ for rocky planets (Zeng et al 2016), we obtain:

$$\Pi_o \sim 4.9 \cdot 10^{13} \text{ kg yr}^{-1} \left[\left(\frac{1-f_o}{1-f_\oplus} \right) + 3.3 \cdot 10^{-3} \right] \left(\frac{f_o}{f_\oplus} \right)^2 \left(\frac{R}{R_\oplus} \right)^{0.3} \tag{6.20}$$

Since the totality of the ocean is considered to be productive and its area is clearly $\propto (R/R_\oplus)^2 \cdot (f_o/f_\oplus)$, the *productivity per unit area* π_o - which we will call *specific productivity* - scales with:

$$\pi_o \propto \left[\left(\frac{1-f_o}{1-f_\oplus} \right) + 3.3 \cdot 10^{-3} \right] \left(\frac{f_o}{f_\oplus} \right) \left(\frac{R}{R_\oplus} \right)^{-1.7} \tag{6.21}$$

This quantity is crucial, because it will be compared to F_{PAR} to establish the boundary between nutrient-limited and light-limited regimes.

Turning now our attention to the net primary production of lands Π_l, we notice that this quantity is dictated primarily by the access to water (Lingam & Loeb 2019a):

$$\Pi_l \sim 5.6 \cdot 10^{13} \text{ kg yr}^{-1} \left(\frac{f_o}{f_\oplus} \right) \left(\frac{1-f_o}{1-f_\oplus} \right) \left(\frac{R}{R_\oplus} \right)^2 \tag{6.22}$$

having assumed, for simplicity, that the whole production occurs on the fraction of land that actually receives precipitation. Being the productive land area $\propto (R/R_\oplus)^2 \cdot (f_o/f_\oplus) \cdot ((1-f_o)/(1-f_\oplus))$, the specific productivity π_l is independent of R and f_o:

$$\pi_l = costant \tag{6.23}$$

The subsequent step will be the conversion between NPP and biomass, mediated by the constants α_1 and α_2 defined in Section 6.4; then, the O_2 production rate is given by 6.11.

These considerations no longer apply when the stellar PAR flux is so weak to stop biomass growth before the nutrient limit is encountered. In this case, the net primary production is found by simply rescaling it from terrestrial values:

$$NPP_l = NPP_\oplus \left(\frac{F_{PAR}}{\tilde{F}_l} \right) \left(\frac{1-f_o}{1-f_\oplus} \right) \left(\frac{R}{R_\oplus} \right)^2 \tag{6.24}$$

$$NPP_o = NPP_\oplus \left(\frac{F_{PAR}}{\tilde{F}_o} \right) \left(\frac{f_o}{f_\oplus} \right) \left(\frac{R}{R_\oplus} \right)^2 \tag{6.25}$$

After distinguishing the cases in which light-limited and nutrient-limited conditions hold, the logical chain to be followed will be therefore:

$$\text{Integration of the star spectrum} \rightarrow \text{available PAR} \rightarrow NPP \rightarrow F_{bur}$$

in the former case, and

$$\text{Available nutrients} \rightarrow \text{biomass} \rightarrow NPP \rightarrow F_{bur}$$

in the latter.

Chapter 7

Setting the stage: Earth as a test case

"The Earth is a very small stage in a vast cosmic arena."
Carl Sagan, Pale Blue Dot, 1994

7.1 Experimental data

What was sketched in the previous chapter was the set of phenomena involved in production and consumption of O_2. Reconstructing in broad terms the oxygenation of the Earth will be theoretically feasible, provided that data on the oxygen levels are present. As we will see, this is not always ensured. Yet, a general understanding of the behaviour of the processes at work will allow to gauge parameters and obtain a reliable fit to be later extended to exoplanets.

7.1.1 Origin and evolution of the Earth's atmosphere

The primary atmosphere of a terrestrial planet directly forms from gravitationally captured gas from the surrounding protoplanetary nebula. The quantity of captured gas is unknown and probably case specific (Seager 2014), although a certain dependence on planet mass and gas temperature is intuitable. This atmosphere quickly undergoes escape of its lightest components (hydrogen and helium), retaining only little trace of hydrogen-bearing compounds like methane, ammonia and water.

A secondary atmosphere soon begins forming because of outgassing from an active young interior and, to a lesser extent, bombardment by asteroids and comets. Back in the protoplanetary disk, the solid rocky particles that were forming were partially coated by volatile molecules; as these particles stack together, growing more and more, these volatiles remained trapped in the protoplanetary embryos. The newly-formed planet hence includes, jealously hidden in its bowels, a significative inventory of volatiles. Differentiation of the interior, eventually leading to the formation of the mantle and the core, releases trapped gas as the rocks containing it melt. Outgassing from volcanoes in this early stage creates an atmosphere rich in *sticky* gases like CO_2, CO, N_2 and H_2O.

Sunlight can drive chemical reactions that consume some gases. Methane (CH_4) and ammonia (NH_3), in absence of a replenishing source, would have a lifetime of less than one million years (Kasting 1982; Kasting et al. 1983). Water, too, is unstable against sunlight and, if an ozone layer is absent, can be photolysed leading to hydrogen escape and oxygen buildup. The importance of this process as an abiotic source of oxygen has been already discussed in Chapter 3. A stronger solar wind and more severe far-UV and X fluxes from the early Sun also contributed to sculpt the atmosphere, carrying away gaseous molecules in the earliest phases of its development.

Following condensation of degassed water vapour, oceans began covering much of the planet's surface, perhaps as soon as 4.4 Gyr ago (Wilde et al. 2001). The main effect of liquid water on atmospheric evolution has been mentioned in Section 4.1: water acts like a catalyst for the Urey reaction (Equation 4.6), enhancing the weathering of silicates and the formation of carbonate deposits. At this point, the evolutionary histories of Earth and Venus forked: only on Earth was the process able to impede the accumulation of degassed CO_2 to levels that would have triggered a runaway greenhouse and caused a fast removal of the oceans. CO_2 has been since a minor component of a N_2-dominated atmosphere.

The appearance of life was the decisive event that shaped Earth's atmosphere to its present form. In the beginning, life was probably heterotrophic (Fenchel et al. 1998) and thermophilic (Baross & Hoffman 1985; Pace 1997). Long before photosynthesis evolved, some organisms developed chemical pathways to produce energy (Walker 1977; Margulis 1980; Wächtershäuser 1990), such as methanogenesis:

$$CO_2 + 4H_2 \rightarrow CH_4 + 2H_2O \tag{7.1}$$

exploiting the readily available hydrogen supply found in hydrothermal vents. As a consequence of their activity, methane atmospheric mixing ratio rose to $\sim 3 \cdot 10^{-3}$ (Kasting & Brown 1998; Claire et al. 2006).

It is thought that, at some point, some of these organisms evolved to adapt to shallower waters, where collection of sunlight was possible (Nisbet 1995; Nisbet & Fowler 1999; Des Marais 2000). The first photosynthetic beings, likely resembling modern purple bacteria and green sulphur bacteria (cf. Chapter 5), employed H_2S as reductant (Olson 2006); oxygenic photosynthesis arose later, together with cyanobacteria (Ward et al. 2016). When the latter first entered the stage, large fluxes of oxygen came in contact and promptly reacted with metals dissolved in the oceans forming insoluble iron oxides, which precipitated out, leaving thin layers on the ocean floor which we can see today in stratigraphic record as *banded iron formations*. Eventually, the Fe^{2+} supply ran out and the oceans became oxygenated. O_2 started leaking in the air, where it rapidly destroyed methane and accumulated, until an equilibrium with weathering of surface rocks was reached. This *Great Oxidation Event* ($\sim$ 2.4 Gyr ago) irreparably altered the weakly reducing properties of the atmosphere.

This event marks the starting point of our simulation. Let us focus now on the evolution of the oxidising atmosphere, comparing it with geological evidence.

7.1.2 The oxygen curve

Figure 8.1 represents the proposed time evolution of Earth's free oxygen levels. Rather than precise measurements of O_2 in time, it is constrained by the existence of some upper and/or lower thresholds in geological records; any quantitative consideration based on it is prone, therefore, to non-negligible errors.

The constraints on the oxygen mixing ratio r are:

- $t \approx 4.4$ Gyr ago: photochemical models indicate $r \sim 10^{-11}$;

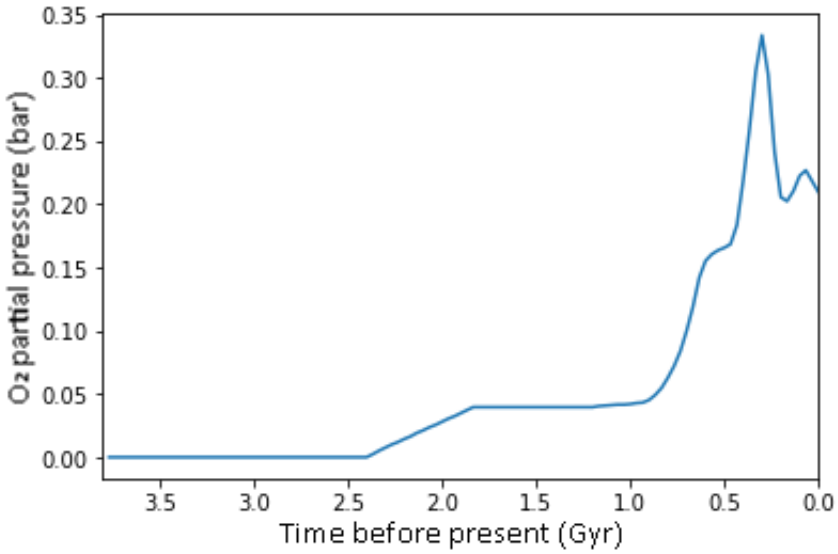

Figure 7.1: Time evolution of O_2 partial pressure. Adapted from Holland (2006)

- $t \approx 2.9$ Gyr ago: the existence of poly-sulphur (S8) aerosols and the mass-independent isotope fractionation in sulphur compounds (Zahnle et al. 2006; Kasting & Pavlov 2001; Pavlov & Kasting 2002) suggests $r < 2 \cdot 10^{-7}$;
- $t \approx 2.2$ Gyr ago: low sulphate concentrations require $r < 0.04$ (Canfield et al. 2000); paleosols begin showing evidence for oxidative weathering, suggesting $r > 0.01$ (Rye & Holland 1998);
- $t \approx 2.1$ Gyr ago: iodine incorporation into carbonates (Hardisty et al. 2014) requires $r > 9 \cdot 10^{-4}$;
- $t \approx 1.9$ Gyr ago: the proposed absence of oxidative weathering of chromium (Planavsky et al. 2014) sets $r < 2 \cdot 10^{-4}$;
- $t \approx 1.9$ Gyr ago: a photochemically stable ozone layer (Zahnle et al. 2006) requires $r > 6 \cdot 10^{-4}$; it conflicts with the previous one;
- $t \approx 0.6$ Gyr ago: macroscopic Ediacaran biota appear, suggesting $r > 0.02$;
- $t \approx 0.4$ Gyr ago: the presence of charcoal indicates that there was enough O_2 to ignite wood (Glasspool & Scott 2010): $r > 0.15$.

Following Holland (2006), the oxygenation history of our planet has been divided into 5 salient phases.

During stage 1 ($t > 2.45$ Gyr ago), free O_2 was virtually absent. The oceans were anoxic, too, since life relied on different chemical pathways to produce energy; some small "oxygen oases" may have been present during the last 200-300 Myr of this stage, following the appeareance of photosynthetical cyanobacteria (Brasier et al. 2006). Stage 2 ($2.45 < t < 1.85$ Gyr ago) was characterised by a sudden and steep rise in free O_2 known as *Great Oxidation Event*. The O_2 mixing ratio at the end of this phase is not known, but it is certainly within the range $0.02 < r < 0.2$. Stage 3 ($1.85 < t < 0.85$ Gyr ago) appears static, with no significant variation of O_2. The deep ocean was moderately oxygenated. During stage 4 ($0.85 < t < 0.54$ Gyr ago)

the Earth alternated unusually hot climates and its most severe ice ages (Hoffman & Schrag 2002); evolution sped up, culminating in the appearance of animals and the blossoming at the Cambrian–Precambrian boundary (Knoll et al. 2006; Conway Morris 2006). Observed δ^{13}C in marine carbonates points to an increase of carbon burial: O_2 levels greatly increased, almost approaching present levels (Berner 2004). Finally, stage 5 ($t < 0.54$ Gyr ago) began with the so-called *Cambrian Explosion*, the most extraordinary creative period of terrestrial life: in just 10-30 Myr, all modern animal phyla but one appeared (Bowring et al. 1993). As oxygen continued to rise, increasingly complex lifeform came into being, in an evolutionary arms-race which strongly stimulated genetic diversification. This pulled the trigger on land colonisation ($\sim$ 420 Myr ago). Just 30 million years later, great forests had appeared, skyrocketing photosynthetic production and oxygen levels $r \approx 0.35$ during the Permo–Carboniferous (Berner 2004) because of both biomass accretion and burial of matter rich in lignine, an insoluble structural polymer found in wood that long escaped decomposition by microorganisms (Robinson 1990). Evidence for this bump comes from the isotopic composition of fossil plants and from the short-lived presence of giant insects (Graham et al. 1995; Dudley 1998; Lane 2002). After reaching its highest value, oxygen decreased, perhaps following an irregular path, up to its present value of $r = 0.2096$.

7.1.3 Modern O_2 fluxes

We report here the estimates of O_2 sources and sinks at present time, taken from Catling & Kasting (2017). The fluxes will be evolved in time through the functions in Section 7.2. The reductant fluxes are weighted by their stoichiometric coefficients to yield the O_2 variation flux.

Name	Species	Flux (Tmol yr^{-1})	Stoichiometry	O_2 loss (Tmol yr^{-1})
	Surface volcanism			
	H_2	1 ± 0.5	$H_2 + 1/2O_2 \rightarrow H_2O$	0.5 ± 0.3
F_{volc}	CO	0.1 ± 0.05	$CO + 1/2O_2 \rightarrow CO_2$	0.05 ± 0.03
	H_2S	0.03 ± 0.015	$H_2 + 2O_2 \rightarrow H_2SO_4$	0.06 ± 0.03
	SO_2	1.8 ± 0.6	$H_2O + SO_2 + 1/2O_2 \rightarrow H_2SO_4$	0.9 ± 0.3
			subtotal	$\mathbf{1.5 \pm 0.7}$
	Submarine volcanism			
	H_2	0.1 ± 0.05	$H_2 + 1/2O_2 \rightarrow H_2O$	0.05 ± 0.03
F_{volc}	H_2S	0.28 ± 0.10	$H_2S + 2O_2 \rightarrow H_2SO_4$	0.6 ± 0.2
	CH_4 (axial)	0.01 ± 0.005	$CH_4 + 2O_2 \rightarrow CO_2 + 2H_2O$	0.02 ± 0.01
	CH_4 (off-axis)	0.03 ± 0.02	$CH_4 + 2O_2 \rightarrow CO_2 + 2H_2O$	0.06 ± 0.04
			subtotal	$\mathbf{0.7 \pm 0.3}$
	Surface metamorphism			
F_{abm}	CH_4 (abiotic)	0.3	$CH_4 + 2O_2 \rightarrow CO_2 + 2H_2O$	0.6
F_{thm}	CH_4 (thermogenic)	1.25	$CH_4 + 2O_2 \rightarrow CO_2 + 2H_2O$	2.5
			subtotal	**3.1**
	Serpentinisation			
F_{se}	Fe^{2+} oxid. (serpent.)	–	$3FeO + H_2O \rightarrow Fe_3O_4 + H_2$	0.2 ± 0.1
			subtotal	$\mathbf{0.2 \pm 0.1}$
			total $\mathbf{F_v}$	$\mathbf{-2.8 \pm 1.0}$
			total $\mathbf{F_{thm}}$	$\mathbf{-2.5}$
			total $\mathbf{F_{se}}$	$\mathbf{-0.2 \pm 0.1}$
			Total sink	$\mathbf{-5.5 \pm 1.1}$

Table 7.1: O_2 sinks from volcanism, metamorphism and serpentinisation.

Name	Species	Weight (%)	Stoichiometry	O_2 gain (Tmol yr^{-1})
F_{oc}	Organic carbon burial	0.6 ± 0.1 as C^0	$CO_2 \rightarrow C + O_2$	10 ± 1.7
F_{pyr}	Pyrite burial	0.4 ± 0.1 as S^{2-}	$Fe(OH)_3 + 2H_2SO_4 \rightarrow FeS_2 + 15/4O_2 + 7/2H_2O$	4.7 ± 1.2
$F_{Fe^{2+}}$	Fe^{2+} burial	1.6 ± 0.6 as FeO	$1/2Fe_2O_3 \rightarrow FeO + 1/4O_2$	1.1 ± 0.4
			Total F_{bur}	$\mathbf{15.8 \pm 3.3}$

Table 7.2: O_2 sources from burial.

Name	Process	Weight (%)	Stoichiometry	O_2 loss (Tmol yr^{-1})
	Continental weathering			
F_{cw}	Organic carbon weath.	0.45 ± 0.1 as C^0	$C + O_2 \rightarrow CO_2$	7.5 ± 1.7
F_{sw}	Sulphide weath.	0.3 ± 0.1 as S^{2-}	$FeS_2 + 15/4O_2 + 7/2H_2O \rightarrow Fe(OH)_3 + 2H_2SO_4$	3.5 ± 1.2
F_{Few}	Fe^{2+} weath.	1.9 ± 0.6 as FeO	$FeO + 1/4O_2 \rightarrow 1/2Fe_2O_3$	1.3 ± 0.4
	Seafloor+hydr. Fe oxid.			
F_{sf}	Fe^{2+} oxid. (sulphate)	–	$6FeO + O_2 \rightarrow 2Fe_3O_4$	0.14 ± 0.07
	hydroth. Fe^{2+} oxid.	0.25 ± 0.09	$2FeO + 1/2O_2 \rightarrow Fe_2O_3$	0.06 ± 0.02
			Total F_{weath}	$\mathbf{-12.2 \pm 3.4}$

Table 7.3: O_2 sinks from weathering.

We see that $F_{source} \approx F_{sink}$: they are compatible within 0.4 σ. They actually *have* to be so, because a difference of ~ 1 Tmol yr^{-1} would deplete the whole atmospheric reservoir in just ~ 40 Myr. So, it was adopted a value of 17.7 Tmol yr^{-1} for the present source flux, too.

7.2 Sources vs sinks: the equations

Let R be the amount of oxygen in the atmosphere, B the living biomass. F always indicates a flux. For an explanation to the functional form used to model the different processes, see Chapter 6. A list of abbreviations will be provided at the end of this chapter for the sake of clarity.

The oxygen flux at time t is given by summing sources and sinks:

$$\frac{dR}{dt} = F_{source} + F_{sink} = F_{bur} + (F_{volc} + F_{meta} + F_{weath}) \tag{7.2}$$

where of course every sink has a negative value. Every contribution will be evaluated below.

Burial

$$F_{bur} = F_{oc} + F_{pyr} + F_{Fe^{2+}} \tag{7.3}$$

$$F_{oc}(t) = \frac{1000}{30}[S_{land} \cdot B_{land}(t) + S_{ocean} \cdot B_{ocean}(t)] \tag{7.4}$$

$$F_{pyr}(t) = \frac{4.7}{10}\frac{1000}{30}[S_{land} \cdot B_{land}(t) + S_{ocean} \cdot B_{ocean}(t)] \tag{7.5}$$

$$F_{Fe^{2+}}(t) = \frac{1.1}{10}\frac{1000}{30}[S_{land} \cdot B_{land}(t) + S_{ocean} \cdot B_{ocean}(t)] \tag{7.6}$$

where $S_{land} = 3.6 \cdot 10^{-4} yr^{-1}$, $S_{ocean} = 0.1421 yr^{-1}$.

Weathering

$$F_{weath} = F_{cw} + F_{sw} + F_{Few} + F_{sf} \tag{7.7}$$

evolving in time as a function of the oxygen level:

$$F_{weath}(t) = -k_w \cdot [O(t)]^{\beta} \tag{7.8}$$

k_w and β are treated as free parameters, with the caveat that $F_{weath}(t_{now}) = 12.2$ Tmol yr^{-1}.

Volcanism

$$F_{volc}(t) = -F_{volc,0} e^{-\frac{t+2.1}{\tau}} \tag{7.9}$$

where $\tau = 4.4 \cdot 10^9$ yr.

Metamorphism

$$F_{meta} = F_{sm} + F_{se} \tag{7.10}$$

$$F_{sm} = F_{abm} + F_{thm} \tag{7.11}$$

while abiotic methane obeys the same law as volcanic emissions:

$$F_{abm} = -F_{CH_4,0} \cdot e^{-\frac{t+2.1}{\tau}}, \tag{7.12}$$

We may define $F_0 := F_{volc,0} + F_{CH_4,0}$ and $F_v := F_{volc} + F_{abm}$, so that:

$$F_v = -F_0 \cdot e^{-\frac{t+2.1}{\tau}}. \tag{7.13}$$

Catling & Kasting (2017) compute an amount ~ 11 Tmol yr^{-1} of hydrogen equivalents (including abiotic methane, but excluding SO_2) for the early Earth; accounting for SO_2, rescaled from its current value through the exponential in eq. (7.9), we obtain a H_2 equivalent flux of ~ 16.10 Tmol yr^{-1}, corresponding to an early oxygen consumption $F_0 = -8.05$ Tmol yr^{-1} (2 moles of H_2 are required to remove 1 mole of O_2).

Thermogenic methane is assumed to be released whenever some the buried biomass reaches conditions of temperature and pressure that trigger metamorphism. Assuming that the time lag between burial and methanogenesis is negligible with respect to the timescales we consider, we can write:

$$F_{thm} = -\frac{2.5}{30} \cdot [S_{ocean} \cdot B_{ocean} + S_{land} \cdot B_{land}]. \tag{7.14}$$

The factor 2.5 is found by imposing that the present biomass yields a methane flux of 2.5 Tmol yr^{-1}.

Finally, serpentinisation evolves through equation:

$$F_{se} = -k_{so} \cdot \left(\frac{4.5}{t + 2.1} \right)^{0.7} \tag{7.15}$$

where $k_{so} = 0.2$ Tmol $\mathrm{yr}^{-1} = 4 \cdot 10^8$ Tmol Gyr^{-1}.

Biomass evolution

$$B(t) = B_0 + \frac{B_1}{1 + e^{-\lambda_1 (t - t_1)}} + \frac{B_2}{1 + e^{-\lambda_2 (t - t_2)}} + \frac{B_3}{1 + e^{-\lambda_3 (t - t_3)}} + \frac{B_4}{1 + e^{-\lambda_4 (t - t_4)}} \tag{7.16}$$

in order to take into account up to four different episodes of biomass accretion. The limit of B as $t \to \infty$ is $B_0 + B_1 + B_2 + B_3 + B_4$. The parameters B_0, B_1 and B_2 were considered as purely oceanic, because they predate colonisation of land; $B : 3$ was treated as a purely land term, while B_4 was allowed to represent both of them. The parameters $\{k_i\}$ are related to the rapidity of the exponential growth, while the $\{t_i\}$ represent the central time of the accretion episodes.

7.3 Simulations

Having discussed the sources and sinks of oxygen in Chapter 6 and presented the related equations in Section 7.2, let us now recall the fundamental equation used to reconstruct the evolution of oxygen:

$$\frac{dR}{dt} = F_{source} + F_{sink} \tag{7.17}$$

Direct integration of all the equations but (7.8) was used to retrieve the atmospheric $O_{2,nw}$, were weathering non-existent, at each step ($\Delta t = 1$ Myr); then, the real O_2 profile was reconstructed by applying the bisection method to the equation:

$$f(R) = R + \left(\frac{R + R[i-1]}{2} \right)^{\beta} \cdot k_w \cdot \Delta t - O_{2,nw}[i] + (O_{2,nw}[i-1] - R[i-1]) \tag{7.18}$$

The simulation was chosen to start at 2.4 Gyr ago, i.e. at the beginning of the GOE, because whenever $R = 0$ there is no way to know the amount by which sinks exceed sources without possessing additional information. Therefore, $t = 2.4$ corresponds to present time.

The free parameters of the model are:

- biomass: B_0, B_1, B_2, B_3, B_4, λ_1, λ_2, λ_3, λ_4;
- weathering: k_w, β.

A grid was defined for each of them:

$$\begin{aligned}
&B_0 \in [10^7, 3 \cdot 10^{14}] \text{ kg} && B_1 \in [10^7, 3 \cdot 10^{14}] \text{ kg} \\
&B_2 \in [10^8, 10^{15}] \text{ kg} && B_3 \in [10^8, 10^{15}] \text{ kg} \\
&B_4 \in [-10^{15}, -10^8] \text{ kg} && \lambda_1 \in [1, 100] \text{ Gyr}^{-1} \\
&\lambda_2 \in [1, 100] \text{ Gyr}^{-1} && \lambda_3 \in [1, 100] \text{ Gyr}^{-1} \\
&\lambda_4 \in [1, 100] \text{ Gyr}^{-1} && k_w \in [1 \cdot 10^{-4}, 5 \cdot 10^{-4}] \text{ Tmol}^{1-\beta} \text{ yr}^{-1} \\
&\beta \in [0.3, 1]
\end{aligned}$$

The $\{B_i\}$ and the $\{\lambda_i\}$ are logarithmically spaced, while the remaining ones are linearly spaced. The $\{t_i\}$ were slightly varied around the values:

$$t_1 \approx 0.4 \text{ Gyr}, t_2 \approx 1.8 \text{ Gyr}, t_3 \approx 2 \text{ Gyr}, t_4 \approx 2.2 \text{ Gyr}.$$

The recovered $R[j]$ at each sampling step j was compared to data $y[j]$ (Figure 7.1) and the quantity:

$$\zeta = \sum_j (R[j] - y[j])^2 \tag{7.19}$$

was computed for each combination. A lower ζ means, intuitively, a better fit to the curve. The best 101 solutions out of $\sim 100,000$ were then bred to create 4950 genetic combinations. The genetic algorithm was applied iteratively to the best combinations of parameters, until there was no more a significant decrease of ζ. At this point, a perturbative approach was applied to the best solution (each parameter was varied by $\pm 20\%$ at the first run), making the variations smaller and smaller as the curve approached the solution.

The final results of the parameters were:

Parameter	value	unit of measurement
B_0	$7 \cdot 10^{11}$	kg
B_1	$4 \cdot 10^{11}$	kg
B_2	$7.91 \cdot 10^{11}$	kg
B_3	$4.5 \cdot 10^{14}$	kg
B_4	$-8.91 \cdot 10^{11}$	kg
λ_1	10.0	Gyr^-1
λ_2	25.0	Gyr^-1
λ_3	33.4	Gyr^-1
λ_4	90.3	Gyr^-1
t_1	0.10	Gyr
t_2	1.68	Gyr
t_3	2.03	Gyr
t_4	2.14	Gyr
β	0.75	–
k_w	$2.52 \cdot 10^{-5}$	$\text{Tmol}^{0.25}$ yr^{-1}

Table 7.4: Parameters of the best simulation.

and the best-fitting curve is shown in Figure 7.2.

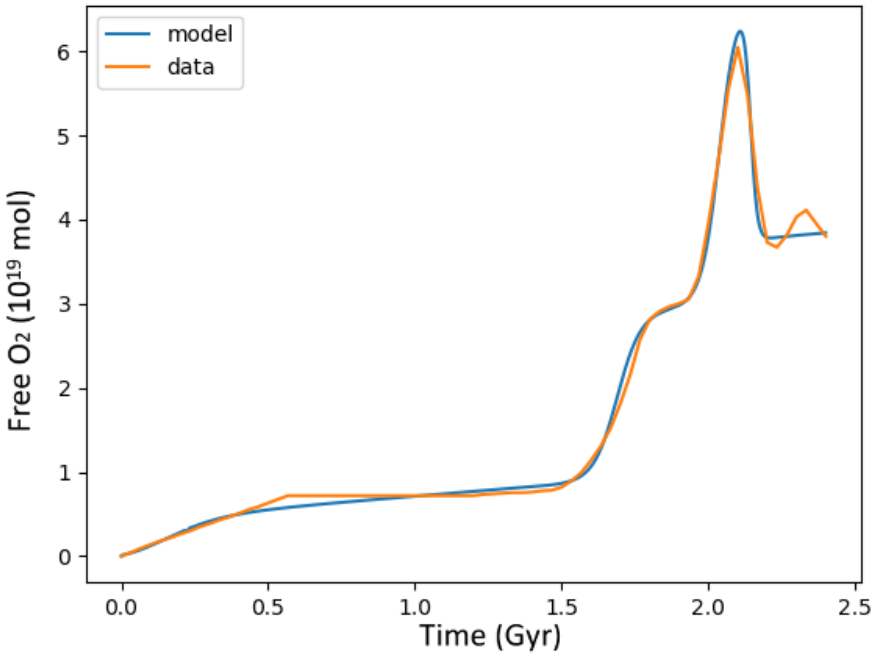

Figure 7.2: The oxygen curve.

The computed total, land and ocean biomass are plotted in Figures 7.3, 7.4 and 7.5.

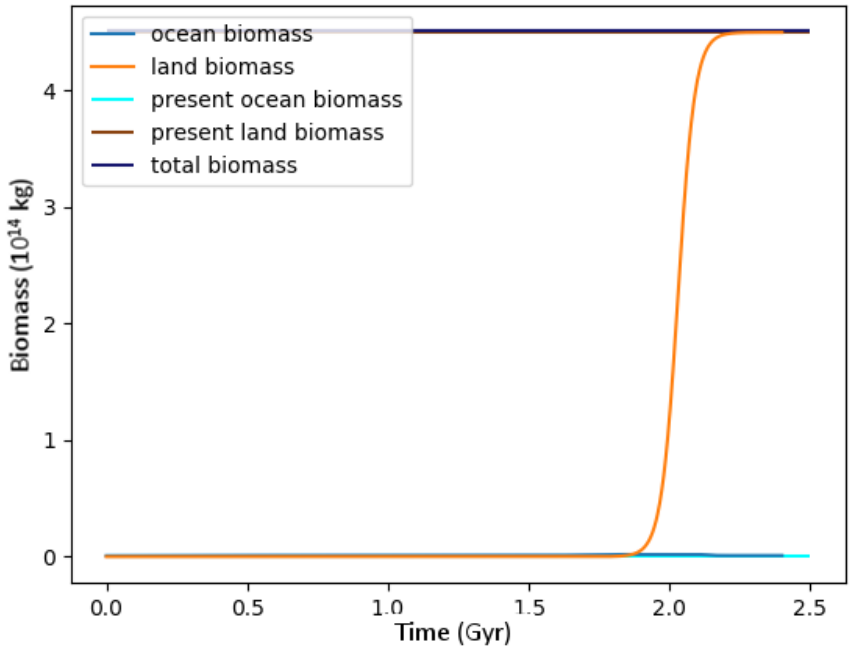

Figure 7.3: Biomass evolution in time. Present terrestrial values are shown as horizontal lines.

Interestingly enough, the best fit attributed the whole biomass depletion episode, modelled by B_4, to ocean biomass.

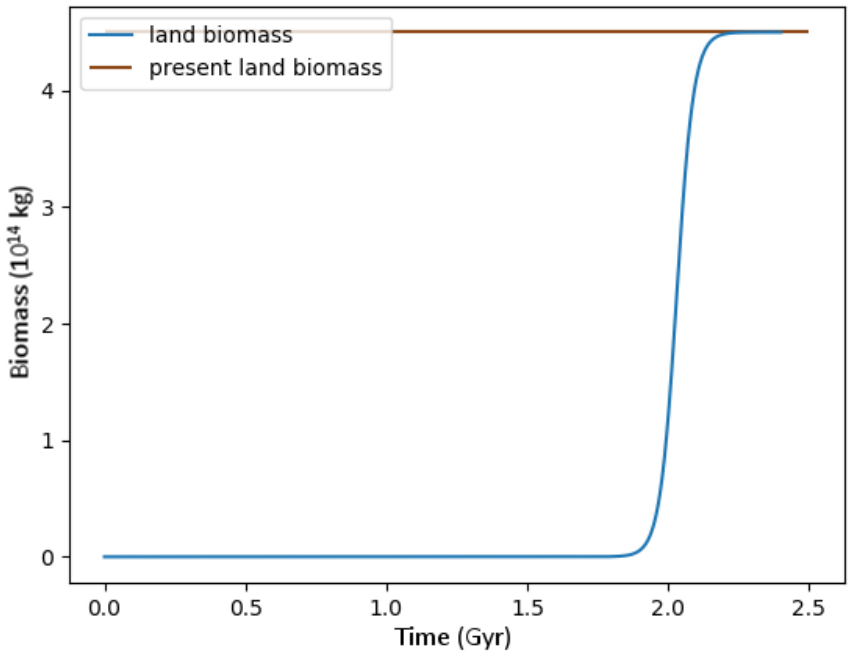

Figure 7.4: Land biomass evolution.

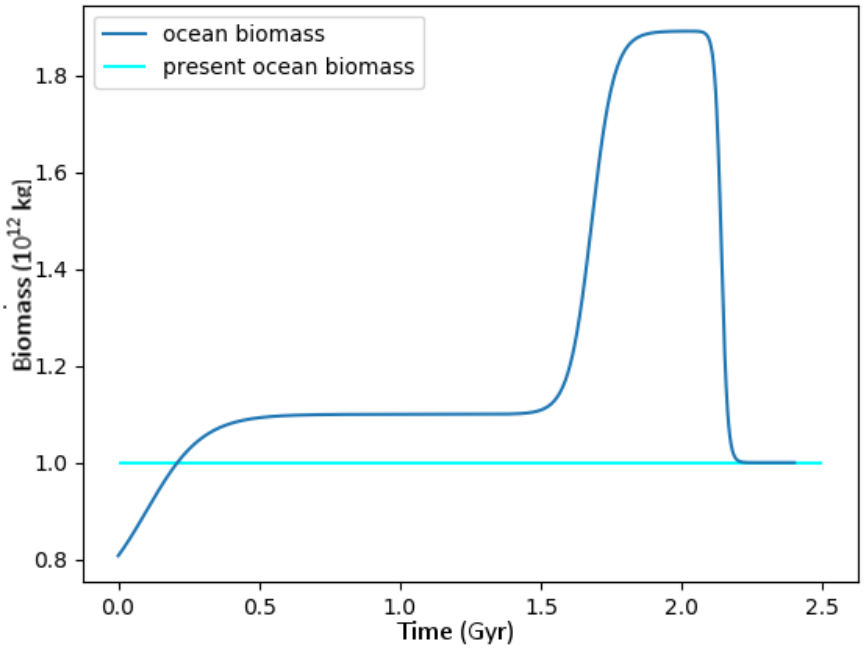

Figure 7.5: Ocean biomass evolution.

Having tuned our model to reproduce the evolution of Earth's free O_2, we will now attempt to extrapolate it to exoplanets. We choose to postpone the discussion of the results from this chapter to Chapter 9.

Appendix: list of abbreviations

F_{bur}: burial of organic or reduced material
B_{land}: land biomass
B_{ocean}: ocean biomass
F_{volc}: volcanic gas flux
F_{meta}: metamorphic degassing
F_v: volcanic+abiotic CH_4 flux
F_{weath}: weathering of organic or reduced material
F_{oc}: burial of organic carbon
F_{pyr}: burial of pyrite (sulphides)
$F_{Fe^{2+}}$: burial of Fe^{2+}
F_{cw}: carbon weathering
F_{sulfw}: sulphide weathering
F_{Few}: Fe^{2+} weathering
F_{sm}: surface metamorphism
F_{sf}: seafloor and hydrothermal iron oxidation
F_{se}: serpentinisation
$F_{CH_{4,ab}}$: abiotic CH_4
$F_{CH_{4,th}}$: thermogenic CH_4

Chapter 8

Planetary models

"Imagination will often carry us to worlds that never were, but without it we go nowhere."

Carl Sagan, Cosmos, 1980

Having calibrated the model to fit the oxygenation history of our planet, we can now move on to the analysis of exoplanets in which some kind of *Earth-like light-harvesting organism* (cf. Section 2.3) has evolved. The equations describing abiotic processes, shown in Section 7.2, will be generalised to planets different from Earth in Section 8.1, while the biomass-dependent term requires more attention and will be the focus of Section 8.2.

8.1 Scaling laws

Weathering

Weathering is, as we have seen, the oxidation of surface rocks operated by free oxygen. Increasing the land fraction of a planet means exposing to O_2 a larger amount of material: it is reasonable to think that $F_{weath} \propto (1 - f_o)/(1 - f_\oplus)$. If we assume that the surface density of substances undergoing weathering does not vary with planet size, their total amount N_w scales with R^2. However, fixing N_{O_2}, the number of moles of free O_2, with increasing R molecules have to spread over a larger area, so their surface density decreases as R^{-2}. Since we have found that $F_{weath} \propto [O_2]^{0.75}$:

$$F_{weath} \propto N_w \cdot [O_2]^{0.75} = k \cdot N_{w,\oplus} \left(\frac{R}{R_\oplus}\right)^2 \left[N_{O_2,\oplus} \cdot \left(\frac{R}{R_\oplus}\right)^{-2}\right]^{0.75} \propto \left(\frac{R}{R_\oplus}\right)^{0.5} \tag{8.1}$$

Hence, we can write:

$$F_{weath} = F_{weath,\oplus} \cdot \left(\frac{R}{R_\oplus}\right)^{0.5} \left(\frac{1 - f_o}{1 - f_\oplus}\right) \tag{8.2}$$

Serpentinisation

Increasing the fraction of water coverage results, of course, in an increase of submarine reactions like serpentinisation. The process fundamentally relies on fresh Fe^{2+} supplies coming from the

newly-formed crust. In presence of plate tectonics, this renewal is far more efficient and can be described by the equation:

$$F_{Fe^{2+}} = C_n \rho f_{FeO} \tag{8.3}$$

where C_n is the crust formation rate, equal to $C_n = l \cdot d \cdot S_c$, product of the total length of the ridges l, the average thickness of the crust d and S_c the crust spreading rate[1] (Guzmán-Marmolejo et al. 2013). Assuming Earth-like values for $f_{FeO} \sim 6{-}10\%$ (Taylor and McLennan, 1985; Condie, 1997), $\rho \approx 3 \cdot 10^3$ kg m^{-3} and the fraction of newly-delivered iron actually experiencing serpentinisation, the value of this contribution for exoplanets[2] is determined by the scaling laws for l, d and S_c, which, according to Valencia et al. (2007), are:

$$l = l_\oplus \cdot M^{0.28} \tag{8.4}$$

$$d = d_\oplus \cdot M^{-0.45} \tag{8.5}$$

$$S_c = S_{c,\oplus} \cdot M^{1.19} \tag{8.6}$$

Recalling the mass-radius proportionality for rocky planets, $M \propto R^{3.7}$, we have:

$$F_{se} \propto \left(\frac{f_o}{f_\oplus}\right) \cdot M^{1.02} \propto \left(\frac{f_o}{f_\oplus}\right) \cdot R^{3.774} \tag{8.7}$$

Volcanism

Assuming that the rate of outgassing depends on the contact area between the lithosphere and the mantle, F_v should scale as $(R/R_\oplus)^2$. However, as we have seen in Section 4.2, larger planets have longer cooling times because of a lower surface/volume ratio; hence, τ too scales with $R/R_\oplus$:

$$F_v = F_0 \cdot e^{-\frac{t}{\tau(R/R_\oplus)}} \cdot \left(\frac{R}{R_\oplus}\right)^2 \tag{8.8}$$

8.2 Biomass

As we have seen, biomass growth is eventually limited by the availability of light and nutrients. Since the current net primary productivity of Earth's land biomass can be sustained by a PAR flux as low as $\tilde{F}_l \approx 3.26 \cdot 10^{20}$ photons m^{-2} s^{-1} (Field et al 1998), some $\sim 40\%$ of the actual $F_{PAR,\oplus}$, while the oceanic biomass requires even lower supplies ($\tilde{F}_o = 7.35 \cdot 10^{19}$ photons m^2 s^{-1}), nutrients are the limiting factor for Earth's life.

The question whether an Earth clone orbiting a star different from the Sun could sustain an Earth-like biomass needs comparison between these minimum energy requirements and the PAR flux reaching its surface (cf. Lehmer et al. 2018). Operating a clear distinction between the two cases will prove valuable to build different models in Section 8.3.

As a starting point, the synthetic spectra presented in Section 6.1.2 were integrated between 400 and 700 nm to yield the amount of PAR received at the distance where the bolometric flux of the star equals the one impacting on Earth, $d(1F_\oplus)$. The results are shown in table 8.1.

[1] It is a geologic process consisting in the slow addition of new oceanic crust at the mid-oceanic ridges, which pushes the older crust away. Proposed by Hess (1962), it is the ultimate cause of the Continental Drift Theory (Wegener 1912).

[2] Under the assumption that plate tectonics is active. See Section 4.2 for a discussion on this topic.

Spectral class	T_{eff}	$d(AU)$	PAR flux
F0	7400	2.81	$1.67 \cdot 10^{21}$
G0	6000	1.31	$1.55 \cdot 10^{21}$
G2	5772	1.00	$1.46 \cdot 10^{21}$
K0	4900	0.74	$1.37 \cdot 10^{21}$
K2	4620	0.63	$1.24 \cdot 10^{21}$
K3	4480	0.58	$1.15 \cdot 10^{21}$
K4	4340	0.56	$1.05 \cdot 10^{21}$
K5	4200	0.52	$9.46 \cdot 10^{20}$
K7	3920	0.43	$8.12 \cdot 10^{20}$
M0	3500	0.36	$6.21 \cdot 10^{20}$
M1	3333	0.25	$5.40 \cdot 10^{20}$
M2	3167	0.18	$4.50 \cdot 10^{20}$
M3	3000	0.13	$2.97 \cdot 10^{20}$
M4	2833	0.10	$1.91 \cdot 10^{20}$
M5	2667	0.08	$9.52 \cdot 10^{19}$
M6	2500	0.07	$4.12 \cdot 10^{19}$

Table 8.1: PAR flux (photon m^{-2} s^{-1}) at $d = d(1F_{\oplus})$ for MS stars of different spectral classes.

A subtler question is the computation of the limit distances d_l and d_o at which F_{PAR}=$\tilde{F}_l$ and $F_{PAR} = \tilde{F}_o$, marking the boundary between a nutrient-limited and a light-limited regime. The results are provided in Table 8.3. However, these distances, *per se*, are not particularly informative: a comparison needs being performed with the boundaries of the habitable zones of the respective stars[3]. The fluxes delimiting the HZ scale with the stellar effective temperature T according to the relation:

$$S_{eff} = S_{eff\odot} + a(T - 5780K) + b(T - 5780K)^2 + c(T - 5780K)^3 + d(T - 5780K)^4 \qquad (8.9)$$

(Kopparapu et al. 2013). The values of the parameters can be found in table 8.2.

	Inner edge	Outer edge
$S_{eff\odot}$	1.0512	0.3438
a	$1.3242 \cdot 10^{-4}$	$5.8942 \cdot 10^{-5}$
b	$1.5418e \cdot 10^{-8}$	$1.6558 \cdot 10^{-9}$
c	$-7.9895 \cdot 10^{-12}$	$-3.0045 \cdot 10^{-12}$
d	$-1.8328 \cdot 10^{-15}$	$-5.2983 \cdot 10^{-16}$

Table 8.2: Parameters to be inserted in Equation 12.1, taken from Kopparapu et al. (2013).

[3]The "runaway greenhouse limit" and the "maximum greenhouse limit" have been chosen as inner and outer edge, respectively. See Section 4.1 for details.

The positions of d_l and d_o with respect to the habitable zone are shown graphically in Figure 8.1.

Spectral class	d_l	d_o	Inner edge	Outer edge
F0	5.74	12.08	2.51	4.31
G0	2.58	5.44	1.26	2.20
G2	1.92	4.04	0.97	1.70
K0	1.37	2.89	0.76	1.36
K2	1.13	2.37	0.66	1.19
K3	0.99	2.09	0.60	1.10
K4	0.91	1.92	0.58	1.07
K5	0.80	1.69	0.54	1.01
K7	0.63	1.32	0.46	0.86
M0	0.45	0.94	0.38	0.72
M1	0.29	0.62	0.27	0.51
M2	0.19	0.41	0.19	0.37
M3	0.12	0.25	0.14	0.28
M4	0.07	0.15	0.11	0.22
M5	0.04	0.08	0.09	0.17
M6	0.02	0.05	0.07	0.15

Table 8.3: Maximum distances at which a planet can sustain an Earth-like land (d_l) and ocean (d_o) biomass.

Looking at table 8.3, we can see that stars earlier than K2 have enough photons in their habitable zones to sustain an Earth-like biomass. On the other hand, planets in the HZ of stars of spectral class ≥M5 are light-limited. The situation in between is blurred, with planets usually having enough photons for oceanic biomass but not terrestrial biomass.

These results, though, assume that the nutrient availability is the same as Earth. Its dependence on planet mass and ocean coverage will be thoroughly examined in Section 8.2.2.

8.2.1 Effect of enhanced photosynthetic response

Let us now hypothesise that life forms can evolve light-harvesting complexes like those discussed by Wolstencroft & Raven (2002) (see Chapter 5). The analysis shown above still holds, but the upper limit of PAR shall be moved to 1050 nm for a photosystem employing 3 photons per CO_2 and to 1400 nm for a four-photon photosystem. The photon energy scaling parameter ε:

$$\varepsilon = \begin{cases} 1 & \text{for } 300 < \lambda \leq 700 \text{ nm} \\ 2/3 & \text{for } 700 < \lambda \leq 1050 \text{ nm} \\ 1/2 & \text{for } 1050 < \lambda \leq 1400 \text{ nm} \end{cases}$$

has been introduced to properly account for the varying photon requirements.

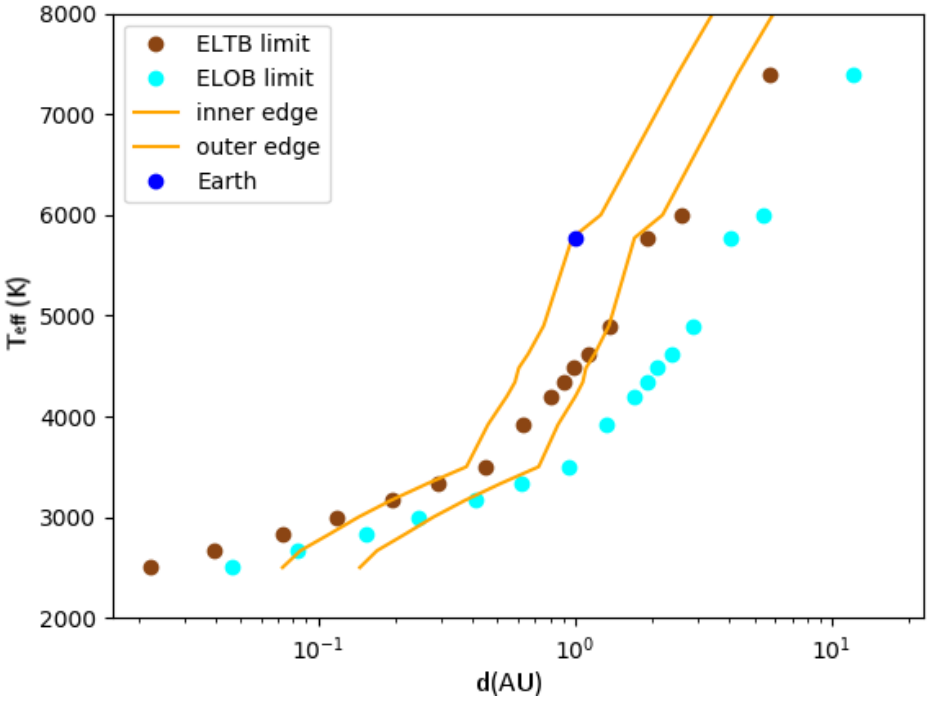

Figure 8.1: Orbital limits for a land (ELTB) and ocean (ELOB) biosphere that is limited by nutrients, compared with the boundaries of the habitable zone.

The maximum distances at which an Earth-like biomass can thrive are clearly larger, because of the extended harvesting capability. They are shown in the subsequent Table 8.4 and, graphically, in Figures 8.2 and 8.3.

Spectral class	$d_{l,3}$	$d_{o,3}$	$d_{l,4}$	$d_{o,4}$	Inner edge	Outer edge
F0	7.23	15.23	7.76	16.35	2.51	4.31
G0	3.47	7.31	3.82	8.05	1.26	2.20
G2	2.62	5.51	2.92	6.14	0.97	1.70
K0	1.93	4.07	2.17	4.58	0.76	1.36
K2	1.63	3.42	1.86	3.93	0.66	1.19
K3	1.47	3.10	1.70	3.58	0.60	1.10
K4	1.40	2.95	1.64	3.45	0.58	1.07
K5	1.28	2.69	1.51	3.18	0.54	1.01
K7	1.07	2.25	1.27	2.68	0.46	0.86
M0	0.80	1.69	1.00	2.11	0.38	0.72
M1	0.56	1.19	0.70	1.48	0.27	0.51
M2	0.39	0.82	0.50	1.06	0.19	0.37
M3	0.28	0.59	0.37	0.78	0.14	0.28
M4	0.20	0.42	0.28	0.59	0.11	0.22
M5	0.13	0.27	0.20	0.42	0.09	0.17
M6	0.10	0.20	0.17	0.35	0.07	0.15

Table 8.4: Same as table 9.3, but with the PAR window extended up to 1050 nm (2^{nd} and 3^{rd} column) or 1400 nm (4^{th} and 5^{th} column).

The possibility to harvest near-infrared light, which is exactly where the emission of M stars peaks, is reflected in much larger values for d_l and d_o. If a three-photon system is present, ocean biomass is always nutrient-limited, while an Earth-like land biomass is sustainable by stars as cool as M3 and even, in some cases, on planets around M4, M5 and M6, depending on their position in the HZ. In case of a four-photon system, neither oceanic nor land biomass it at risk is of running out of light.

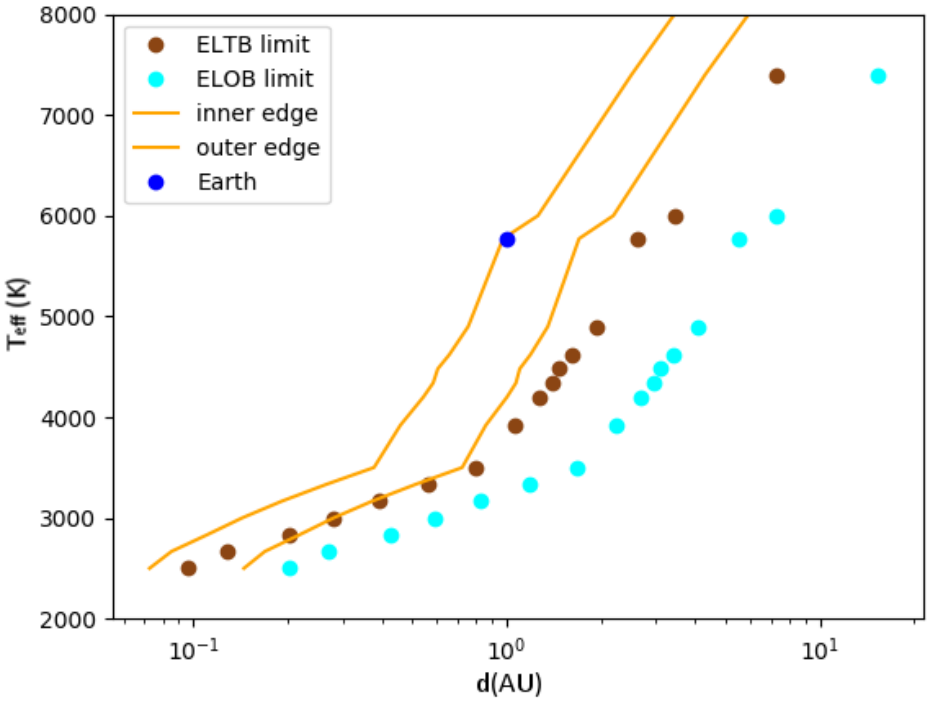

Figure 8.2: Land and ocean habitability with a PAR extended up to 1050 nm, compared with the boundaries of the habitable zone.

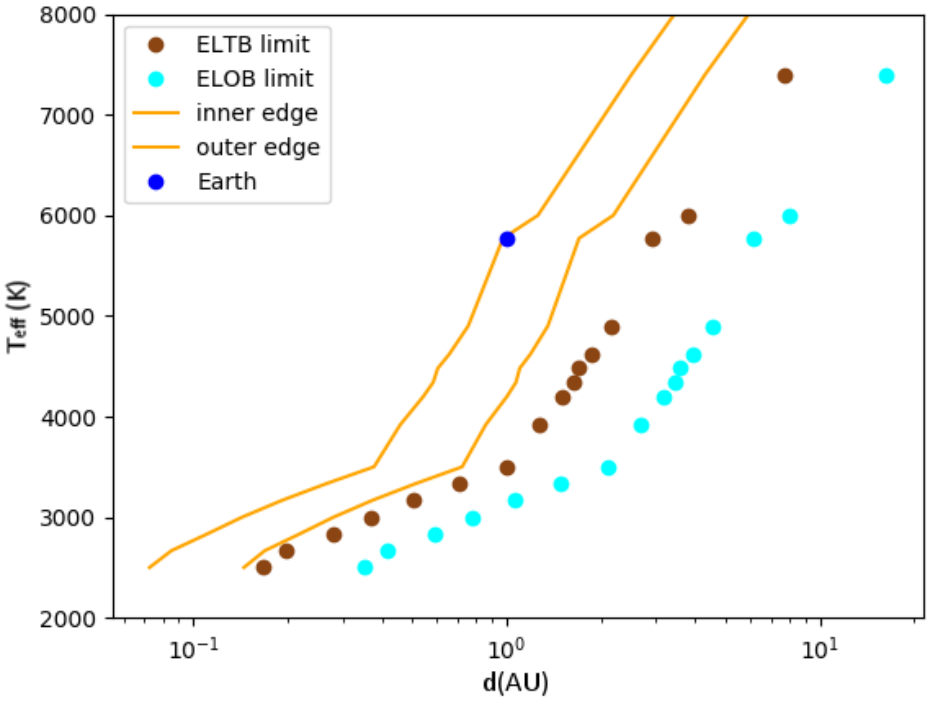

Figure 8.3: Land and ocean habitability with a PAR extended up to 1400 nm, compared with the boundaries of the habitable zone.

8.2.2 Effect of planetary mass and water coverage

The nutrient limits $\tilde{F}_l$ and $\tilde{F}_o$ introduced in the previous section are, of course, Earth-specific. Can an attempt be made to generalise them to different planets? Recalling Section 6.5, the availability of nutrients depends sensitively on the planetary radius and the fraction of surface covered by oceans (Lingam & Loeb 2019a). The behaviours of land and ocean productivity, though, are different (eq. 6.21 and 6.23):

$$\pi_o \propto \left[\left(\frac{1-f_o}{1-f_\oplus}\right) + 3.3 \cdot 10^{-3}\right] \left(\frac{f_o}{f_\oplus}\right) \left(\frac{R}{R_\oplus}\right)^{-1.7} \tag{8.10}$$

$$\pi_l = costant \tag{8.11}$$

The boundary between nutrient-limited and light-limited regimes is encountered when the stellar flux equates the minimum energy requirements for organisms at their maximum density allowed by nutrient availability:

$$F_{PAR} = \tilde{F}_l \propto \pi_l \tag{8.12}$$

for land, and

$$F_{PAR} = \tilde{F}_o \propto \pi_o \tag{8.13}$$

for oceans. From this moment forward, we denote by $\tilde{F}_l$ and $\tilde{F}_o$ the minimum energy requirements of the exoplanet under study, and by $\tilde{F_{l,\oplus}}$ and $\tilde{F_{o,\oplus}}$ the corresponding terrestrial values. Hence:

$$\tilde{F}_l \equiv \tilde{F}_{l,\oplus} \tag{8.14}$$

$$\tilde{F}_o = \frac{\tilde{F}_{o,\oplus}}{1 + 3.3 \cdot 10^{-3}} \cdot \left[\left(\frac{1 - f_o}{1 - f_\oplus} \right) + 3.3 \cdot 10^{-3} \right] \left(\frac{f_o}{f_\oplus} \right) \left(\frac{R}{R_\oplus} \right)^{-1.7} \tag{8.15}$$

Any radius increase makes more likely that a nutrient-limited state is in force for ocean life, pushing outwards the light-limited orbital distance (Figure 8.4). The increase in ocean biomass, consequently, is extremely faint ($\propto R^{0.3}$), more than outweighted by the increase of volcanic sinks ($\propto R^2$, cf. Equation 8.4). If life is confined to marine environments, the situation becomes detrimental for oxygen buildup, as we will see in Section 8.3.

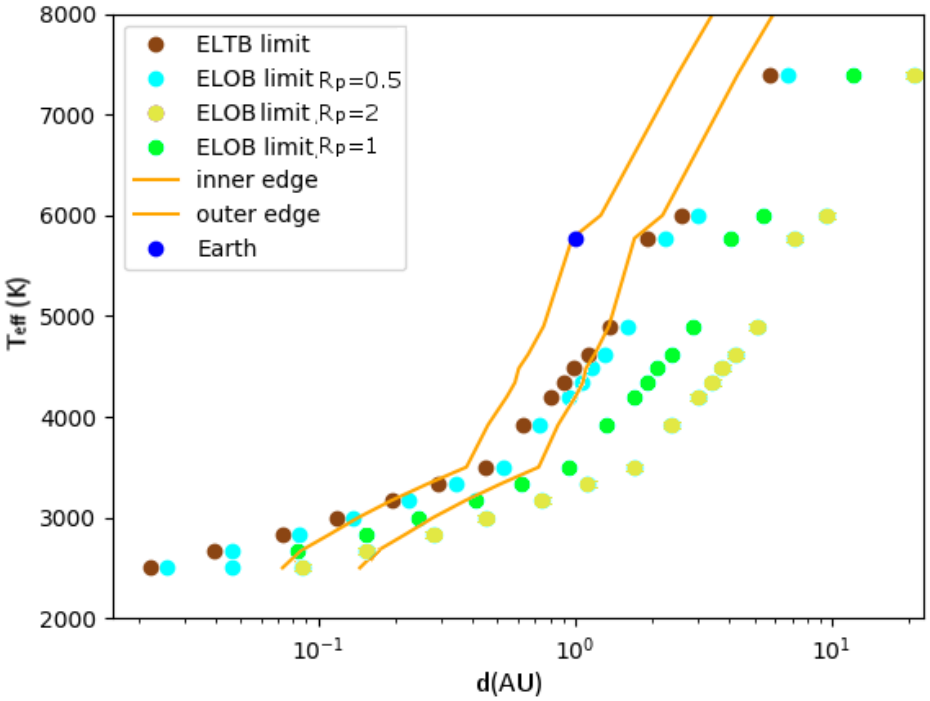

Figure 8.4: Effect of a variation of the planetary radius on $\tilde{F}_o$.

As concerns the ocean fraction f_o, the terrestrial specific productivity is again unperturbed, while the ocean one drops if f_o significantly departs from 0.5: $f_o \cdot (1 - f_o)$ is equal to 0.25 if f_o=0.5 and still to 0.21 if $f_o = f_\oplus = 0.7$, but it is just 0.09 if $f_o = 0.9$. The global production of ocean worlds is seriously hindered; at the other hand, decreasing f_o does not result in an enhanced land production because of the increase of dry lands (cf. Section 6.5.1).

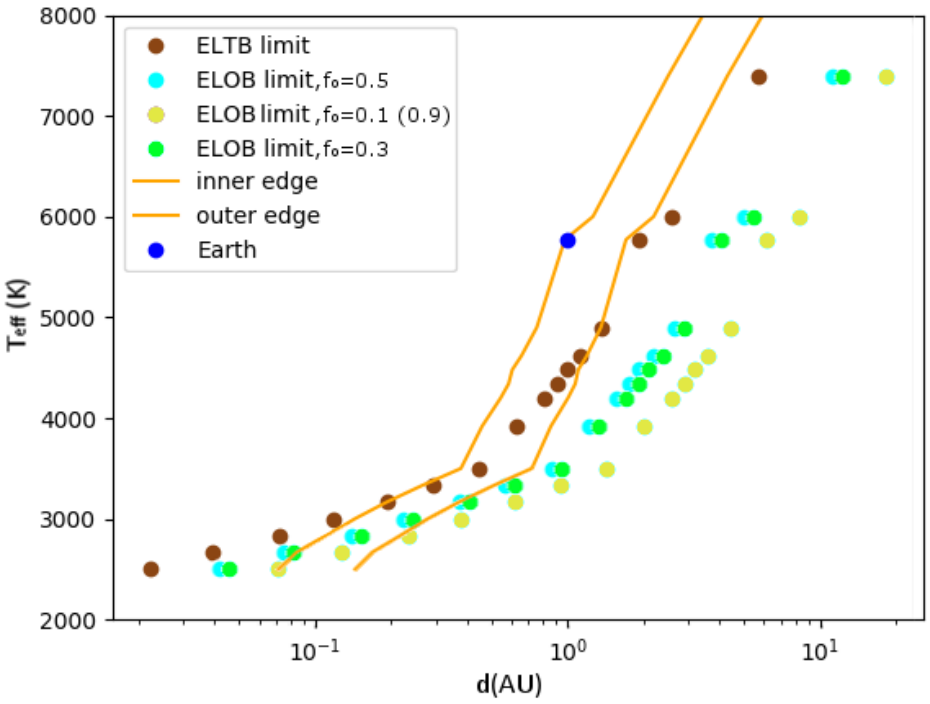

Figure 8.5: The effect of a change in the surficial fraction covered by oceans on $\tilde{F}_o$.

Given the importance of this issue, the parameter space has been explored in higher detail: d_o has been computed for $\sim 10^8$ point pairs (f_o, R). The range of radii considered here is [0.5-2] $R_\oplus$: planets with a radius $R < 0.5R_\oplus$ ($\sim$ Mars) are too low to retain a significant atmosphere and a long-lived geological activity (see Section 4.2); on the other hand, the boundary between Super-Earths and mini-Neptunes is somewhere between 1.5 and 2 $R_\oplus$ (Lopez & Fortney 2014; Marcy et al. 2014a,b; Fulton et al. 2017).

The results are shown in Figures 8.6, 8.7 and 8.8, one for each studied photosystem.

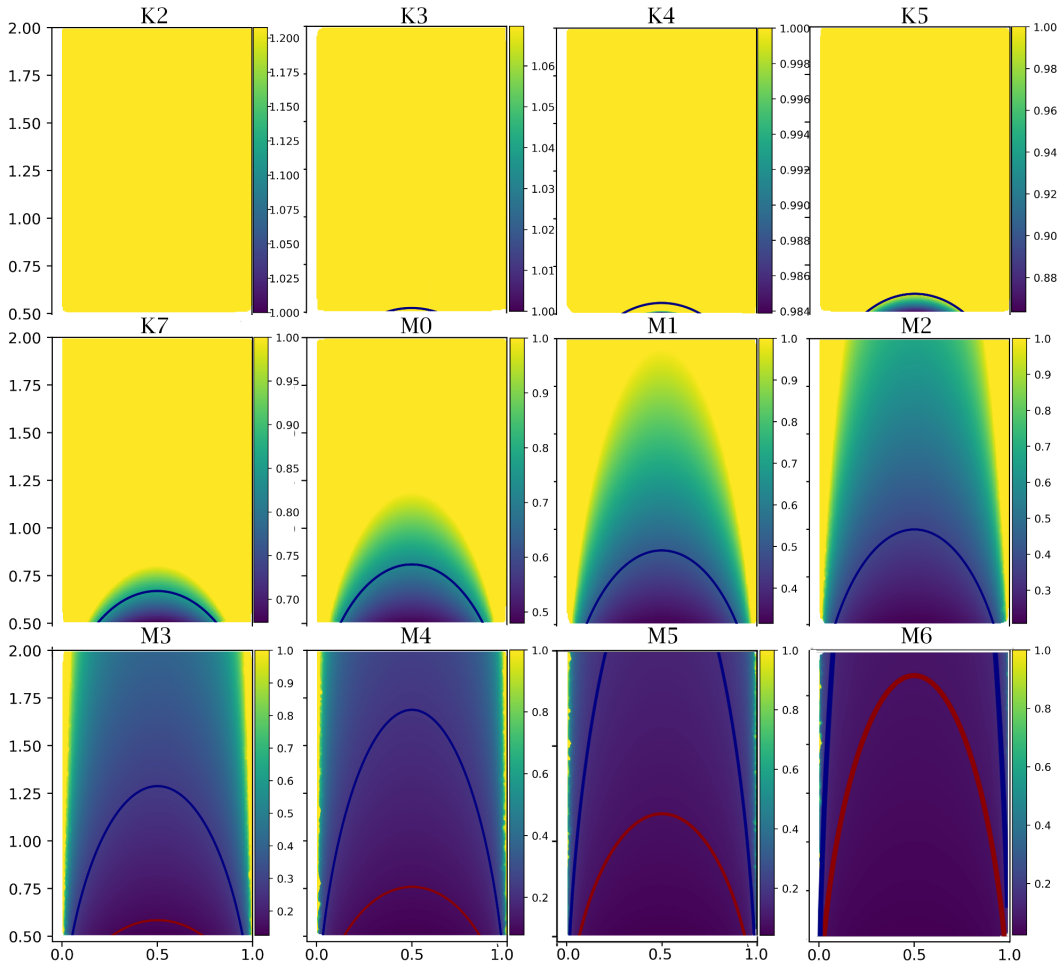

Figure 8.6: Effect of the variation of f_o and R on d_o, shown through a colour scale. The values in the colourbar are in AU. From the upper left to the lower right, cooler and cooler stars are shown. The blue and red curves indicate the outer and the inner edge, respectively. All the combinations (f_o, R) above the outer edge indicate a nutrient-limited regime throughout the HZ; combinations below the inner edge suggest instead light-limited conditions; the area between the curves gathers point pairs for which the boundary is encountered within the HZ.

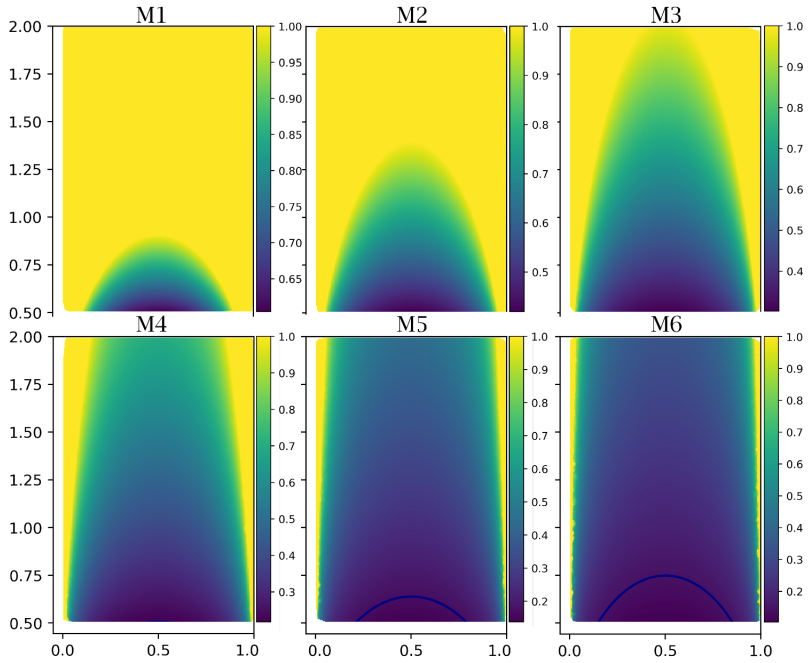

Figure 8.7: Same as Figure 8.6, but with a PAR extended up to 1050 nm. Stars earlier than M1 are not shown because they are, like M1, M2 and M3, always nutrient-limited.

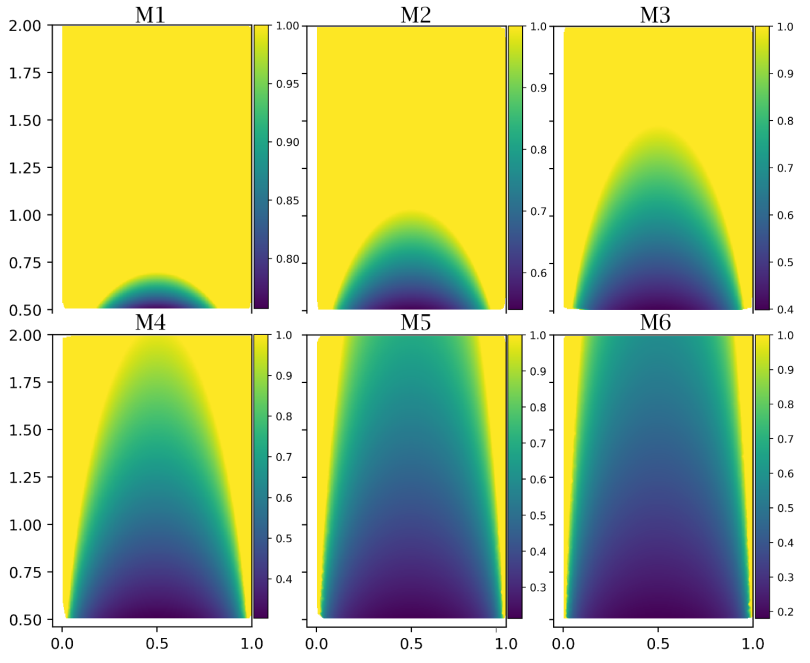

Figure 8.8: Same as Figure 8.6, but with a PAR extended up to 1400 nm. Every ocean biosphere should be nutrient-limited.

The figures clearly show that:

- ocean worlds and (marine environments on) desert worlds are extremely prone to a nutrient-limited behaviour, just like Earth; however, rather than a consequence of abundant starlight, this fact stems from the extremely low delivery of crucial materials to the oceans, as shown by Equation 8.10;
- extending the PAR window up to 1050 nm renders the light-limited conditions unlikely even around the coolest stars, whilst an extention to 1400 nm causes the limitation to disappear altogether.

We have now all the elements to try to simulate the oxygenation history of exoplanets.

8.3 The oxygen curves

8.3.1 Nutrient-limited planets

Planets whose biomass is limited by the availability of nutrients have been modelled by varying the radius and the ocean coverage, as shown by equations from Section 8.1. As regards the biological term, since Earth itself has experienced during its history some variations of the nutrient flow, reflected in the ocean biomass evolution and dictated by somewhat random processes, we are not able to predict the form that such evolution may take on other planets. Hence, the following choices have been made:

- ocean photosynthetic life is already present at t=0 and follows the same biomass evolution as on our planet -included the giant extinction of the Permian- opportunely scaled through Equation 6.20;
- land life starts, ending the *aquatic era*, whenever the concentration of free O_2 reaches the value proper of Earth at the time of land colonisation (0.79 PAL); it then follows the same evolution of its terrestrial counterpart, scaled through Equation 6.22;
- the simulation ends at $t = 10$.

It has been kept track of the time evolution of land and ocean biomass, alongside the profile of atmospheric oxygen.

Let us see in Figures 8.9 and 8.10 how the variation of radius affects the oxygenation history of an Earth-like planet.

Since the NPP of the oceans is almost independent of the planetary radius, while sinks (especially outgassing) strongly increase with increasing R, low mass planets become easily oxygenated even before the second biomass bump at $t = t_2$: the Mars-sized planet reaches ~ 0.6 PAL, almost three times the coeval terrestrial levels. However, the dependence of B_l on R^2 (Equation 6.22) makes the contribution of land life far less significative than Earth's. Curiously, the highest O_2 content is similar among all the planets, and consistent with the Carboniferous peak. Less massive planets recover more easily from the mass extinction because of a shorter e-folding time for volcanic activity decay.

On the contrary, larger planets than the Earth struggle to accumulate enough oxygen during their aquatic era because of stronger sinks. Land colonisation occurs ~ 1.8 Gyr *later* than on Earth for the $R = 1.1R_\oplus$ planet, 3.6 Gyr later for the $R = 1.2R_\oplus$ planet and 9.8 Gyr later for the $R = 1.4R_\oplus$ planet. At the end of the simulation, land life has not yet appeared on the two most massive planets.

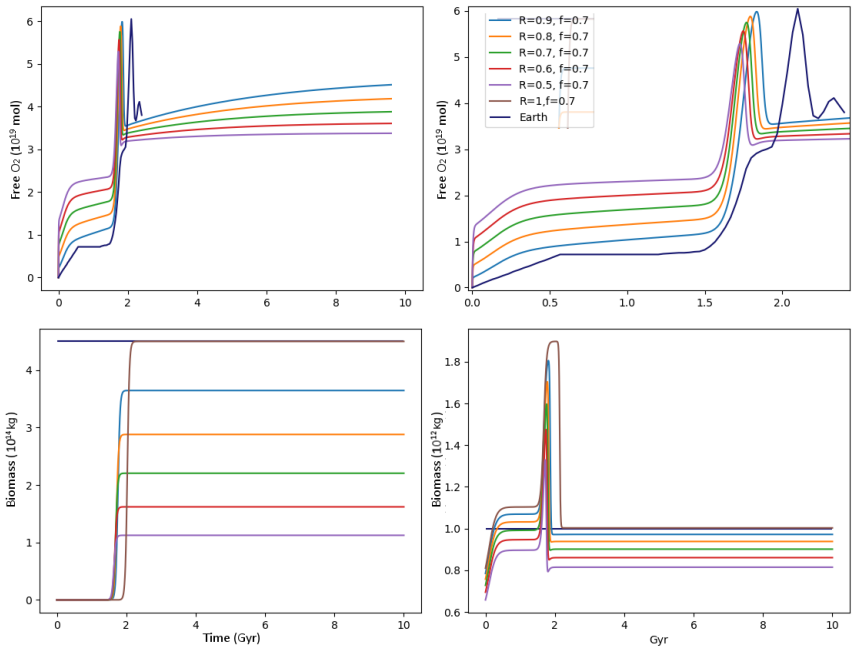

Figure 8.9: Oxygenation history of planets with the same f_o as Earth, but with a shorter radius. Top left: O_2 profile in time. Top right: a zoom of the previous graph. Bottom left: land biomass evolution. Bottom right: ocean biomass evolution. The blue horizontal lines mark the current levels of Earth's ocean and land biomass.

The effect of f_o on the planet oxygenation history is even more intriguing. Looking at Figure 8.11, we see that the ocean world ($f_o = 0.9$) has a negligible O_2 content until the second biomass bump, then in just $\sim$ 300 Myr it soars up to $\sim$ 1.9 PAL. This is caused by the suppression of continental weathering ($\propto 1 - f_o$), which explains also the quick recovery after the global stress episode. Apart from the ocean world, none of the other planets develops land life; only the planet with $f_o = 0.5$ is able to retain a significant amount of O_2 ($\sim$ 0.4 PAL) at the end of the simulation. Figure 8.12 shows the consequence of a variation of f_o in the range [0.55-0.8]. While the planet with $f_o = 0.6$ never develops land life, the one with $f_o = 0.75$ does: still, a difference as low as 5% in the ocean coverage delays the time of the oxygen bump by more than 3 Gyr. Given the unexpected influence of small variations of f_o near the terrestrial value, an additional simulation has been performed in the range $f_o \in [0.63, 0.68]$. The results are shown in Figure 8.13.

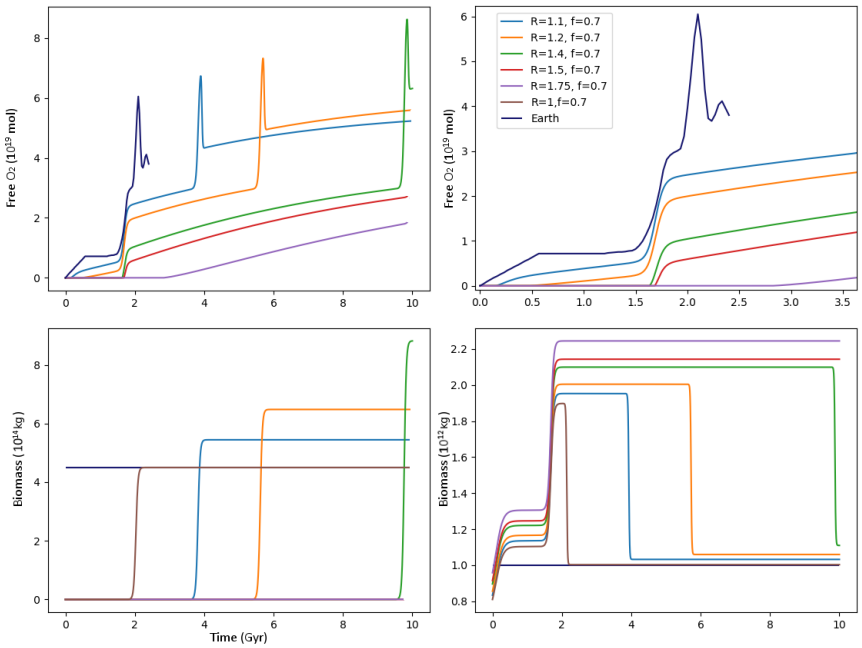

Figure 8.10: Oxygenation history of planets with $f_o = f_\oplus$, but larger than the Earth.

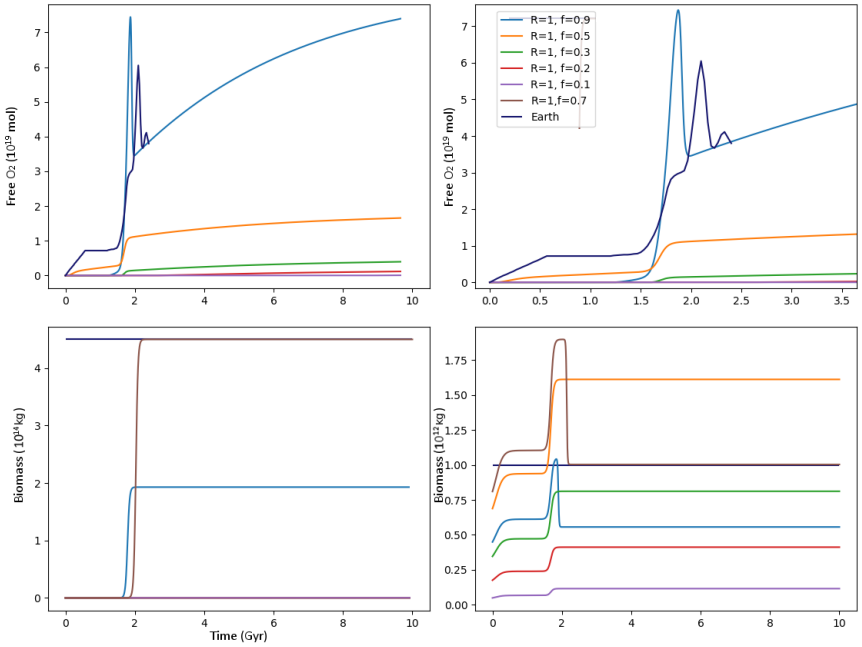

Figure 8.11: Oxygenation history of planets with $R = R_\oplus$, but with different f_o.

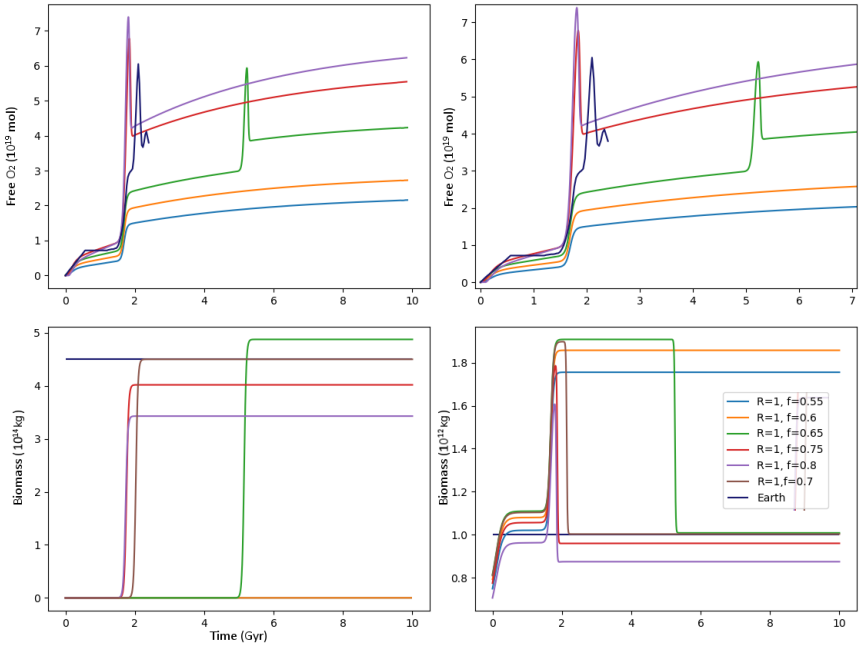

Figure 8.12: Varying f_o from 0.6 to 0.75 has an enormous influence over the oxygen curve.

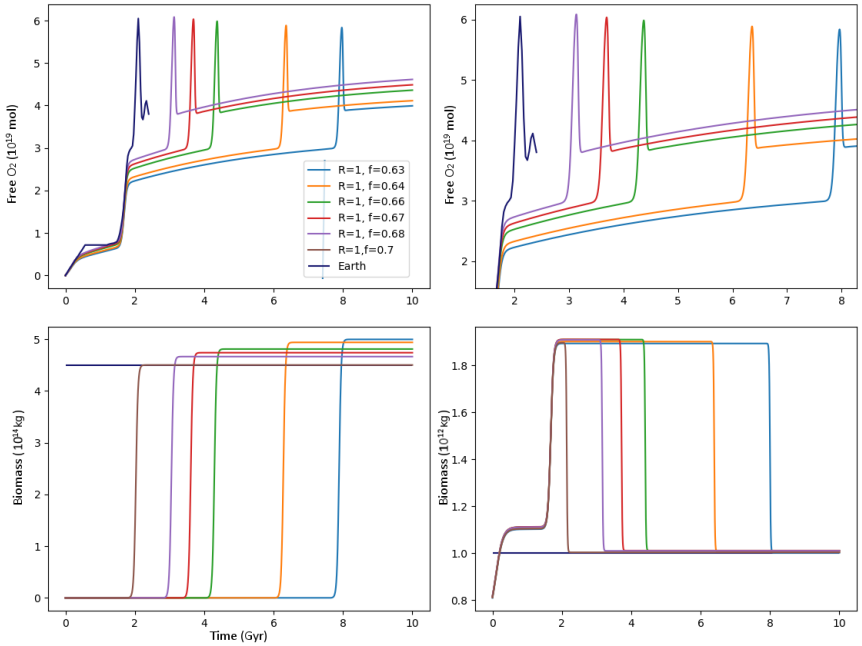

Figure 8.13: Sensitivity of land colonisation time on a small variation in f_o.

It is evident that the cause of this enormous time lag is the variation of the maximum O_2 level reached after the second biomass bump, coupled with the nearly null rate of oxygen buildup that

follows it.

The nutrient-limited regime applies to stars with spectral class $\leq$ K2 for a two-photon photosystem (M1 if we consider the innermost part of the HZ), $\leq$ M3 for a three-photon one (M6 in the innermost HZ) and in every case for a four-photon one.

Let us now see what happens in a light-limited regime.

8.3.2 Light-limited planets

Whenever this condition holds, biomass cannot completely exploit the resources of its planet to grow. The specific productivity of lands and oceans, therefore, will be constant, dictated by the received PAR.

Different simulations were set up, varying the spectral type, R and f_o. The planet's orbital position was fixed, for each star, halfway between the inner and the outer edge. The saturation value of biomass $\hat{B_o}$ and $\hat{B_l}$ are now computed from equations 6.24 and 6.25:

$$\hat{B_o} = \alpha_l NPP_l \tag{8.16}$$

$$\hat{B_l} = \alpha_o NPP_o \tag{8.17}$$

with α_l and α_o defined in Section 6.4. The time evolution of biomass is given again by the logistic equation:

$$B_o(t) = \frac{\hat{B_o}}{1 + e^{-\lambda_o t}} \tag{8.18}$$

$$B_l(t) = \frac{\hat{B_l}}{1 + e^{-\lambda_l (t - t_l)}} \tag{8.19}$$

with $\lambda_o = \lambda_l = 30$ and t_l corresponding again, as in the nutrient-limited case, to the moment when O_2 first reached the critical value of 0.79 PAL.

The parameter space is wider for cooler stars, as it was shown in Figure 8.6. Any increase in radius results in an increased amount of free oxygen, in contrast with the behaviour of nutrient-limited worlds: this is because the biotic source and the volcanic sink both increase $\propto R^2$, while weathering only $\propto R^{0.5}$. Warmer stars emit a higher F_{PAR}, hence raising the specific productivity: O_2 levels, at given f_o and R, are correspondingly higher. The effect of f_o in the curves is simply interpreted as the fact that, being biomass at the start of the simulation only oceanic, NPP scales with f_o (Equation 6.25).

Never was a planet capable of evolving land life before the end of the simulation.

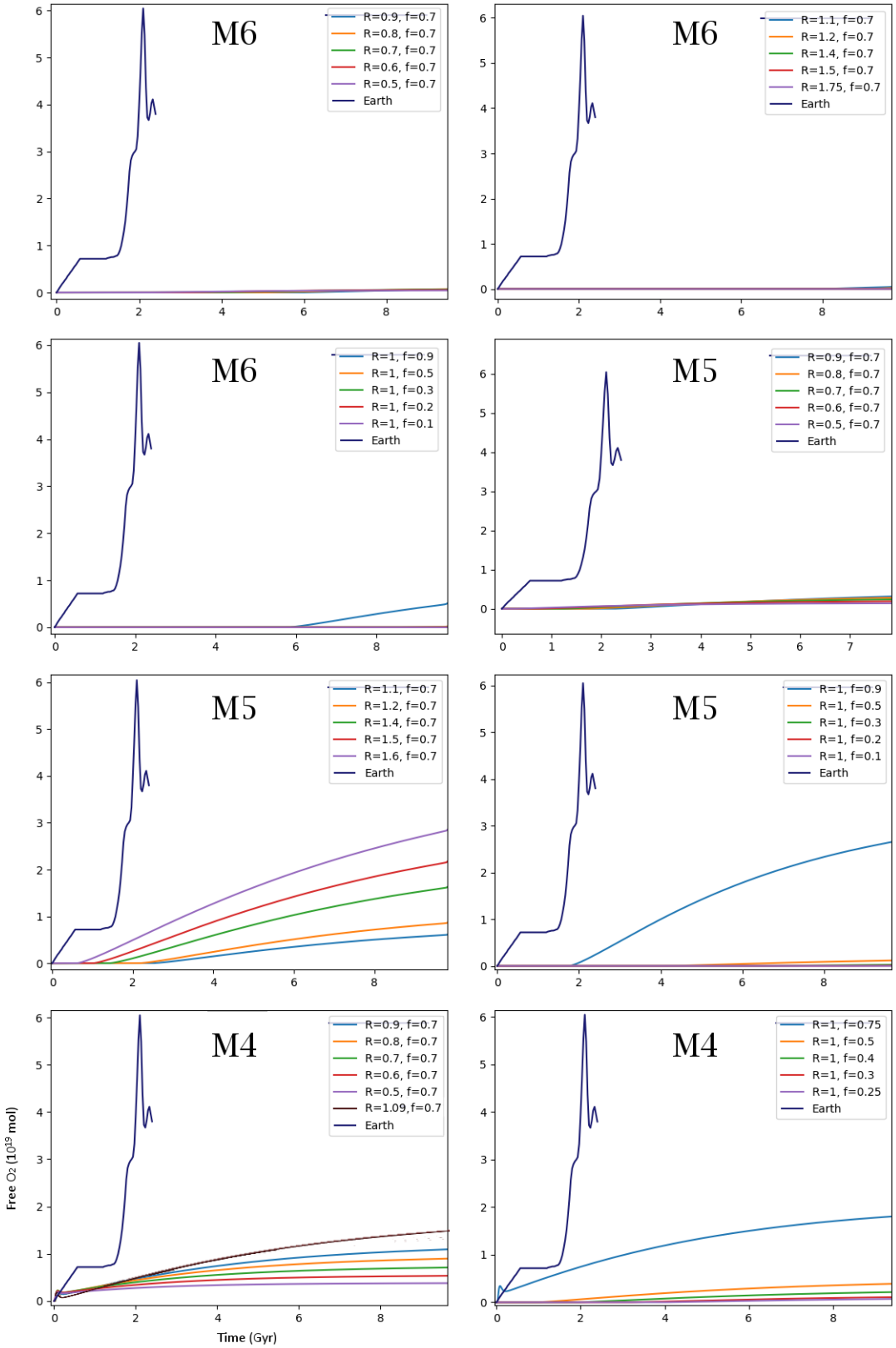

Figure 8.14: Oxygen buildup on light-limited worlds orbiting stars from M6 to M4.

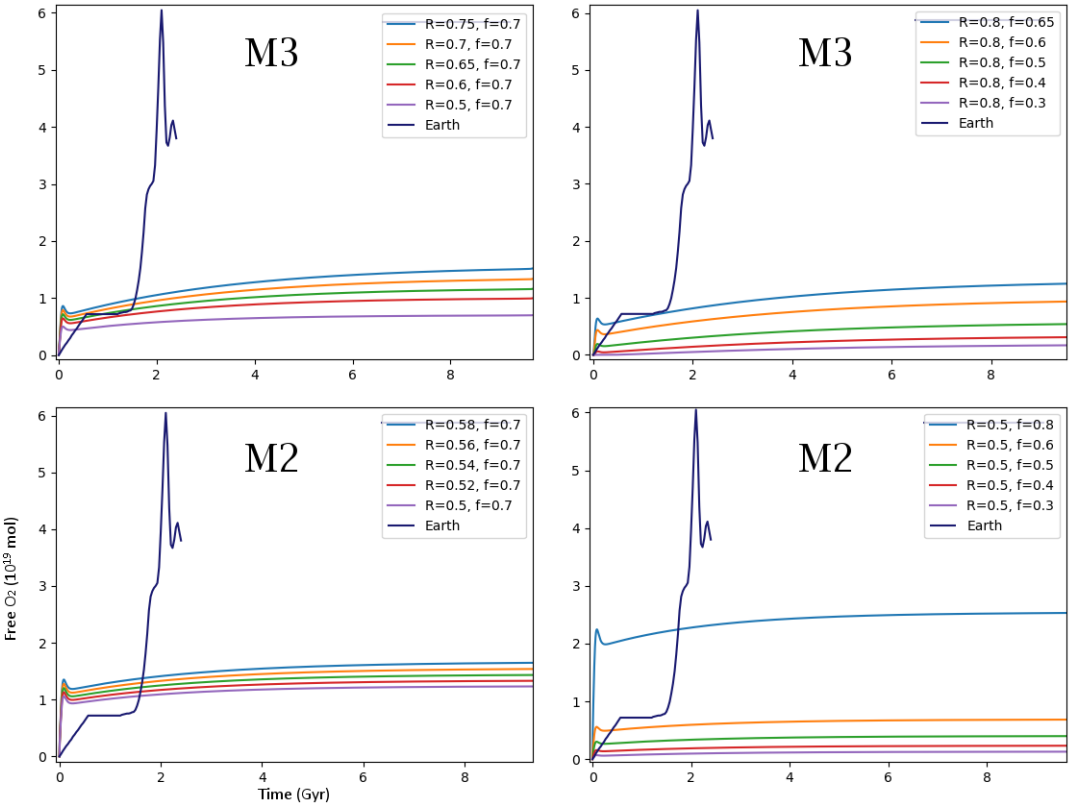

Figure 8.15: Oxygen buildup on light-limited worlds orbiting M3 and M2 stars.

8.3.3 Chimera planets

We may define *chimera planets* the worlds that appear, like mythological beings, as an odd cross-breed between two distinct entities: they are light-limited with respect to land life, nutrient-limited with respect to ocean life. They occupy a narrow region in the parameter space defined by the conditions:

$$d_l < d < d_o \quad \wedge \quad d_i < d < d_o \tag{8.20}$$

A necessary condition for a point pair (f_o, R) to belong to this regime consists in being located above the red curve in Figure 8.6.

Since ocean biomass is the only kind of life present at the beginning of the simulation, the analysis will resemble, in general terms, the one of Section 8.3.1.

For the coolest stars, the region is very narrow: it is either necessary that $f_o \to 1$ or that $R \to 2R_\oplus$[4]. The tiny variation of f_o from 0.99 to 1 has dramatic consequences on oxygen evolution: recalling Equation 8.10, it is evident that ocean productivity drops by about one order of magnitude, due to complete suppression of nutrient delivery from continents. Worlds with $f_o = 0.99$[5] always develop landlife, albeit at very different timescales, up to $R = 1.2R_\oplus$ before sinks start dominating, and -with the exclusion of the $0.5R_\oplus$ one- suffer total depletion of their

[4]Even when $R = 2R_\oplus$, the region $f_o \in [0.14, 0.86]$ is prohibited.

[5]To give an idea, the Earth would have $f_o \approx 0.99$ if its landmass were reduced only to the European Union.

O_2 reservoir soon after the mass extinction. Among the land-free worlds, only the $0.5R_\oplus$ is able to build up a significant amount of free O_2.

Moving to warmer stars, the region of the parameter space occupied by chimera planets increases: Earth-like worlds ($f_o = 0.7$, $R = R_\oplus$) start belonging to the category from stellar class M3 (cf. Table 8.3). Planets with $R = R_\oplus$ develop landlife only if $f_o \geq f_\oplus$, while planets with $f_o = f_\oplus$ do only when $R \leq 1.4R_\oplus$. The evolution is conceptually similar for K7-M3 stars. Interestingly enough, smaller planets than the Earth orbiting the M0 star have very similar curves after the second biomass bump, both horizontally and vertically. For planets orbiting earlier stars than K7, land habitability is no more restricted by light and this hybrid regime disappears altogether.

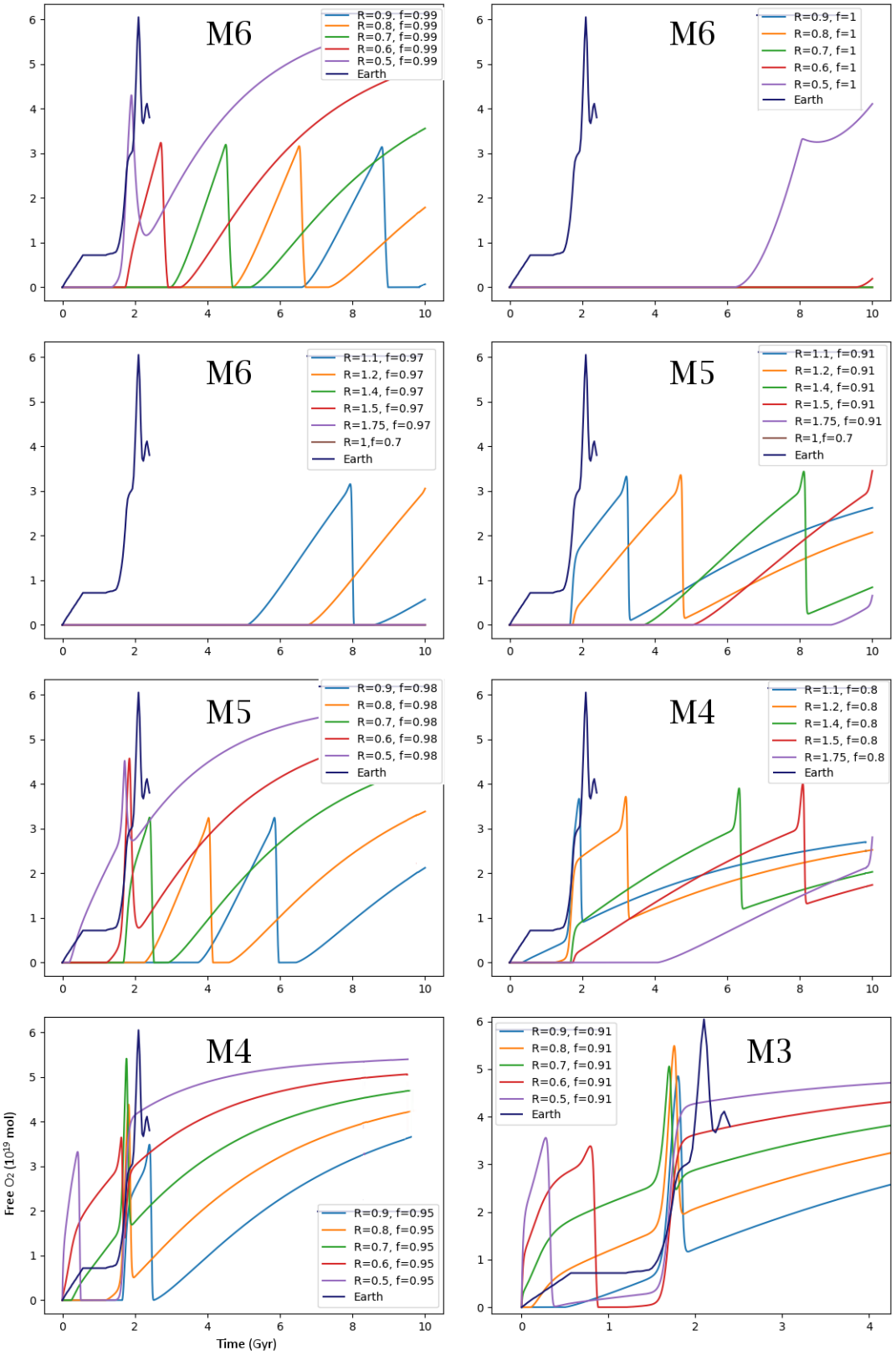

Figure 8.16: Oxygen buildup on planets with an hybrid behaviour (M3-M6).

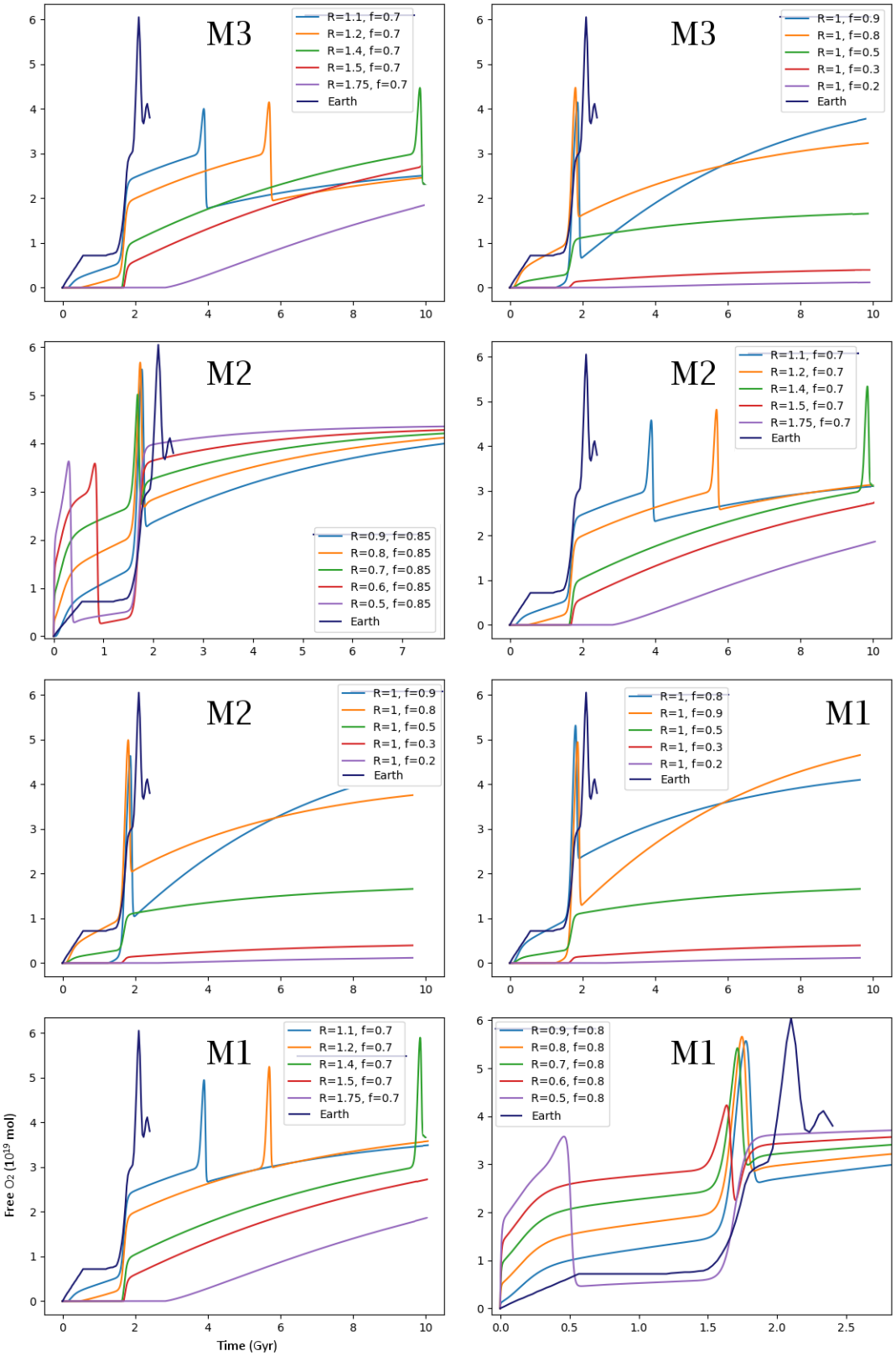

Figure 8.17: Oxygen buildup on planets with an hybrid behaviour (M1-M3).

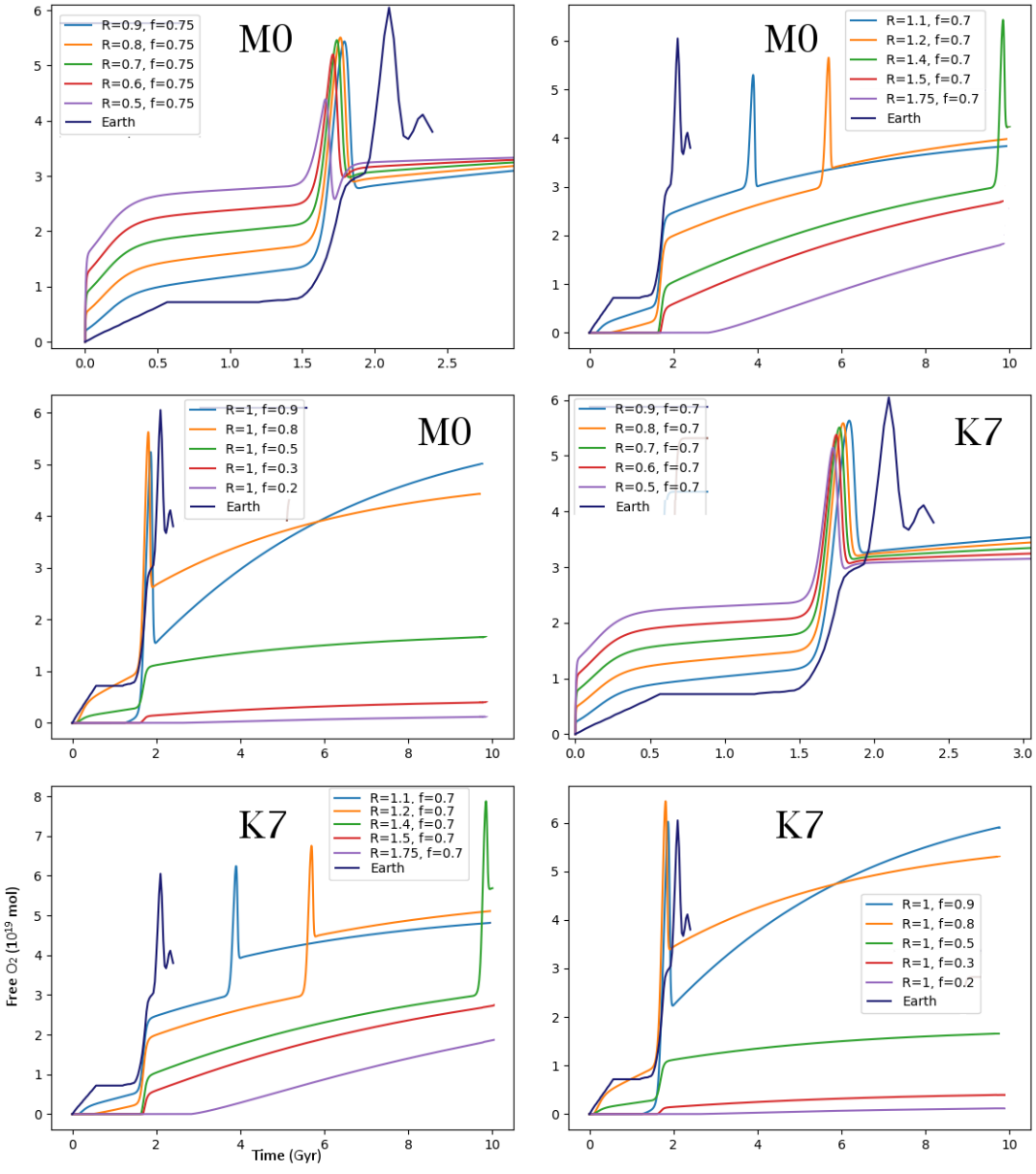

Figure 8.18: Oxygen buildup on chimera planets orbiting K7 and M0 stars.

Chapter 9

Discussion

"The important thing is not to stop questioning. Curiosity has its own reason for existence. One cannot help but be in awe when he contemplates the mysteries of eternity, of life, of the marvelous structure of reality. It is enough if one tries merely to comprehend a little of this mystery each day."

Albert Einstein, 1955

The model presented in this dissertation has been thought as an attempt to put together knowledge from different scientific fields (physics, astronomy, geology, chemistry, biology) with the aim of shedding light on the issue of exoplanet habitability. The importance of oxygen as a biomarker has been thoroughly discussed, alongside the plausibility of biological evolution of light-harvesting complexes. The exquisite diversity of planets has just begun to be unravelled, and a lot of work still needs being done. Spectroscopic characterisation of planetary atmospheres, the holy grail of exoplanetary studies, is expected to provide a significant boost to our knowledge of their origin and evolution in the next decade, by means of new-generation space and ground-based instruments.

9.1 The Earth

As it was mentioned in Section 2.24, Earth itself can be studied *as if* it were an exoplanet. As a first step of this study, the oxygenation history of our planet was examined in order to understand which processes determine the long-time evolution of molecular oxygen: it turns out that free O_2 is a small residue of interactions involving atmosphere, lithosphere, hydrosphere and biosphere, the result of an intricate balance between sources and sinks. During the first phases of Earth's history, water photolysis, driven by a much higher solar XUV flux than today, created a source of abiotic oxygen, promptly sequestered by Earth's crust. Evidence for the process comes from the observed discrepancy between trapped oxygen and carbon reservoirs. When oxygenic photosynthesis first entered the stage ($\sim$ 2.7 Gyr ago), O_2 started reacting with reduced ions like Fe^{2+} dissolved in water. After $\sim$ 300 Myr, when eventually the iron sink was exhausted, oxygen began leaking in the atmosphere, rapidly bestowing upon it an oxidising character. This *Great Oxidation Event* marks the initial point of our simulation.

The sinks considered in the model were volcanic and metamorphic outgassing, weathering and serpentinisation. Starting from the present values of sources and sinks, analytical forms for their

time evolution were searched. Three hypotheses were made, namely tying serpentinisation to planetary heat flow, and pyrite/Fe^{2+} burial and thermogenic methane production to biomass burial. The exact dependence of weathering on oxygen concentration, highly disputed in the literature, was treated as a free parameter. The biomass term was modelled using a well-known functional form for bacterial growth, and allowing for up to four different episodes of accretion. Despite many simplifications[1], the model yielded a close fit to the reconstructed O_2 time evolution[2]. Biomass has been found to experience four bumps at $t = 2.3$ Gyr, $t = 720$ Myr, $t = 370$ Myr and $t = 260$ Myr ago. Comparing them with paleontological evidence, we see that:

- the first bump corresponds, intuitively, to the diffusion of light-harvesting organisms;
- the second episode preceded the Cambrian explosion, the event that shaped Earth's modern life;
- the third one closely matches the timing of appearance of complex land lifeforms;
- the fourth one is actually negative, coinciding with the greatest threat ever faced by terrestrial life: the Permian extinction.

The model describes *how* biomass changed, not *why*. Some hypotheses have been put forward to explain, in particular, the blossoming of the Cambrian era. Ocean productivity was reduced before then because of a lower availability of phosphorus compared to the present one (Bjerrum & Canfield 2002; Kipp & Stüeken 2017). The increase of nutrient flux, indicated by the widespread presence of phosphorites (Cook & Shergold 1984), can be related to a major shift in the phosphorus cycle following global-scale glaciations (Planavsky et al. 2010; Reinhard et al. 2017). The consequent increase in ocean productivity affected shallow marine biomass, that raised free O_2, and this in turn provided a necessary[3] condition for the appearance of large animals which first came into being during the Cambrian (Canfield & Teske 1996; Knoll & Carroll 1999; Lenton & Watson 2004; Hurtgen et al. 2005).

This is effectively what has been observed: according to the model, the bump happened at ~ 720 ago Myr with a e-folding time $\Delta t \sim 40$ Myr. Paleontological evidence shows that, between 700 and 600 Myr ago, the first animals -the *Ediacarian fauna*- emerged; multicellular algae were already present $\sim$ 700 Myr ago and, after experiencing a series of genetic adaptations, were finally able to survive in terrestrial environments; colonisation of land, started $\sim 400Myr$ ago (Cloud 1976), was actually a rapid process, with an estimated Δt of $\sim$ 30 Myr. The steep rise of photosynthetic production lead to a dramatic increase of atmospheric O_2, which could even overcome, for a short period, the present level.

A negative sigmoid was used to model the decrease of oxygen from $pO_2 = 0.35$ to $pO_2 = 0.21$. Centred at ~ 260 Myr ago, it closely matches, although with a more extended timescale ($\Delta t \sim 11$), the Permian extinction (Knoll et al. 2007). The model attributes the whole biomass decline to ocean biosphere. While it has been long established that the event wiped out nearly 96% of marine species (Benton 2015), whether the balance of biomass decline completely sways to one side is a matter of difficult assessment.

It is not known whether the intricate interplay between geological, biological and chemical processes on Earth is just the unique way followed by our life or there is some general mechanism

[1]For instance: 1) assuming that the burial efficiency κ is constant in time; 2) neglecting the evolution of O_2 dissolved in water. Although clearly related to atmospheric reservoir, the oxygenation of oceans is not uniform, with important differences between shallow and deep waters.

[2]Even if, as it has been underlined in Section 7.1.2, the curve itself is far from being 100% reliable.

[3]Multicellular organisms relying on diffusion alone to oxygenate themselves are limited in size by pO_2. At 0.01 PAL, the greatest attainable size is $\sim 10^2 \mu$m, equal to that of a single eukaryotic cell. When p$O_2 \approx 0.1$ PAL, the limit is pushed to $\sim$ 1 mm and cellular differentiation can lead to the evolution of a primitive circulation system (Catling et al. 2005).

underlying it. Burial of organic sediments, together with creation of pyrite and Fe^{2+} mediated by microorganisms, have been assumed to follow the same rules as on Earth. If, on the one side, it appears reasonable to envisage a universal underwater birth of life, on the other side it can't be known when complex life will start colonising mainland. In the simulation, the critical time has been defined as the moment when oxygen first reached the concentration it had on Earth back then (0.79 PAL). This is clearly a naïve assumption: contrary to common conception (e.g., Berkner & Marshall 1964), land colonisation was not impeded by UV radiation because, as photochemical models show, oxygen levels as low as 0.01 PAL would suffice to shield the surface from radiation in the dangerous range [200–300] nm (Levine et al. 1979; Kasting & Donahue 1980; Kasting 1987; Segura et al. 2003). Nevertheless, oxygen levels have been on Earth a necessary condition for the development of complex lifeforms (Catling et al. 2005) which, after evolving the needed adaptations to thrive in a totally different environment as land is with respect to ocean, turned into what we call *plants*. It might be thought that a similar correlation between oxygen levels and complex life be at work elsewhere, too.

9.2 The heavens

After gauging the model to provide a good fit to the Earth, the subsequent step was an attempt to generalise it to exoplanets. Absence of data compulsorily required a whole series of assumptions. Geological factors, like the presence of plate tectonics and of a strong magnetic field, are highly uncertain and rely on models lacking, of course, any observational verification. This is particularly true for seafloor oxidation, which additionally assumed that the pH of exoplanetary oceans is similar to its terrestrial counterpart (~ 8.0). The dependence on pH was implicit in the equation for nutrient delivery, as the pH difference determines the relative weight of riverine and oceanic inputs. As regards volcanism, whilst the adopted scaling law seems reasonable, the total degassing output hinges upon factors like the core mass fraction (Noack et al. 2017), the mass fraction of volatiles and the redox state of the mantle (Catling & Kasting 2017): a precise knowledge of the formation of every planet would be needed before quantitatively studying it.

The dependence of weathering on oxygen content is highly disputed in the literature; therefore, the choice was made to leave it as a free parameter. The normalisation factor, i.e. the amount of reduced material exposed to oxidation, was again scaled from earthly values.

Moving on now to the biological source, an underlying assumption behind the PAR limit for ocean and land biomass and the productivity of light-limited worlds is that the harvesting efficiency ε of extraterrestrial autotrophs, i.e. the fraction of impacting PAR actually collected by organisms, defined by equation:

$$F_{abs} = \varepsilon F_{*,PAR} \tag{9.1}$$

is the same as Earth's. The factor, opportunely averaged to describe the whole PAR range, ultimately stems from the superposition of absorption spectra of chlorophylls and accessory pigments (cf. Chapter 4) and critically depends on temperature, CO_2 concentration, hydration and, to a lesser extent, on O_2 itself (e.g., Potter et al. 1993). Again, in absence of information regarding alien pigments and biochemistry and the mentioned physical conditions, Earth-like conditions have been assumed. The dependence of land productivity for nutrient-limited worlds on the globally-averaged precipitation rate was neglected, since it would have required a delicate analysis of temperature effects and cloud coverage (Lingam & Loeb 2019a).

The underlying criticality of the model, ensued from the entire set of assumptions, is the risk of being strongly Earth-biased. This is the inevitable fate of any theoretical work trying to extrapolate, by means of inductive reasoning, a body of knowledge whose foundations lie in a single benchmark case. An attempt to depart from geocentrism was made with respect to the biological factor: extended PAR windows for stars cooler than the Sun were considered, as the

emergence of similar complexes would be favoured by a strong evolutionary thrust (Wolstencroft & Raven 2002).

A clear distinction has emerged between nutrient-limited and light-limited worlds. Nutrient-limited worlds are virtually unaffected by the spectral class of their host star and follow a similar evolutionary history as the Earth. A decrease of the radius causes higher O_2 contents than the Earth's whenever life is confined to marine environments, due to the almost null dependence of ocean NPP on planetary radius, and lower contents in the long run, because of the weaker dependence on R of weathering, compared with land NPP. A consequence is that larger planets than the Earth may take several billion years before evolving land life, perhaps posing a physical limitation to higher habitability. The effect of a different water coverage is a delicate balance between varying ocean NPP (peaked at $f_o = 0.67$) and continental weathering ($\propto 1 - f_o$). Worlds with $f_o \sim 0.9$ that somehow increase their nutrient delivery, in a similar way as Earth did in the Precambrian bump, skyrocket their O_2 content to nearly 2 PAL. Worlds with slight departures from $f_o = 0.67$ undergo enormous variations in the timing of land colonisation, until for $f_o < 0.6$ it is not reached anymore. Desert worlds, due to their low ocean NPP, never reach the level of 0.1 PAR.

Light-limited worlds, which should be common around M stars if the PAR window were the same as Earth's, never managed to overcome the critical O_2 threshold for land colonisation. Nonetheless, concentrations as high as 0.65 PAL were reached in two cases: for the Earth-sized ocean planet ($f_o = 0.9$) around the M5 star and for the Mars-sized one ($f_o = 0.8$) orbiting an M2 primary. The latter is particularly intriguing, because the convergence of a high ocean productivity and small sinks causes an extremely quick saturation: the O_2 signal would be very stable and easily detectable for at least 10 Gyr.

Chimera planets, defined as those with a light-limited land NPP and a nutrient-limited ocean NPP, look especially attractive, for they manage to accumulate significant amounts of oxygen, sometimes even higher than 1 PAL, even when the primary is an M6 star. The Mars-sized worlds around M3 ($f_o = 0.91$) and M4 stars ($f_o = 0.95$) are able to develop land habitability in the first Gyr of the simulation, creating the conditions for a high-paced biological evolution. However, the reduced land NPP makes their O_2 reservoir extremely sensitive to variations in ocean biomass: extreme O_2 depletion episodes can occur, rapidly turning the atmosphere to an anoxic state that would be lethal for life forms thriving on oxygen.

Two seemingly contradictory conclusions could be drawn:

- biotic oxygen accumulates in a wide variety of planetary environments, including light-starving M-star systems;
- an O_2-rich atmosphere -as most of Earth's history witnesses- is not an inevitable outcome of the presence of photosynthesis. Only if the biotic source outweights sinks, can oxygen begin to accumulate.

A factor that was not computed in the model is the abiotic O_2 contribution from water and carbon dioxide photolysis. As it was underlined in Chapter 4, under the severe environmental stress suffered in the first phases of stellar life, M-star habitable planets could build up atmospheres hundred to thousand bars thick (Luger & Barnes 2015). Some authors (e.g., Hamano et al. 2013) have argued that planets that start off in a runaway greenhouse state could have their O_2 absorbed by the magma ocean, and evidence for the efficiency of this process would be, according to Ramirez (2018), the lack of free O_2 from Venus atmosphere. As early oxygen accrual is actually a strong buffer *against* the appearance of life, since it quickly oxidises and breaks down any precursor of biochemistry, the process raises many issues which merit further consideration and shall be taken into account in future studies.

9.3 Conclusions

The discovery of more than 4000 exoplanets in the last 25 years, coupled with a fast-paced technological improvement of both space and ground-based capabilities, has suddenly opened a window into a universe of possibilities: the outstanding diversity of planetary environments, which we just beginning to grasp, by far overcomes our most whimsical thoughts. For the first time in human history, the search for life outside the Earth can be assessed in a scientific way. Atmospheric characterisation of distant worlds is expected to shed light on one of the most profound human questions: "Are we alone?". Well, *the universe is a pretty big place. If it's just us, seems like an awful waste of space*[4].

[4]Carl Sagan, *Contact* (1985).

Bibliography

Abe, Y., Abe-Ouchi, A., Sleep, N. H., & Zahnle, K. J. 2011, Astrobiology, 11, 443, pMID: 21707386

Acuña, M. H., Connerney, J. E. P., Ness, F. N., et al. 1999, Science, 284, 790

Adelman, B. 1986, Journal of the British Interplanetary Society, 39, 256

Airapetian, V. S., Glocer, A., Khazanov, G. V., et al. 2017, The Astrophysical Journal, 836, L3

Alibert, Y. & Benz, W. 2017, Astronomy and Astrophysics, 598, L5

Allard, F., Hauschildt, P. H., Alexander, D. R., & Starrfield, S. 1997, Annual Review of Astronomy and Astrophysics, 35, 137

Angel, J. R. P., Cheng, A. Y. S., & Woolf, N. J. 1986, Nature, 322, 341

Anglada-Escudé, G., Tuomi, M., Gerlach, E., et al. 2013, Astronomy and Astrophysics, 556, A126

Arcichovsky, V. M. 1912, Annales de l'Institut Polytechnique Don Cesarevitch Alexis a Novotcherkassk, 17

Armstrong, J., Barnes, R., Domagal-Goldman, S., et al. 2014, Astrobiology, 14, 277, pMID: 24611714

Arnold, L., Gillet, S., Lardière, O., Riaud, P., & Schneider, J. 2002, Astronomy and Astrophysics, 392, 231

Audard, M., Güdel, M., Drake, J. J., & Kashyap, V. L. 2000, The Astrophysical Journal, 541, 396

Ayres, T. R. 1997, Journal of Geophysical Research, 102, 1641

Bailer-Jones, C. A. L. 2005, in ESA Special Publication, Vol. 576, The Three-Dimensional Universe with Gaia, ed. C. Turon, K. S. O'Flaherty, & M. A. C. Perryman, 393

Bains, W. 2004, Astrobiology, 4, 137

Bar-On, Y. M., Phillips, R., & Milo, R. 2018, Proceedings of the National Academy of Sciences, 115, 6506

Barnes, R., Jackson, B., Greenberg, R., & Raymond, S. N. 2009, The Astrophysical Journal Letters, 700, L30

Barnes, R., Mullins, K., Goldblatt, C., et al. 2013, Astrobiology, 13, 225, pMID: 23537135

Barnes, R., Raymond, S. N., Jackson, B., & Greenberg, R. 2008, Astrobiology, 8, 557, pMID: 18598142

Baross, J. 2007, The Limits of Organic Life in Planetary Systems (Washington, DC: The National Academies Press)

Baross, J. A. 1983, Nature, 303, 423

Baross, J. A. & Hoffman, S. E. 1985, Origins of life and evolution of the biosphere, 15, 327

Battista, J. R. 1997, Annual Review of Microbiology, 51, 203, pMID: 9343349

Bean, J. L., Miller-Ricci Kempton, E., & Homeier, D. 2010, Nature, 468, 669

Becker, M. M. & Wang, Z. 1989, Journal of Molecular Biology, 210, 429

Beichman, C. A., Fridlund, M., Traub, W. A., et al. 2007, in Protostars and Planets V, ed. B. Reipurth, D. Jewitt, & K. Keil, 915

Benton, M. 2015, When Life Nearly Died: The Greatest Mass Extinction of All Time (Revised edition) (Thames & Hudson)

Berkner, L. V. & Marshall, L. C. 1964, in The Origin and Evolution of Atmospheres and Oceans, ed. P. J. Brancazio & A. G. W. Cameron, 102

Berner, R. 2004, The Phanerozoic Carbon Cycle (Oxford University Press)

Berner, R. A., Lasaga, A. C., & Garrels, R. M. 1983, American Journal of Science, 283, 641

Beuzit, J.-L., Feldt, M., Dohlen, K., et al. 2008, in Society of Photo-Optical Instrumentation Engineers (SPIE) Conference Series, Vol. 7014, Ground-based and Airborne Instrumentation for Astronomy II, 701418

Biller, B. A., Liu, M. C., Wahhaj, Z., et al. 2013, The Astrophysical Journal, 777, 160

Bin, J., Tian, F., & Liu, L. 2018, Earth and Planetary Science Letters, 492, 121

Bjerrum, C. J. & Canfield, D. E. 2002, Nature, 417, 159

Blake, C., Johnson, J., Plavchan, P., et al. 2015, in American Astronomical Society Meeting Abstracts, Vol. 225, American Astronomical Society Meeting Abstracts #225, 257.32

Bleam, W. 2017, in Soil and Environmental Chemistry (Second Edition), second edition edn., ed. W. Bleam (Academic Press), 445 – 489

Bolmont, E., Libert, A.-S., Leconte, J., & Selsis, F. 2016, Astronomy and Astrophysics, 591, A106

Bolmont, E., Selsis, F., Owen, J. E., et al. 2017, Monthly Notices of the Royal Astronomical Society, 464, 3728

Bourrier, V., de Wit, J., Bolmont, E., et al. 2017, The Astronomical Journal, 154, 121

Bowring, S. A., Grotzinger, J. P., Isachsen, C. E., et al. 1993, Science, 261, 1293

Boyce, C. K. & Knoll, A. H. 2002, Paleobiology, 28, 70

Brack, A., Horneck, G., Cockell, C. S., et al. 2010, Astrobiology, 10, 69

Brain, D. A., McFadden, J. P., Halekas, J. S., et al. 2015, Geophysical Research Letters, 42, 9142

Brasier, M., McLoughlin, N., Green, O., & Wacey, D. 2006, Philosophical Transactions of the Royal Society B: Biological Sciences, 361, 887

Brock, T. D. 1967, Science, 158, 1012

Broeg, C., Fortier, A., Ehrenreich, D., et al. 2013, in European Physical Journal Web of Conferences, Vol. 47, European Physical Journal Web of Conferences, 03005

Brown, T. M. 2001, The Astrophysical Journal, 553, 1006

Bryant, D. A., Costas, A. M. G., Maresca, J. A., et al. 2007, Science, 317, 523

Bryant, D. A. & Frigaard, N.-U. 2006, Trends in Microbiology, 14, 488

Buccino, A. P., Lemarchand, G. A., & Mauas, P. J. D. 2007, Icarus, 192, 582

Budyko, M. I. 1969, Tellus, 21, 611

Bulat, S. A., Alekhina, I. A., Blot, M., et al. 2004, International Journal of Astrobiology, 3, 1–12

Burrows, A., Hubbard, W. B., Lunine, J. I., & Liebert, J. 2001, Reviews of Modern Physics, 73, 719

Busse, F. 1976, Physics of the Earth and Planetary Interiors, 12, 350

Cabrol, N. A. 2016, Astrobiology, 16, 661

Caldwell, M. M. 1981, Plant Response to Solar Ultraviolet Radiation, ed. O. L. Lange, P. S. Nobel, C. B. Osmond, & H. Ziegler (Berlin, Heidelberg: Springer Berlin Heidelberg), 169–197

Canfield, D., Habicht, K., & Thamdrup, B. 2000, Science (New York, N.Y.), 288, 658

Canfield, D. E. & Teske, A. 1996, Nature, 382, 127

Cannat, M., Fontaine, F., & Escartín, J. 2010, Washington DC American Geophysical Union Geophysical Monograph Series, 188, 241

Catling, D. C., Glein, C. R., Zahnle, K. J., & McKay, C. P. 2005, Astrobiology, 5, 415

Catling, D. C. & Kasting, J. F. 2017, Atmospheric Evolution on Inhabited and Lifeless Worlds

Catling, D. C., Zahnle, K. J., & McKay, C. P. 2001, Science, 293, 839

Chapman, S. 1930, A Theory of Upper-atmospheric Ozone, Memoirs of the Royal Meteorological Society (Edward Stanford)

Charbonneau, D., Allen, L. E., Megeath, S. T., et al. 2005, The Astrophysical Journal, 626, 523

Charbonneau, D. & Deming, D. 2007, arXiv e-prints, arXiv:0706.1047

Chase, S. C., J., Miner, E. D., Morrison, D., Muench, G., & Neugebauer, G. 1976, Icarus, 28, 565

Chassefière, E. 1996, Icarus, 124, 537

Chauvin, G., Lagrange, A. M., Zuckerman, B., et al. 2005, Astronomy and Astrophysics, 438, L29

Chyba, C. F. & Hand, K. P. 2005, Annual Review of Astronomy and Astrophysics, 43, 31

Chyba, C. F. & Phillips, C. B. 2002, Origins of life and evolution of the biosphere, 32, 47

Claire, M. W., Catling, D. C., & Zahnle, K. J. 2006, Geobiology, 4, 239

Clampin, M. 2014, in Society of Photo-Optical Instrumentation Engineers (SPIE) Conference Series, Vol. 9143, Space Telescopes and Instrumentation 2014: Optical, Infrared, and Millimeter Wave, 914302

Clampin, M. & Pham, T. 2014, in Society of Photo-Optical Instrumentation Engineers (SPIE) Conference Series, Vol. 9154, High Energy, Optical, and Infrared Detectors for Astronomy VI, 91542N

Clark, R., Swayze, G., Gallagher, A., King, T., & Calvin, W. 1993, U.S. Geological Survey, Reston, VA. Available online at: http://speclab.cr.usgs.gov

Claudi, R. 2017, arXiv e-prints, arXiv:1708.05829

Claudi, R., Benatti, S., Carleo, I., et al. 2018, in Society of Photo-Optical Instrumentation Engineers (SPIE) Conference Series, Vol. 10702, Ground-based and Airborne Instrumentation for Astronomy VII, 107020Z

Claudi, R., Pace, E., Ciaravella, A., et al. 2016, Memorie della Societá Astronomica Italiana, 87, 104

Cloud, P. 1976, Paleobiology, 2, 351–387

Cnossen, I., Sanz-Forcada, J., Favata, F., et al. 2007, Journal of Geophysical Research: Planets, 112

Cocconi, G. & Morrison, P. 1959, Nature, 184, 844

Cockell, C. S. 1998, Journal of Theoretical Biology, 193, 717

Cockell, C. S. 2014, Philosophical Transactions of the Royal Society of London Series A, 372, 20130082

Cockell, C. S. & Raven, J. A. 2004, Icarus, 169, 300

Conway Morris, S. 1998, The Crucible of Creation : the Burgess Shale and the Rise of Animals (Oxford University Press)

Conway Morris, S. 2006, Philosophical Transactions of the Royal Society B: Biological Sciences, 361, 1069

Cook, P. J. & Shergold, J. H. 1984, Nature, 308, 231

Cox, C. S. 1993, Origins of life and evolution of the biosphere, 23, 29

Craddock, R. A. & Howard, A. D. 2002, Journal of Geophysical Research: Planets, 107, 21

Cui, J., Wu, X. S., Gu, H., Jiang, F. Y., & Wei, Y. 2019, Astronomy and Astrophysics, 621, A23

Cullum, J., Stevens, D., & Joshi, M. 2014, Astrobiology, 14, 645

Cuntz, M. & Guinan, E. F. 2016, The Astrophysical Journal, 827, 79

Danchi, W. C. & Lopez, B. 2013, The Astrophysical Journal, 769, 27

DasSarma, S. & Schwieterman, E. W. 2018, International Journal of Astrobiology, 1–10

del Moral, R. 1972, Oecologia, 9, 289

Demarque, P., Guenther, D. B., & van Altena, W. F. 1986, The Astrophysical Journal, 300, 773

Deming, D., Wilkins, A., McCullough, P., et al. 2013, The Astrophysical Journal, 774, 95

Des Marais, D. J. 2000, Science, 289, 1703

Des Marais, D. J., Harwit, M. O., Jucks, K. W., et al. 2002, Astrobiology, 2, 153

Diaz, B. & Schulze-Makuch, D. 2006, Astrobiology, 6, 332, pMID: 16689650

Dobrovolskis, A. R. 2013, Icarus, 226, 760

Dole, S. H. 1964, Habitable planets for man

Domagal-Goldman, S. D., Meadows, V. S., Claire, M. W., & Kasting, J. F. 2011, Astrobiology, 11, 419

Domagal-Goldman, S. D., Segura, A., Claire, M. W., Robinson, T. D., & Meadows, V. S. 2014, The Astrophysical Journal, 792, 90

Donahue, T. M., Hoffman, J. H., Hodges, R. R., & Watson, A. J. 1982, Science, 216, 630

Dorn, R. J., Anglada-Escude, G., Baade, D., et al. 2014, The Messenger, 156, 7

Dose, K., Bieger-Dose, A., Dillmann, R., et al. 1995, Advances in Space Research, 16, 119 , eURECA Scientific Results

Driscoll, P. & Barnes, R. 2015, Astrobiology, 15, 739, pMID: 26393398

Dudley, R. 1998, Journal of Experimental Biology, 201, 1043

Edson, A., Lee, S., Bannon, P., Kasting, J. F., & Pollard, D. 2011, Icarus, 212, 1

Ehrenfreund, P., Irvine, W., Becker, L., et al. 2002, Reports on Progress in Physics, 65, 1427

Elkins-Tanton, L. T. & Seager, S. 2008, The Astrophysical Journal, 685, 1237

Erkaev, N. V., Kulikov, Y. N., Lammer, H., et al. 2007, Astronomy and Astrophysics, 472, 329

Erkaev, N. V., Lammer, H., Odert, P., et al. 2013, Astrobiology, 13, 1011, pMID: 24251443

Etiope, G. 2009, Atmospheric Environment, 43, 1430

Etiope, G., Lassey, K. R., Klusman, R. W., & Boschi, E. 2008, Geophysical Research Letters, 35, L09307

F. Chyba, C. 2000, Nature, 403, 381

Falkowski, P. G. & Raven, J. A. 1997, Aquatic Photosynthesis (Princeton University Press)

Fenchel, T., King, G., & Blackburn, T. 1998, Bacterial biogeochemistry : the ecophysiology of mineral cycling (San Diego Academic Press)

Field, C. B., Behrenfeld, M. J., Randerson, J. T., & Falkowski, P. 1998, Science, 281, 237

Foley, B. J. & Smye, A. J. 2018, Astrobiology, 18, 873

Ford, E. B., Seager, S., & Turner, E. L. 2001, Nature, 412, 885

Forget, F. & Pierrehumbert, R. T. 1997, Science, 278, 1273

Forget, F., Wordsworth, R., Millour, E., et al. 2013, Icarus, 222, 81

Fredrickson, J. K., Zachara, J. M., Kennedy, D. W., et al. 1998, Geochimica et Cosmochimica Acta, 62, 3239

Fulton, B. J., Petigura, E. A., Howard, A. W., et al. 2017, The Astronomical Journal, 154, 109

Gaidos, E., Deschenes, B., Dundon, L., et al. 2005, Astrobiology, 5, 100

Gaidos, E. & Selsis, F. 2007, in Protostars and Planets V, ed. B. Reipurth, D. Jewitt, & K. Keil, 929

Gale, J. & Wandel, A. 2017, International Journal of Astrobiology, 16, 1

Garraffo, C., Drake, J. J., Cohen, O., Alvarado-Gómez, J. D., & Moschou, S. P. 2017, The Astrophysical Journal, 843, L33

Garrett, R. & Grisham, C. 2008, Biochemistry (Cengage Learning)

Gates, D. M., Gates, H. J., Gates, J. C., & Gates, V. R. 1965, Applied Optics, 4, 11

Gershberg, R. E. 2005, Solar-Type Activity in Main-Sequence Stars

Gershberg, R. E. & Shakhovskaia, N. I. 1983, Astrophysics and Space Science, 95, 235

Giampapa, M. S. & Liebert, J. 1986, The Astrophysical Journal, 305, 784

Gillmann, C. & Tackley, P. 2014, Journal of Geophysical Research (Planets), 119, 1189

Gillon, M., Triaud, A. H. M. J., Demory, B.-O., et al. 2017, Nature, 542, 456

Glasspool, I. J. & Scott, A. C. 2010, Nature Geoscience, 3, 627

Godolt, M., Stracke, B., Tosi, N., & Grenfell, J. L. 2018, in European Planetary Science Congress, EPSC2018–780

Gough, D. O. 1981, Solar Physics, 74, 21

Gould, S. 1989, Wonderful Life: The Burgess Shale and the Nature of History (W. W. Norton & Company), 323

Graham, J. B., Aguilar, N. M., Dudley, R., & Gans, C. 1995, Nature, 375, 117

Grasset, O., Schneider, J., & Sotin, C. 2009, THe Astrophysical Journal, 693, 722

Gregory, R. 1977, Biochemistry of Photosynthesis (Wiley)

Grenfell, J. L., Stracke, B., von Paris, P., et al. 2007, Planetary and Space Science, 55, 661

Grenfell, J. L., von Paris, P., Stracke, B., & Rauer, H. 2008, in European Planetary Science Congress 2008, 819

Grießmeier, J. M., Stadelmann, A., Grenfell, J. L., Lammer, H., & Motschmann, U. 2009, Icarus, 199, 526

Grießmeier, J.-M., Stadelmann, A., Motschmann, U., et al. 2005, Astrobiology, 5, 587

Grosch, E. G. & Hazen, R. M. 2015, Astrobiology, 15, 922, pMID: 26430911

Güdel, M., Audard, M., Reale, F., Skinner, S. L., & Linsky, J. L. 2004, Astronomy and Astrophysics, 416, 713

Gueymard, C. A. 2001, Solar Energy, 71, 325

Gueymard, C. A. 2003, Solar Energy, 74, 355

Guo, J. H. 2011, The Astrophysical Journal, 733, 98

Guzmán-Marmolejo, A., Segura, A., & Escobar-Briones, E. 2013, Astrobiology, 13, 550, pMID: 23742231

Haberle, R. M., McKay, C. P., Tyler, D., & Reynolds, R. T. 1996, in Circumstellar Habitable Zones, ed. L. R. Doyle, 29

Haisch, B., Strong, K. T., & Rodono, M. 1991, Annual Review of Astronomy and Astrophysics, 29, 275

Haldane, J. 1929, The Rationalist Annual, 3

Hamano, K., Abe, Y., & Genda, H. 2013, Nature, 497, 607

Hamdani, S., Arnold, L., Foellmi, C., et al. 2006, Astronomy and Astrophysics, 460, 617

Hansen, B. M. S. 2015, International Journal of Astrobiology, 14, 267

Hardisty, D. S., Lu, Z., Planavsky, N. J., et al. 2014, Geology, 42, 619

Harm, W. 1980, Biological Effects of Ultraviolet Radiation, IUPAB Biophysics Series (Cambridge University Press)

Harman, C. E., Schwieterman, E. W., Schottelkotte, J. C., & Kasting, J. F. 2015, The Astrophysical Journal, 812, 137

Hart, M. H. 1978, Icarus, 33, 23

Hauck, S. A. & Phillips, R. J. 2002, Journal of Geophysical Research (Planets), 107, 5052

Heath, M. J., Doyle, L. R., Joshi, M. M., & Haberle, R. M. 1999, Origins of Life and Evolution of the Biosphere, 29, 405

Heller, R. & Armstrong, J. 2014, Astrobiology, 14, 50

Heng, K. 2016, American Scientist, 146, arXiv:1604.05078

Henry, T. J. 2004, in Astronomical Society of the Pacific Conference Series, Vol. 318, Spectroscopically and Spatially Resolving the Components of the Close Binary Stars, ed. R. W. Hilditch, H. Hensberge, & K. Pavlovski, 159–165

Herrick, R. R. 1994, Geology, 22, 703

Herzberg, C., Condie, K., & Korenaga, J. 2010, Earth and Planetary Science Letters, 292, 79

Hess, H. H. 1962, in Petrologic Studies (Geological Society of America)

Hill, R. & Bendall, F. 1960, Nature, 186, 136

Hill, R. & Rich, P. R. 1983, Proceedings of the National Academy of Science, 80, 978

Hirschmann, M. M. & Withers, A. C. 2008, Earth and Planetary Science Letters, 270, 147

Hoffman, P. F. & Schrag, D. P. 2002, Terra Nova, 14, 129

Holland, H. 1978, The chemistry of the atmosphere and oceans, Wiley-Interscience publication (Wiley)

Holland, H. D. 1973, Economic Geology, 68, 1169

Holland, H. D. 2002, Geochimica et Cosmochimica Acta, 66, 3811

Holland, H. D. 2003, Geochimica et Cosmochimica Acta, 67, 787

Holland, H. D. 2006, Philosophical Transactions of the Royal Society B: Biological Sciences, 361, 903

Horowitz, N. H., Hobby, G. L., & Hubbard, J. S. 1976, Science, 194, 1321

Hoyle, F. 1958, Ricerche Astronomiche, 5, 223

Hu, R., Seager, S., & Bains, W. 2012, The Astrophysical Journal, 761, 166

Hu, Y. & Yang, J. 2014, Proceedings of the National Academy of Science, 111, 629

Huang, S.-S. 1959, American Scientist, 47, 397

Huang, S.-S. 1960, Publications of the Astronomical Society of the Pacific, 72, 489

Hunten, D. M. 1973, Journal of Atmospheric Sciences, 30, 1481

Hunten, D. M., Pepin, R. O., & Walker, J. C. G. 1987, Icarus, 69, 532

Hurtgen, M. T., Arthur, M. A., & Halverson, G. P. 2005, Geology, 33, 41

Hüve, K., Bichele, I., Rasulov, B., & Niinemets, Ü. 2011, Plant, Cell & Environment, 34, 113

Ingersoll, A. P. 1969, Journal of Atmospheric Sciences, 26, 1191

Irwin, J., Charbonneau, D., Nutzman, P., & Falco, E. 2009, in IAU Symposium, Vol. 253, Transiting Planets, ed. F. Pont, D. Sasselov, & M. J. Holman, 37–43

Jackson, B., Barnes, R., & Greenberg, R. 2008, Monthly Notices of the Royal Astronomical Society, 391, 237

Jagger, J. 1985

Jakosky, B. M., Grebowsky, J. M., Luhmann, J. G., et al. 2015, Science, 350, 0210

Jiang, G., Shi, X., Zhang, S., Wang, Y., & Xiao, S. 2011, Gondwana Research, 19, 831

Johnson, J. A., Butler, R. P., Marcy, G. W., et al. 2007, The Astrophysical Journal, 670, 833

Joshi, M. 2003, Astrobiology, 3, 415

Joshi, M. M., Haberle, R. M., & Reynolds, R. T. 1997, Icarus, 129, 450

Kaltenegger, L. 2017, Annual Review of Astronomy and Astrophysics, 55, 433

Kaltenegger, L., Eiroa, C., & Fridlund, C. V. M. 2010a, Astrophysics and Space Science, 326, 233

Kaltenegger, L., Jucks, K., & Traub, W. 2006, in IAU Colloq. 200: Direct Imaging of Exoplanets: Science & Techniques, ed. C. Aime & F. Vakili, 259–264

Kaltenegger, L. & Sasselov, D. 2010, The Astrophysical Journal, 708, 1162

Kaltenegger, L. & Selsis, F. 2007, Biomarkers Set in Context, 79

Kaltenegger, L., Selsis, F., Fridlund, M., et al. 2010b, Astrobiology, 10, 89

Kaltenegger, L., Traub, W. A., & Jucks, K. W. 2007, The Astrophysical Journal, 658, 598

Kasper, M., Verinaud, C., & Mawet, D. 2013, in Proceedings of the Third AO4ELT Conference, ed. S. Esposito & L. Fini, 8

Kasting, J. F. 1982, Journal of Geophysical Research, 87, 3091

Kasting, J. F. 1987, Precambrian Research, 34, 205

Kasting, J. F. 1988, Icarus, 74, 472

Kasting, J. F. 1991, Icarus, 94, 1

Kasting, J. F. 1997, Habitable Zones Around Low Mass Stars and the Search for Extraterrestrial Life

Kasting, J. F. 2004, Scientific American, 291, 78

Kasting, J. F. 2010, in Astronomical Society of the Pacific Conference Series, Vol. 430, Pathways Towards Habitable Planets, ed. V. Coudé du Foresto, D. M. Gelino, & I. Ribas, 3

Kasting, J. F. & Brown, L. L. 1998, Setting the Stage: the Early Atmosphere as a Source of Biogenic Compounds, ed. A. Brack, 35–56

Kasting, J. F. & Catling, D. 2003, Annual Review of Astronomy & Astrophysics, 41, 429

Kasting, J. F. & Donahue, T. M. 1980, Journal of Geophysical Research, 85, 3255

Kasting, J. F., Holland, H. D., & Pinto, J. P. 1985, Journal of Geophysical Research, 90, 10,497

Kasting, J. F., Liu, S. C., & Donahue, T. M. 1979, Journal of Geophysical Research, 84, 3097

Kasting, J. F. & Pavlov, A. A. 2001, in Eleventh Annual V. M. Goldschmidt Conference, 3051

Kasting, J. F. & Pollack, J. B. 1983, Icarus, 53, 479

Kasting, J. F. & Walker, J. C. G. 1981, Journal of Geophysical Research, 86, 1147

Kasting, J. F., Whitmire, D. P., & Reynolds, R. T. 1993, Icarus, 101, 108

Kasting, J. F., Zahnle, K. J., & Walker, J. C. G. 1983, Precambrian Research, 20, 121

Kay, C., Opher, M., & Kornbleuth, M. 2016, The Astrophysical Journal, 826, 195

Keir, R. S. 2010, Geophysical Research Letters, 37, L24609

Kelley, D. S., Karson, J. A., Früh-Green, G. L., et al. 2005, Science, 307, 1428

Keppens, R., MacGregor, K. B., & Charbonneau, P. 1995, Astronomy and Astrophysics, 294, 469

Kerrick, D. M. 2001, Reviews of Geophysics, 39, 565

Kerrick, D. M., McKibben, M. A., Seward, T. M., & Caldeira, K. 1995, Chemical Geology, 121, 285

Khare, B. N., Sagan, C., Ogino, H., et al. 1986, Icarus, 68, 176

Khodachenko, M. L., Ribas, I., Lammer, H., et al. 2007, Astrobiology, 7, 167

Khodachenko, M. L., Shaikhislamov, I. F., Lammer, H., & Prokopov, P. A. 2015, The Astrophysical Journal, 813, 50

Kiang, N. Y. 2008, Scientific American, 298, 48

Kiang, N. Y., Segura, A., Tinetti, G., et al. 2007a, Astrobiology, 7, 252

Kiang, N. Y., Siefert, J., Govindjee, & Blankenship, R. E. 2007b, Astrobiology, 7, 222

Kipp, M. A. & Stüeken, E. E. 2017, Science Advances, 3, eaao4795

Kitzmann, D. 2017, Astronomy and Astrophysics, 600, A111

Knoll, A., Javaux, E., Hewitt, D., & Cohen, P. 2006, Philosophical Transactions of the Royal Society B: Biological Sciences, 361, 1023

Knoll, A. H., Bambach, R. K., Payne, J. L., Pruss, S., & Fischer, W. W. 2007, Earth and Planetary Science Letters, 256, 295

Knoll, A. H. & Carroll, S. B. 1999, Science, 284, 2129

Kopparapu, R. K. 2018, The Habitable Zone: The Climatic Limits of Habitability, 58

Kopparapu, R. K., Ramirez, R., Kasting, J. F., et al. 2013, The Astrophysical Journal, 765, 131

Kopparapu, R. K., Ramirez, R. M., SchottelKotte, J., et al. 2014, The Astrophysical Journal Letters, 787, L29

Kopparapu, R. k., Wolf, E. T., Arney, G., et al. 2017, The Astrophysical Journal, 845, 5

Kraft, R. P. 1967, The Astrophysical Journal, 150, 551

Kreidberg, L., Bean, J. L., Désert, J.-M., et al. 2014, Nature, 505, 69

Krumbein, W. E., Gorbushina, A. A., & Holtkamp-Tacken, E. 2004, Astrobiology, 4, 450, pMID: 15684726

Kulikov, Y. N., Lammer, H., Lichtenegger, H. I. M., et al. 2007, Space Science Reviews, 129, 207

Kump, L. R., Brantley, S. L., & Arthur, M. A. 2000, Annual Review of Earth and Planetary Sciences, 28, 611

Kunkel, W. E. 1969, Nature, 222, 1129

Lafrenière, D., Doyon, R., Marois, C., et al. 2007, The Astrophysical Journal, 670, 1367

Lammer, H., Bredehöft, J. H., Coustenis, A., et al. 2009, The Astronomy and Astrophysics Review, 17, 181

Lammer, H., Erkaev, N. V., Odert, P., et al. 2013, Monthly Notices of the Royal Astronomical Society, 430, 1247

Lammer, H., Kasting, J. F., Chassefière, E., et al. 2008, Space Science Reviews, 139, 399

Lammer, H., Kislyakova, K. G., Holmström, M., Khodachenko, M. L., & Grießmeier, J. M. 2011, Astrophysics and Space Science, 335, 9

Lammer, H., Lichtenegger, H. I. M., Kulikov, Y. N., et al. 2007, Astrobiology, 7, 185

Lane, N. 2002, Oxygen: The Molecule That Made the World

Larkin, J. E., Chilcote, J. K., Aliado, T., et al. 2014, in Society of Photo-Optical Instrumentation Engineers (SPIE) Conference Series, Vol. 9147, Ground-based and Airborne Instrumentation for Astronomy V, 91471K

Laughlin, G., Bodenheimer, P., & Adams, F. C. 1997, The Astrophysical Journal, 482, 420

Leconte, J., Wu, H., Menou, K., & Murray, N. 2015, Science, 347, 632

Leger, A., Pirre, M., & Marceau, F. J. 1993, Astronomy and Astrophysics, 277, 309

Léger, A., Selsis, F., Sotin, C., et al. 2004, Icarus, 169, 499

Lehmer, O. R., Catling, D. C., Parenteau, M. N., & Hoehler, T. M. 2018, The Astrophysical Journal, 859, 171

Lenardic, A., Jellinek, A. M., Foley, B., O'Neill, C., & Moore, W. B. 2016, Journal of Geophysical Research (Planets), 121, 1831

Lenton, T. & Watson, A. 2004, AGU Fall Meeting Abstracts

Levin, G. V. & Straat, P. A. 1976, Science, 194, 1322

Levine, J. S., Hays, P. B., & Walker, J. C. G. 1979, Icarus, 39, 295

Lillis, R. J., Robbins, S., Manga, M., Halekas, J. S., & Frey, H. V. 2013, Journal of Geophysical Research: Planets, 118, 1488

Lindberg, C. & Horneck, G. 1991, Journal of Photochemistry and Photobiology B: Biology, 11, 69

Lingam, M. & Loeb, A. 2018, The Astronomical Journal, 156, 151

Lingam, M. & Loeb, A. 2019a, The Astronomical Journal, 157, 25

Lingam, M. & Loeb, A. 2019b, Monthly Notices of the Royal Astronomical Society, 485, 5924

Lippincott, E. R., Eck, R. V., Dayhoff, M. O., & Sagan, C. 1967, The Astrophysical Journal, 147, 753

Lissauer, J. J. 2007, The Astrophysical Journal, 660, L149

Lopez, E. D. & Fortney, J. J. 2014, The Astrophysical Journal, 792, 1

Lovelock, J. E. 1965, Nature, 207, 568

Lovelock, J. E. & Whitfield, M. 1982, Nature, 296, 561

Luger, R. & Barnes, R. 2015, Astrobiology, 15, 119

Lundin, R., Barabash, S., Andersson, H., et al. 2004, Science, 305, 1933

Mahadevan, S., Ramsey, L., Wright, J., et al. 2010, in Society of Photo-Optical Instrumentation Engineers (SPIE) Conference Series, Vol. 7735, Ground-based and Airborne Instrumentation for Astronomy III, 77356X

Manabe, S. & Wetherald, R. T. 1967, Journal of Atmospheric Sciences, 24, 241

Marcy, G. W., Isaacson, H., Howard, A. W., et al. 2014a, The Astrophysical Journal Supplement Series, 210, 20

Marcy, G. W., Weiss, L. M., Petigura, E. A., et al. 2014b, Proceedings of the National Academy of Science, 111, 12655

Margulis, L. 1980, Origin of Eukaryotic Cells (Yale University Press, New Haven)

Marion, G. M., Fritsen, C. H., Eicken, H., & Payne, M. C. 2003, Astrobiology, 3, 785, pMID: 14987483

Maruyama, S., Ikoma, M., Genda, H., et al. 2013, in AGU Fall Meeting Abstracts, Vol. 2013, P43E–07

Mayor, M. & Queloz, D. 1995, Nature, 378, 355

McDermott, J. M., Seewald, J. S., German, C. R., & Sylva, S. P. 2015, Proceedings of the National Academy of Science, 112, 7668

McElroy, M. B. 1972, Science, 175, 443

McKay, C. P., Friedmann, E. I., Gómez-Silva, B., et al. 2003, Astrobiology, 3, 393, pMID: 14577886

Miller, S. L. 1953, Science, 117, 528

Mirzoyan, L. V. 1990, Symposium - International Astronomical Union, 137, 1–13

Mizutani, H., Yamamoto, T., & Fujimura, A. 1992, Advances in Space Research, 12, 265

Moore, W. B., Lenardic, A., Jellinek, A. M., et al. 2017, Nature Astronomy, 1, 0043

Morbidelli, A., Bitsch, B., Crida, A., et al. 2016, Icarus, 267, 368

Mörner, N.-A. & Etiope, G. 2002, Global and Planetary Change, 33, 185

Mulders, G. D., Pascucci, I., & Apai, D. 2015, The Astrophysical Journal, 814, 130

Mykytczuk, N., Foote, S., Omelon, C., et al. 2013, The ISME journal, 7

Navarro-González, R., Rainey, F. A., Molina, P., et al. 2003, Science, 302, 1018

Newkirk, G., J. 1980, in The Ancient Sun: Fossil Record in the Earth, Moon and Meteorites, ed. R. O. Pepin, J. A. Eddy, & R. B. Merrill, 293–320

Newton, E. R., Irwin, J., Charbonneau, D., Berta-Thompson, Z. K., & Dittmann, J. A. 2016, The Astrophysical Journal, 821, L19

Nisbet, E. & Fowler, C. 1999, Proceedings of the Royal Society of London. Series B: Biological Sciences, 266, 2375

Nisbet, E. G. 1995, Nature, 373, 479

Noack, L. 2014, Planetary and Space Science, 98, 14 , planetary evolution and life

Noack, L. & Breuer, D. 2014, Planetary and Space Science, 98, 41 , planetary evolution and life

Noack, L., Höning, D., Rivoldini, A., et al. 2016, Icarus, 277, 215

Noack, L., Rivoldini, A., & Van Hoolst, T. 2017, Physics of the Earth and Planetary Interiors, 269, 40

Noll, L. C. 2014, Stellar Classification Table. [online]

North, G. R. 1975, Journal of Atmospheric Sciences, 32, 2033

Olson, J. M. 2006, Photosynthesis Research, 88, 109

O'Malley-James, J. T., Cockell, C. S., Greaves, J. S., & Raven, J. A. 2014, International Journal of Astrobiology, 13, 229

O'Neill, C. & Lenardic, A. 2007, Geophysical Research Letters, 34

Oparin, A. 1924, in The Origin of Life, J.D. Bernal, 1967, World, Cleveland, OH

Osten, R. A., Hawley, S. L., Allred, J. C., Johns-Krull, C. M., & Roark, C. 2005, The Astrophysical Journal, 621, 398

Owen, T. 1980, in Strategies for the Search for Life in the Universe. Astrophysics and Space Sciences Library, M.D. Papagiannis, ed. Springer, Vol. 83, 177

P McKay, C. 2000, Geophysical research letters, 27, 2153

Pace, N. R. 1997, Science, 276, 734

Paulino-Lima, I., Pilling, S., Janot-Pacheco, E., et al. 2010, Planetary and Space Science, 58, 1180

Pavlov, A., Blinov, A., & Konstantinov, A. 2002, Planetary and Space Science, 50, 669 , exobiology: the search for extraterrestrial life and prebiotic ch emistry

Pavlov, A. A. & Kasting, J. F. 2002, Astrobiology, 2, 27

Peale, S. J. 1977, in IAU Colloq. 28: Planetary Satellites, 87

Penz, T., Erkaev, N., Kulikov, Y., et al. 2008, Planetary and Space Science, 56, 1260

Penz, T. & Micela, G. 2008, Astronomy and Astrophysics, 479, 579

Permentier, H. P., Neerken, S., Overmann, J., & Amesz, J. 2001, Biochemistry, 40, 5573, pMID: 11331023

Pettersen, B. R. & Coleman, L. A. 1981, The Astrophysical Journal, 251, 571

Pianka, E. 1974, Evolutionary Ecology (Eric R. Pianka)

Pickles, A. J. 1998, The Publications of the Astronomical Society of the Pacific, 110, 863

Pierrehumbert, R. & Gaidos, E. 2011, The Astrophysical Journal Letters, 734, L13

Pilcher, C. B. 2003, Astrobiology, 3, 471

Pinto, J. P., Gladstone, G. R., & Yung, Y. L. 1980, Science, 210, 183

Planavsky, N. J., Reinhard, C. T., Wang, X., et al. 2014, Science, 346, 635

Planavsky, N. J., Rouxel, O. J., Bekker, A., et al. 2010, Nature, 467, 1088

Pollack, J. B., Kasting, J. F., Richardson, S. M., & Poliakoff, K. 1987, Icarus, 71, 203

Pope, E. C., Bird, D. K., & Rosing, M. T. 2012, Proceedings of the National Academy of Science, 109, 4371

Popp, M., Schmidt, H., & Marotzke, J. 2016, Nature Communications, 7, 10627

Potter, C. S., Randerson, J. T., Field, C. B., et al. 1993, Global Biogeochemical Cycles, 7, 811

Prieur, D., Erauso, G., & Jeanthon, C. 1995, Planetary and Space Science, 43, 115 , exobiology

Prigogine, I., Nicolis, G., & Babloyantz, A. 1972, Physics Today, 25, 23

Priscu, J. C., Fritsen, C. H., Adams, E. E., et al. 1998, Science, 280, 2095

Quintana, E. V., Barclay, T., Raymond, S. N., et al. 2014, Science, 344, 277

Quirrenbach, A., Amado, P. J., Seifert, W., et al. 2012, CARMENES. I: instrument and survey overview

Rambler, M. B. & Margulis, L. 1980, Science, 210, 638

Ramirez, R. 2014, PhD thesis

Ramirez, R. M. 2017, Icarus, 297, 71

Ramirez, R. M. 2018, Geosciences, 8, 280

Ramirez, R. M. & Craddock, R. A. 2017, in Fourth International Conference on Early Mars: Geologic, Hydrologic, and Climatic Evolution and the Implications for Life, Vol. 2014, 3003

Ramirez, R. M. & Kaltenegger, L. 2014, The Astrophysical Journal Letters, 797, L25

Ramirez, R. M. & Kaltenegger, L. 2016, The Astrophysical Journal, 823, 6

Ramirez, R. M. & Kaltenegger, L. 2017, The Astrophysical Journal Letters, 837, L4

Rasool, S. I. & de Bergh, C. 1970, Nature, 226, 1037

Rauer, H., Catala, C., Aerts, C., et al. 2014, Experimental Astronomy, 38, 249

Rauer, H., Catala, C., Aerts, C., et al. 2014, Experimental Astronomy, 38, 249

Rauer, H., Gebauer, S., Paris, P. V., et al. 2011, Astronomy and Astrophysics, 529, A8

Raymond, S. N., Scalo, J., & Meadows, V. S. 2007, The Astrophysical Journal, 669, 606

Reinhard, C. T., Planavsky, N. J., Gill, B. C., et al. 2017, Nature, 541, 386

Ribas, I., Guinan, E. F., Güdel, M., & Audard, M. 2005, The Astrophysical Journal, 622, 680

Ricker, G. R., Vanderspek, R., Winn, J., et al. 2016, in Society of Photo-Optical Instrumentation Engineers (SPIE) Conference Series, Vol. 9904, Space Telescopes and Instrumentation 2016: Optical, Infrared, and Millimeter Wave, 99042B

Ries, G., Heller, W., Puchta, H., et al. 2000, Nature, 406, 98

Robinson, J. M. 1990, Geology, 18, 607

Rodono, M. 1986, NASA Special Publication, 492

Rothschild, L. 2008, Philosophical transactions of the Royal Society of London. Series B, Biological sciences, 363, 2787

Rothschild, L. & Mancinelli, R. 2001, Nature, 409, 1092

Rowe, J. F., Bryson, S. T., Marcy, G. W., et al. 2014, The Astrophysical Journal, 784, 45

Rugheimer, S., Kaltenegger, L., Zsom, A., Segura, A., & Sasselov, D. 2013, Astrobiology, 13, 251

Rushby, A. J., Claire, M. W., Osborn, H., & Watson, A. J. 2013, Astrobiology, 13, 833

Russell, M. J., Hall, A. J., & Martin, W. 2010, Geobiology, 8, 355

Rye, R. & Holland, H. D. 1998, American Journal of Science, 298, 621

Sagan, C. 1962, Icarus, 1, 151

Sagan, C., Thompson, W. R., Carlson, R., Gurnett, D., & Hord, C. 1993, Nature, 365, 715

Salaris, M. & Cassisi, S. 2005, Evolution of Stars and Stellar Populations, 400

Sano, Y. 1993, Journal of Geomagnetism and Geoelectricity, 45, 65

Scalo, J., Kaltenegger, L., Segura, A., et al. 2007, Astrobiology, 7, 85

Schiffbauer, J. D., Xiao, S., Sharma, K. S., & Wang, G. 2012, Geology, 40, 223

Schindler, T. L. & Kasting, J. F. 2000a, in ESA Special Publication, Vol. 451, Darwin and Astronomy : the Infrared Space Interferometer, ed. B. Schürmann, 159

Schindler, T. L. & Kasting, J. F. 2000b, Icarus, 145, 262

Schwieterman, E. W., Kiang, N. Y., Parenteau, M. N., et al. 2018, Astrobiology, 18, 663

Schwieterman, E. W., Meadows, V. S., Domagal-Goldman, S. D., et al. 2016, The Astrophysical Journal Letters, 819, L13

Seager, S. 2014, Proceedings of the National Academy of Science, 111, 12634

Seager, S., Bains, W., & Hu, R. 2013a, The Astrophysical Journal, 775, 104

Seager, S., Bains, W., & Hu, R. 2013b, The Astrophysical Journal, 777, 95

Seager, S., Bains, W., & Petkowski, J. J. 2016, Astrobiology, 16, 465

Seager, S., Turner, E. L., Schafer, J., & Ford, E. B. 2005, Astrobiology, 5, 372

Segerer, A. H., Burggraf, S., Fiala, G., et al. 1993, Origins of life and evolution of the biosphere, 23, 77

Segura, A. & Kaltenegger, L. 2010, Search for Habitable Planets

Segura, A., Kasting, J. F., Meadows, V., et al. 2005, Astrobiology, 5, 706

Segura, A., Krelove, K., Kasting, J. F., et al. 2003, Astrobiology, 3, 689

Segura, A., Meadows, V. S., Kasting, J. F., Crisp, D., & Cohen, M. 2007, Astronomy and Astrophysics, 472, 665

Segura, A., Walkowicz, L. M., Meadows, V., Kasting, J., & Hawley, S. 2010, Astrobiology, 10, 751, pMID: 20879863

Sellers, W. D. 1969, Journal of Applied Meteorology, 8, 392

Selsis, F. 2003, in Astronomical Society of the Pacific Conference Series, Vol. 321, Detection and Characterization of Extrasolar Planets: Today and Tomorrow, ed. J. Beaulieu, A. Lecavelier des Etangs, & C. Terquem, 170–182

Selsis, F., Despois, D., & Parisot, J. P. 2002, Astronomy and Astrophysics, 388, 985

Selsis, F., Kasting, J. F., Levrard, B., et al. 2007, Astronomy and Astrophysics, 476, 1373

Shaikhislamov, I. F., Khodachenko, M. L., Sasunov, Y. L., et al. 2014, The Astrophysical Journal, 795, 132

Shields, A. L., Ballard, S., & Johnson, J. A. 2016, Physics Reports, 663, 1

Shields, A. L., Barnes, R., Agol, E., et al. 2016, Astrobiology, 16, 443, pMID: 27176715

Shields, A. L., Meadows, V. S., Bitz, C. M., et al. 2013, Astrobiology, 13, 715

Skumanich, A. 1972, The Astrophysical Journal, 171, 565

Sleep, N. H. 2000, Journal of Geophysical Research, 105, 17563

Sleep, N. H. & Zahnle, K. 2001, Journal of Geophysical Research, 106, 1373

Snellen, I. A. G., de Kok, R. J., de Mooij, E. J. W., & Albrecht, S. 2010, Nature, 465, 1049

Soderblom, D. R. 1982, The Astrophysical Journal, 263, 239

Sotin, C., Grasset, O., & Mocquet, A. 2007, Icarus, 191, 337

Sozzetti, A., Giacobbe, P., Lattanzi, M. G., et al. 2013, Monthly Notices of the Royal Astronomical Society, 437, 497

Sparks, W. B., DasSarma, S., & Reid, I. N. 2006, in Bulletin of the American Astronomical Society, Vol. 38, American Astronomical Society Meeting Abstracts, 901

Spencer, J. R. & Schneider, N. M. 1996, Annual Review of Earth and Planetary Sciences, 24, 125

Spiegel, D. S., Menou, K., & Scharf, C. A. 2009, The Astrophysical Journal, 691, 596

Spiegel, D. S., Raymond, S. N., Dressing, C. D., Scharf, C. A., & Mitchell, J. L. 2010, The Astrophysical Journal, 721, 1308

Stamenković, V., Noack, L., Breuer, D., & Spohn, T. 2012, The Astrophysical Journal, 748, 41

Stauffer, J. R., Giampapa, M. S., Herbst, W., et al. 1991, The Astrophysical Journal, 374, 142

Stauffer, J. R. & Hartmann, L. W. 1986, The Astrophysical Journal Supplement Series, 61, 531

Stevenson, D. J. 1983, Reports on Progress in Physics, 46, 555

Stevenson, D. J. 2003, Earth and Planetary Science Letters, 208, 1

Stoeckenius, W. 1976, Scientific American, 234, 38

Stomp, M., Huisman, J., de Jongh, F., et al. 2004, Nature, 432, 104

Sullivan, P. W., Winn, J. N., Berta-Thompson, Z. K., et al. 2015, The Astrophysical Journal, 809, 77

Summers, M. E., Stern, S. A., Gladstone, G. R., et al. 2015, in AAS/Division for Planetary Sciences Meeting Abstracts #47, AAS/Division for Planetary Sciences Meeting Abstracts, 105.11

Svensen, H. & Jamtveit, B. 2010, Elements, 6, 179

Sverdrup, K., Duxbury, A., & Duxbury, A. 2003, An introduction to the world's oceans (McGraw-Hill)

Tajika, E. 2007, Earth, Planets, and Space, 59, 293

Takai, K., Nakamura, K., Toki, T., et al. 2008, Proceedings of the National Academy of Sciences, 105, 10949

Tarter, J. C., Backus, P. R., Mancinelli, R. L., et al. 2007, Astrobiology, 7, 30

Tasker, E., Tan, J., Heng, K., et al. 2017, Nature Astronomy, 1, 0042

Tian, F. 2009, The Astrophysical Journal, 703, 905

Tian, F. 2015, Earth and Planetary Science Letters, 432, 126

Tian, F., France, K., Linsky, J. L., Mauas, P. J. D., & Vieytes, M. C. 2014, Earth and Planetary Science Letters, 385, 22

Tian, F. & Ida, S. 2015, Nature Geoscience, 8, 177

Tian, F., Kasting, J. F., Liu, H.-L., & Roble, R. G. 2008, Journal of Geophysical Research (Planets), 113, E05008

Tian, F., Kasting, J. F., & Solomon, S. C. 2009, Geophysical Research Letters, 36

Tian, F., Toon, O. B., Pavlov, A. A., & De Sterck, H. 2005, The Astrophysical Journal, 621, 1049

Étienne Artigau, Kouach, D., Donati, J.-F., et al. 2014, SPIRou: the near-infrared spectropolarimeter/high-precision velocimeter for the Canada-France-Hawaii telescope

Tikhov, G. A. 1914, Mitteilungen der Nikolai-Hauptsternwarte zu Pulkowo, 6

Tinetti, G., Drossart, P., Eccleston, P., et al. 2018, Experimental Astronomy, 46, 135

Tinetti, G., Rashby, S., & Yung, Y. L. 2006, The Astrophysical Journal Letters, 644, L129

Tinetti, G., Vidal-Madjar, A., Liang, M.-C., et al. 2007, Nature, 448, 169

Toupance, G., Bossard, A., & Raulin, F. 1977, Origins of Life, 8, 259

Traub, W. A. 2003, in Astronomical Society of the Pacific Conference Series, Vol. 294, Scientific Frontiers in Research on Extrasolar Planets, ed. D. Deming & S. Seager, 595–602

Tsiaras, A., Waldmann, I. P., Tinetti, G., Tennyson, J., & Yurchenko, S. N. 2019, arXiv e-prints, arXiv:1909.05218

Turbet, M., Forget, F., Leconte, J., Charnay, B., & Tobie, G. 2017, Earth and Planetary Science Letters, 476, 11

Turcotte, D. L., Morein, G., Roberts, D., & Malamud, B. D. 1999, Icarus, 139, 49

Turnbull, M. C., Traub, W. A., Jucks, K. W., et al. 2006, The Astrophysical Journal, 644, 551

Unterborn, C. T., Desch, S. J., Hinkel, N. R., & Lorenzo, A. 2018, Nature Astronomy, 2, 297

Urey, H. C. 1951, Geochimica et Cosmochimica Acta, 1, 209

Valencia, D., O'Connell, R. J., & Sasselov, D. D. 2007, The Astrophysical Journal, 670, L45

Vanderburg, A., Plavchan, P., Johnson, J. A., et al. 2016, Monthly Notices of the Royal Astronomical Society, 459, 3565

Villaver, E. & Livio, M. 2007, The Astrophysical Journal, 661, 1192

von Bloh, W., Bounama, C., Cuntz, M., & Franck, S. 2007, Astronomy and Astrophysics, 476, 1365

Wächtershäuser, G. 1990, Origins of Life and Evolution of the Biosphere, 20, 173

Walker, J. C. G. 1977, Evolution of the atmosphere (Macmillan Publishing, New York)

Walker, J. C. G., Hays, P. B., & Kasting, J. F. 1981, Journal of Geophysical Research, 86, 9776

Ward, L. M., Kirschvink, J. L., & Fischer, W. W. 2016, Origins of Life and Evolution of Biospheres, 46, 51

Ward, P. & Brownlee, D. 2000, Rare earth : why complex life is uncommon in the universe

Ward, P. D. & Brownlee, D. 2004, The life and death of planet Earth: how the new science of astrobiology charts the ultimate fate of our world, first owl books edition edn. (Judy Piatkus Publishers Ltd)

Ward, W. R. 1974, Journal of Geophysical Research (1896-1977), 79, 3375

Warren, P. H. & Kallemeyn, G. W. 1996, Meteoritics & Planetary Science, 31, 97

Wedepohl, K. H. 1995, Geochimica et Cosmochimica Acta, 59, 1217

Wegener, A. 1912, Geologische Rundschau, 3, 276

West, A. A., Hawley, S. L., Bochanski, J. J., et al. 2008, The Astronomical Journal, 135, 785

Westall, F., Foucher, F., Cavalazzi, B., et al. 2011, Planetary and Space Science, 59, 1093 , comparative Planetology: Venus-Earth-Mars

Whitmire, D. P., Reynolds, R. T., & Kasting, J. F. 1991, Habitable Zones for Earth-like Planets Around Main Sequence Stars, ed. J. Heidmann & M. J. Klein, Vol. 390, 173–178

Wilde, S. A., Valley, J. W., Peck, W. H., & Graham, C. M. 2001, Nature, 409, 175

Wildi, F., Blind, N., Reshetov, V., et al. 2017, in Society of Photo-Optical Instrumentation Engineers (SPIE) Conference Series, Vol. 10400, Society of Photo-Optical Instrumentation Engineers (SPIE) Conference Series, 1040018

Williams, D. M., Kasting, J. F., & Wade, R. A. 1997, Nature, 385, 234

Williams, D. M. & Pollard, D. 2003, International Journal of Astrobiology, 2, 1–19

Wilson, O. C. 1966, The Astrophysical Journal, 144, 695

Wolf, E. T. & Toon, O. B. 2015, Journal of Geophysical Research (Atmospheres), 120, 5775

Wolstencroft, R. D. & Raven, J. A. 2002, Icarus, 157, 535

Woods, T. N., Eparvier, F. G., Fontenla, J., et al. 2004, Geophysical Research Letters, 31, L10802

Woolf, N. J., Smith, P. S., Traub, W. A., & Jucks, K. W. 2002, Astronomy and Astrophysics, 574, 430

Worden, S. P., Schneeberger, T. J., Giampapa, M. S., Deluca, E. E., & Cram, L. E. 1984, The Astrophysical Journal, 276, 270

Wordsworth, R., Kalugina, Y., Lokshtanov, S., et al. 2017, Geophysical Research Letters, 44, 665

Wordsworth, R. & Pierrehumbert, R. 2014, The Astrophysical Journal, 785, L20

Wordsworth, R. D., Forget, F., Selsis, F., et al. 2010, Astronomy and Astrophysics, 522, A22

Wordsworth, R. D. & Pierrehumbert, R. T. 2013, The Astrophysical Journal, 778, 154

Yang, J. & Abbot, D. S. 2014, The Astrophysical Journal, 784, 155

Yang, J., Boué, G., Fabrycky, D. C., & Abbott, D. S. 2014, The Astrophysical Journal, 787, L2

Yang, J., Cowan, N. B., & Abbot, D. S. 2013a, The Astrophysical Journal, 771, L45

Yang, J., Cowan, N. B., & Abbot, D. S. 2013b, The Astrophysical Journal, 771, L45

Yelle, R. V. 2004, Icarus, 170, 167

Zahnle, K., Claire, M., & Catling, D. 2006, Geobiology, 4, 271

Zahnle, K. J. & Kasting, J. F. 1986, Icarus, 68, 462

Zheng, X., Beard, B., Roden, E., Czaja, A., & Johnson, C. 2018, Goldschmidt abstracts, 3033

Zwietering, M., Jongenburger, I., Rombouts, F., & Van, T. 1990, Applied and environmental microbiology, 56, 1875